

The fine scale structure of synaptic inputs in developing hippocampal neurons

Dissertation zur Erlangung
des Doktorgrades der Naturwissenschaften

der Fakultät für Biologie
der Ludwig-Maximilians-Universität München

vorgelegt von

Thomas Kleindienst
München, 29. April 2010

Erstgutachter: Prof. Dr. Tobias Bonhoeffer
Zweitgutachter: Prof. Dr. Axel Borst

Tag der mündlichen Prüfung : 28. Juli 2010

Die vorliegende Arbeit wurde zwischen Januar 2006 und April 2010 am
Max-Planck Institut für Neurobiologie in Martinsried
sowie am
Netherlands Institute for Neuroscience in Amsterdam
durchgeführt.

Ehrenwörtliche Versicherung:

Ich versichere hiermit ehrenwörtlich, dass Ich die Dissertation mit dem Titel „The fine scale structure of synaptic inputs in developing hippocampal neurons“ selbständig und ohne unerlaubte Beihilfe angefertigt habe. Ich habe mich dabei keiner anderen als der von mir ausdrücklich bezeichneten Hilfen und Quellen bedient.

Erklärung:

Hiermit erkläre ich, dass ich mich nicht anderweitig einer Doktorprüfung ohne Erfolg unterzogen habe. Die Dissertation wurde in ihrer jetzigen oder ähnlichen Form bei keiner anderen Hochschule eingereicht und hat noch keinen sonstigen Prüfungszwecken gedient.

München, 28 April 2010

Thomas Kleindienst

Meiner Familie

TABLE OF CONTENT

Table of Content	vii
Table of Figures	ix
Abbreviations	xi
1 Summary	1
2 Introduction	3
2.1 Synapses and synapse formation	3
2.2 The hippocampus	8
2.3 Calcium and Calcium imaging	10
2.4 Development of specificity	15
2.5 Spontaneous activity	17
2.6 Dendritic computation	19
2.7 Objectives of this study	24
3 Materials and Methods	25
3.1 Material	25
3.1.1 Chemicals	25
3.1.2 Drugs	26
3.1.3 Media	26
3.1.4 Equipment	28
3.1.5 Programs	30
3.2 Method	31
3.2.1 Cultures	31
3.2.2 Patch Clamp Recordings	32
3.2.3 Stimulation	32
3.2.4 Imaging	33
3.2.5 Image analysis	35
3.2.6 Electrophysiological analysis	43
3.2.7 Temporal alignment of datasets	45

Table of Content

4	Results	47
4.1	Electrophysiological recordings.....	47
4.2	Ca ²⁺ -transients	47
4.2.1	Global Ca ²⁺ -transients	47
4.2.2	Local Ca ²⁺ -transients and their correlation with synaptic currents	49
4.2.3	Stimulated Ca ²⁺ -transients	50
4.2.4	Local Ca ²⁺ -transients as reporters of glutamatergic transmission .	52
4.2.5	Properties of synaptic and non-synaptic Ca ²⁺ -transients	54
4.3	Developmental changes.....	55
4.4	Mapping synaptic inputs in individual neurons	56
4.5	Activation-patterns during bursts of synaptic activation.....	61
4.6	Correlated activation of individual pairs of synapses.....	63
4.6.1	Correlation vs. vertical distance from the soma	64
4.6.2	Correlation vs. inter-synapse-distance	66
5	Discussion	71
5.1	Subset of local Ca ²⁺ -transients is linked to glutamatergic transmission.....	72
5.2	Stimulated Ca ²⁺ -transients	74
5.3	Ca ²⁺ -transients as reporter of glutamatergic transmission	76
5.4	Developmental changes.....	79
5.5	Mapping synaptic inputs in individual neurons	82
5.6	Synaptic patterns during bursts of synaptic activation.....	85
5.7	Correlated activation of individual pairs of synapses.....	87
5.7.1	Correlation vs. vertical distance from the soma	87
5.7.2	Correlation vs. inter-synapse-distance	88
6	Conclusion and Outlook	91
7	Bibliography	97
8	Acknowledgements	109
9	Curriculum vitae	111

TABLE OF FIGURES

Figure 2-1 EM picture of a synapse	4
Figure 2-2 Comparison of different types of synapses.....	5
Figure 2-3 Synapse elimination at the NMJ	7
Figure 2-4 Neuronal organization of a hippocampal slice	10
Figure 2-5 Chemical structure of fluorescent dyes.....	12
Figure 2-6 FRET – effect	13
Figure 2-7 Development of the hippocampal circuit in the rat.....	18
Figure 2-8 Dendritic morphologies.....	20
Figure 2-9 Scheme depicting the complex interactions of the integrative properties of dendrites	22
Figure 3-1 The position of the hippocampus in the rodent brain.....	31
Figure 3-2 Setup for simultaneous electrophysiological recording and Ca^{2+} -imaging	34
Figure 3-3 Fast z-stepping.....	35
Figure 3-4 Dendrite detection	36
Figure 3-5 Measuring signal properties	37
Figure 3-6 Sites of local Ca^{2+} -transients	39
Figure 3-7 Manual detection of local Ca^{2+} -transients.....	40
Figure 3-8 Inter-synapse correlation	42
Figure 3-9 Removing current fluctuations induced by the fast z-stepping	44
Figure 3-10 Scheme depicting the aligning principle	46
Figure 4-1 Global Ca^{2+} -transients	48
Figure 4-2 Global Ca^{2+} -transients and spike rate.....	48

Table of Figures

Figure 4-3 Histogram of time differences between local Ca^{2+} -transients and synaptic currents50

Figure 4-4 Spontaneous and stimulated local Ca^{2+} -transients51

Figure 4-5 Synaptic sites show glutamate receptor activation.....52

Figure 4-6 Histogram of the amplitude of miniature EPSCs53

Figure 4-7 Properties of Ca^{2+} -transients at synaptic and at non-synaptic sites.....54

Figure 4-8 Duration of synaptic and non-synaptic transients at different developmental stages56

Figure 4-9 Mapping the synaptome.....58

Figure 4-10 Structural and functional Sholl diagrams.....60

Figure 4-11 Synaptic activity pattern during successive bursts61

Figure 4-12 Activation patterns of individual synapses during consecutive bursts62

Figure 4-13 Correlation of pairs of synapses against their vertical distance65

Figure 4-14 Synaptic activations at two neighboring synapses67

Figure 4-15 Correlation of pairs of synapses against their distance along the dendrite68

Figure 6-1 Scheme of subcellular wiring diagram92

ABBREVIATIONS

3D	Three dimensions
4D	Four dimensions
A	Ampere
BME	Basal Medium Eagle
CA	Cornu Ammonis
CAMs	Cell adhesion molecules
CCD	Charge-coupled device
CNS	Central nervous system
D-APV	(2R)-amino-5-phosphonovaleric acid
DMSO	Dimethyl sulfoxide
EM	Electron microscopy
FRET	Fluorescence resonance energy transfer
GABA	Gamma-aminobutyric acid
GBSS	Gey's Balanced Salt Solution
GDP	Giant depolarization potentials
HBSS	Hank's buffered salt solution
Hz	Hertz
LTD	Long time depression
LTP	Long time potentiation
min	Minute
ml	Milliliter
mm	Millimeter
ms	Millisecond

Abbreviations

mV	Millivolt
µm	Micrometer
n	Number
NBQX	2,3-dihydroxy-6-nitro-7-sulfamoyl-benzo[f]quinoxaline-2,3-dione
NMDA	N-methyl-D-aspartic acid
NMJ	Neuro-muscular junction
OGB-1	Oregon-Green-BAPTA I
P	Probability
P(X)	Post natal day X
pA	Picoampere
rpm	Revolutions per minute
s	Second
s.d.	Standard deviation
Trolox	6-hydroxy-2,5,7,8-tetramethylchroman-2-carboxylic acid
TTX	Tetrodotoxin

1 SUMMARY

During development, the brain forms out of billions of individual neurons. The formation of a functional network is achieved in steps. First, only a coarse wiring diagram is set up guided mainly by fixed genetic programs. Subsequently, this wiring diagram becomes increasingly refined by activity. Even before the onset of sensation the wiring diagram is shaped by spontaneous activity, i.e. activity not evoked by sensory input. There is increasing evidence that the precision which is to be achieved exceeds just cellular resolution. That means it is not only of importance which neurons are connected to each other, but also the exact location of the connecting synapse matters. Since electrophysiological recordings do not provide any information on the subcellular location of synaptic activation, today little is known about the spatio-temporal patterns of synaptic activation in individual neurons. I set out to monitor spontaneous synaptic activity in the dendritic tree of developing hippocampal CA3 pyramidal cells with single synapse resolution.

I combined electrophysiological recordings and calcium imaging to visualize synaptic activation of large parts of the dendritic arborization of individual neurons. To increase the imaged volume and gather information from larger parts of the dendritic tree, I acquired images from three consecutive z-planes using a piezo stepper triggered by the frame trigger signal given from the CCD camera. The software I wrote during this thesis analyzed both, the electrophysiological data and the imaging data, completely automatically and aligned the two datasets in time. The analysis revealed that about 50% of the local Ca^{2+} -transients report for glutamatergic synaptic activity and since these glutamatergic Ca^{2+} -transients can be clearly identified they can be exploited to visualize synaptic activity. Analysis of the spatio-temporal patterns of synaptic activation revealed a local activity pattern: synapses being close to one another are more likely to fire simultaneously than synapses further apart from each other. This finding is in line with recently found plasticity rules showing the existence of mechanisms, which preferentially strengthen

Summary

neighboring synapses carrying similar activation patterns. Furthermore, it shows a subcellular precision of the wiring diagram. This subcellular precision has already been proposed by theoretical work since, in combination with the existing dendritic nonlinearities, it could enhance the computational power of individual neurons and thus the entire brain.

In summary I developed and described a technique to visualize and map the purely glutamatergic synaptic input onto individual neurons with single synapse precision. Using this approach, I investigated the spatio-temporal activity patterns and described a local activity rule which is, according to previous work, an important prerequisite to increase the capacities of neurons. The technique developed here may offer the opportunity to visualize synaptic activity in various other systems, and thus might be useful to investigate spatio-temporal aspects of synaptic activity not only during development but also in mature systems.

2 INTRODUCTION

The mammalian brain is an extraordinary organ, able to process received information extremely fast on the one hand, but on the other hand also capable of storing information over decades. The basic intention of neuroscience is to understand the brain and to decipher the complex interactions which enable the stability to guarantee functionality throughout lifetime but facilitate the plasticity necessary for learning and the formation of memories. During development, when the mammalian brain forms a network out of billions of individual neurons, it is particularly plastic. The function of this network crucially depends on properly connecting these individual neurons. The complexity of the network requires a variety of mechanisms setting up and tuning the wiring diagram. Today we know that the wiring diagram is specified not solely genetically but it is adjusted to a large part by activity (Cline, 2003). These activity dependent refinements are not only important during the initial development of the brain, but they are also the basis for shaping the wiring diagram in the adult brain, and thus, the basis for learning and memory formation. Despite the importance of activity and its influence on shaping the wiring diagram, little is known about the activity patterns impinging onto individual neurons and their impact on the wiring diagram.

2.1 Synapses and synapse formation

Today it is generally accepted, that the brain consists of billions of individual cells, the neurons, but this knowledge was gained only relatively recently. At the beginning of the last century there was still a discussion whether the brain is formed by a “syncytium of continuous cytoplasm”, which was called the reticular theory, or whether it is rather made out of distinct individual cells. By the end of the 19th century, Cajal who claimed to see “*dispositions of engagement*” was convinced that the cell theory was valid. He could convince Sherrington who at the end of the 19th century argued that “*nerve endings are only in contact with other neurons*”. For this contact site between neurons Sherrington coined the

term *Synapse* (Cowan and Kandel, 2001). Nevertheless, final proof for the cell theory came only with the development of electron microscopy (EM) in the 1950th, increasing the achievable resolution, thus making visualization of synaptic membranes possible (Figure 2-1). The emerging question

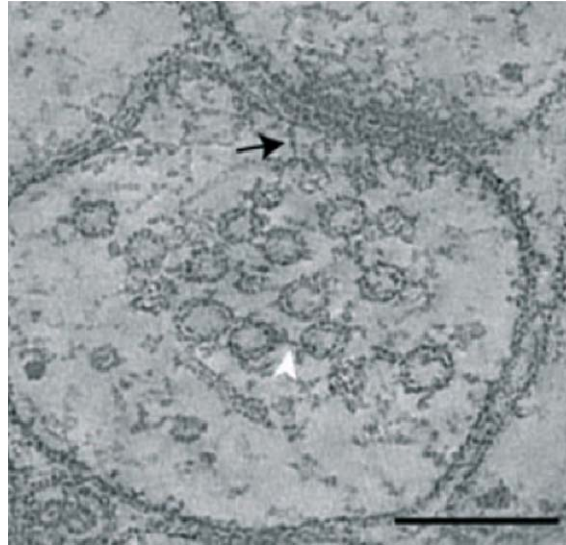


Figure 2-1 EM picture of a synapse

was how information is transmitted from one neuron to the other at the synapse. Is the transmission electrical, like it

Presynaptic densities (black arrow) and short strands linking synaptic vesicles (white arrow). Scale bar: 100 nm (Siksou et al., 2009)

was already known for the spread of information within the neuron, or is it rather a chemical transmission? Experimental findings of Otto Loewi and Henry Dale proofed the existence of chemical transmission at peripheral synapses (Todman, 2008; Karczmar, 1996), at a structure today known as neuromuscular junction (NMJ). Today it is generally known that both ways of transmission, chemical as well as electric, occur although the majority of synapses in the mammalian brain and all synapses referred to in this study are chemical ones (Figure 2-2).

Synapses are sites at which information is transferred from a presynaptic axon terminal of one neuron to the postsynaptic site, in the central nervous system (CNS) most commonly at a dendrite, of another neuron. This information transfer needs to be fast and reliable, thus synapses are highly specialized structures. To understand the development and function of the entire nervous system, it is essential to get insight into the principles of formation, maturation and function of individual synapses. However, since mammalian synapses are diverse, principles valid at one type of synapse are not necessarily valid throughout the nervous system. "Typical synapses" do not exist.

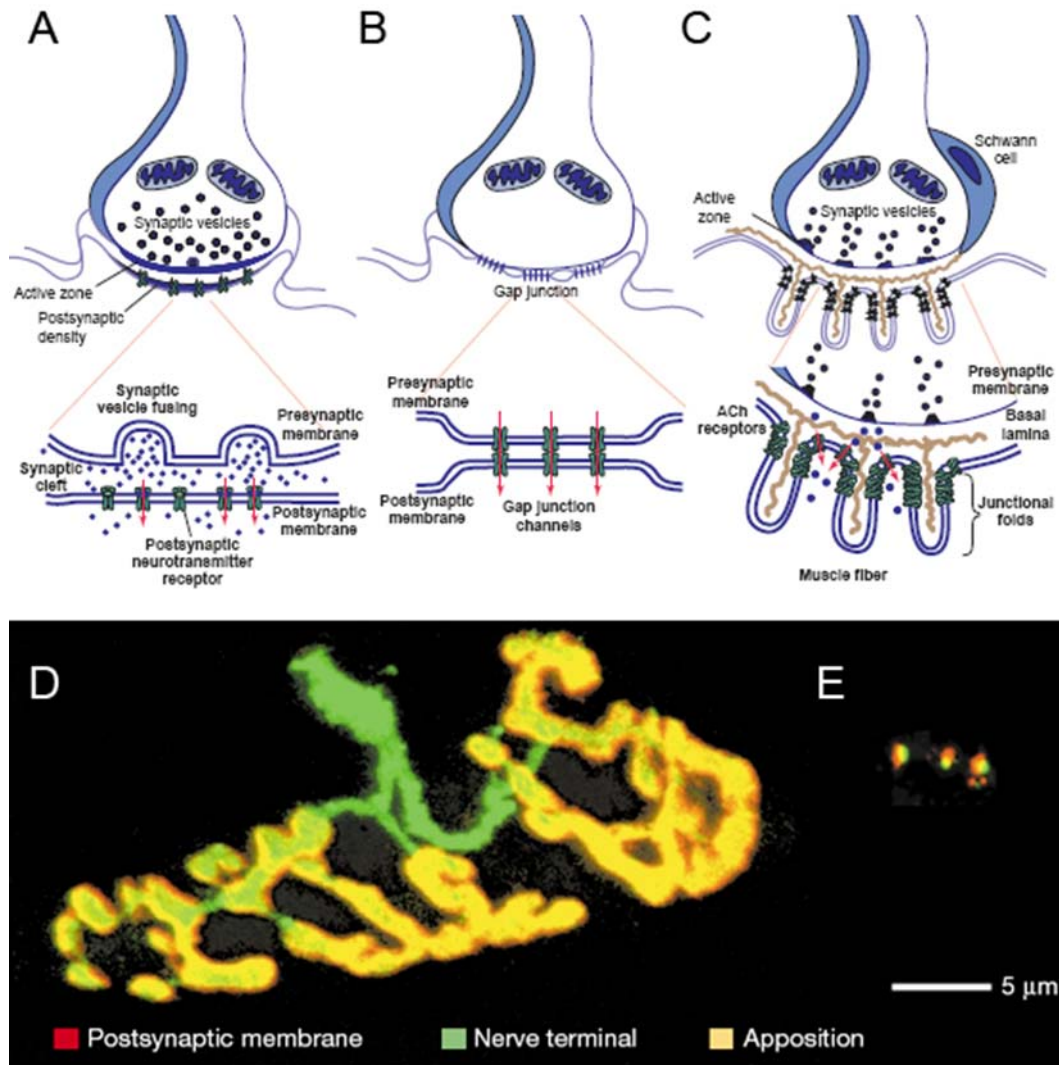


Figure 2-2 Comparison of different types of synapses

A: Chemical synapse in the CNS; B: Electrical synapse; C: NMJ; (Cohen-Cory, 2002)

D and E: Comparison of the size of a NMJ (D) of an adult mouse and a synapse of a cultured hippocampal neuron (E) of the mouse (Sanes and Lichtman, 2001).

One of the best studied synapse is the synaptic structure studied by Otto Loewi and Henry Dale, the NMJ, mostly due to its good accessibility and its sheer size (Sanes and Lichtman, 2001). However, most synapses in the CNS of mammals are much smaller (Figure 2-2), less easy to access, and thus harder to study. Nevertheless, certain common characteristics shared by all CNS synapses can be distilled: At synaptic sites the pre- and the postsynaptic plasma membranes run strictly parallel and build a synaptic cleft (Figure 2-2). This synaptic cleft is not an empty space but it contains even denser concentrations of material than ordinary

extracellular space. The presynaptic site contains synaptic vesicles (Figure 2-1) and at the pre- and postsynaptic sites, structural specializations can be observed (Vaughn, 1989). These are descriptions based on the structure of synapses as visualized by EM studies. These were the bases for subsequent research investigating synapse function, formation and maturation.

At the NMJ several principles triggering the induction, differentiation and maturation of synapses have been discovered and studied in detail. In this system, one molecule, namely z^+ -agrin, which is released from the nerve endings, induces the process of synapse formation and the clustering of postsynaptic receptors (Sanes and Lichtman, 2001). Synapses in the mammalian CNS are more diverse. Up to now, no protein inducing synapse formation in all different types of CNS synapses is discovered. Rather, various proteins are shown to induce synapse formation or at least play an important role in synapse formation (Scheiffele, 2003). Molecules spanning the synaptic cleft and visualized by EM as electron dense structures (Figure 2-1) are important players initiating contact- and synapse formation (Scheiffele, 2003). These so called synaptic adhesion molecules, like integrins (Chavis and Westbrook, 2001), neuroligins and neuexins (Scheiffele et al., 2000), cadherins (Togashi et al., 2002) and SynCAMs (Biederer et al., 2002) also influence the maturation of synapses (Scheiffele, 2003). It has been shown for example that the expression of a synaptic adhesion molecule, SynCAM, expressed in non neuronal cells is sufficient to induce synapse formation with co-cultured hippocampal neurons (Biederer et al., 2002).

The different trans-synaptic signaling pathways seem to cooperate and therefore enable for flexibility but also ensure the robustness needed for creating a functional nervous system (Scheiffele, 2003). After contact formation, responses in the presynaptic and in the postsynaptic compartment differ, as required by the different specializations of those two compartments. Eventually, if the pre- and the postsynaptic cell match, a synapse is formed, leading to the accumulation of a functioning release

machinery and transmitter filled vesicles on the presynaptic side, and matching receptors, scaffolding proteins, etc. on the postsynaptic side. In that way pre- and postsynaptic specializations form a superstructure spanning two cells and link their interiors (Hall and Sanes, 1993), not only in NMJs but also in synapses of the CNS. This newly formed synapse is then to mature and compete with other connections to establish itself in the network (Goodman and Shatz, 1993; Katz and Shatz, 1996).

The competition between synaptic connections is most obvious at the NMJ. Here it has been shown, that individual muscle fibers, which are initially innervated by many axons, lose all but one of their connections during development (Figure 2-3). This refinement of the wiring diagram, which leads to a mature system with each muscle fiber being innervated by exactly one axon, is shown to be activity dependent (Lichtman and Colman, 2000).

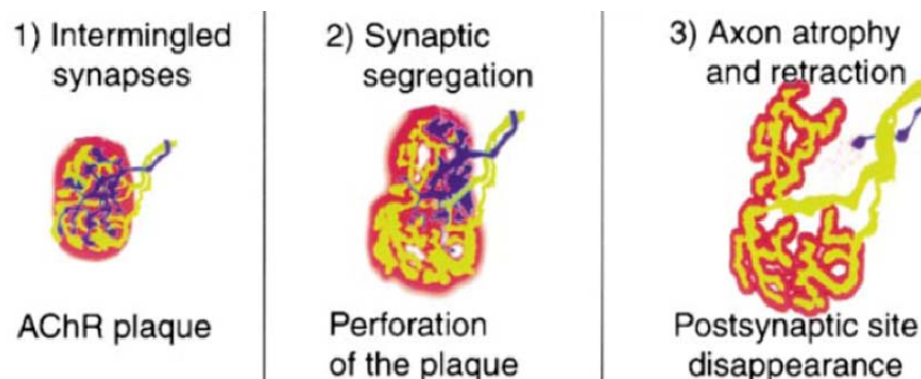


Figure 2-3 Synapse elimination at the NMJ

(Lichtman and Colman, 2000)

Synapse refinement has been observed by now in most parts of the CNS and in many parts it has also been shown that this refinement is activity dependent. One of the most famous and popular examples for activity dependent refinement may be long term potentiation (LTP) discovered by Bliss and Lomo in the hippocampus (Bliss and Lomo, 1973).

2.2 The hippocampus

The hippocampus, a brain structure common to all mammals, is located in both hemispheres in the medio-temporal lobe next to the fornix and the entorhinal cortex. It has a curved shape which according to the anatomist Arantius resembles the shape of a sea horse, thus he called this structure hippocampus, derived from the Greek word for sea horse (Amaral and Lavenex, 2007). The hippocampus was also compared to various other structures for example a banana or ram's horn, inspiring the name for the different regions *Cornu Ammonis* (CA) 1-3. The hippocampus belongs to the limbic system and is a part of the archicortex, what is reflected in its three layered design. One of those layers is the *stratum pyramidale* containing almost exclusively pyramidal neurons.

Traditionally the hippocampus was described to be organized in three units and information was thought to be passed only from one unit to the next. Today it is known that the wiring diagram is more complex and that the single regions are highly interconnected (Amaral, 1993). The main flow of information goes from the entorhinal cortex to the dentate gyrus via the perforant path. From here information is transferred via the mossy fiber path to CA3 pyramidal neurons (Figure 2-4).

The CA3 region of adult Wistar rats consist of around 10,000 CA3 pyramidal cells most of which (approximately 95%) are directly connected via the Schaffer collateral path to CA1 pyramidal neurons (Andersen et al., 1994). Even though most of the CA3 pyramidal neurons make contact to CA1 pyramidal neurons, on average every CA3 pyramidal neuron makes only a single synapse onto an individual CA1 pyramidal neuron (Bolshakov and Siegelbaum, 1995; Stevens and Wang, 1995).

The hippocampus is a well studied brain structure shown to be involved in learning and memory formation but also important in spatial navigation not only in rodents but in basically all mammals including human beings (Gilbert and Brushfield, 2009; Knierim, 2009; Maguire et al., 2006a; Maguire et al., 2006b; Jacobs et al., 1990). Serving such complex tasks it shows a high degree of plasticity making it an interesting model system for

research in neurobiology. Furthermore, the laminar organization permits to prepare transversal slices of the hippocampus which in large parts retain their three dimensional structure and wiring diagram. Those slices can also be kept alive and active in culture for several weeks (Stoppini et al., 1991; Gahwiler, 1981). Slice cultures are not only in their structure and the expression profiles of proteins comparable to the *in vivo* situation they also resemble the development of the hippocampus *in vivo* (Gahwiler et al., 1997). The good accessibility and a relatively easy handling of slice cultures compared to *in vivo* preparations make them an ideal model system particularly for optical approaches at high spatial resolution and electrophysiological investigations.

Not surprisingly, many important findings concerning memory formation and the accompanying functional and structural changes were first shown in hippocampal model systems. The already mentioned LTP which is shown to occur not only *in vitro* but also *in vivo* (Bliss and Lomo, 1973) is just one of them. LTP is a long lasting increase in the efficacy of transmission between two neurons following repeated high frequency stimulation. It can be seen as a direct cellular correlate of Hebb's postulate, which, published already in 1949, predicts that cells that fire together wire together (Hebb, 1949). Functionally, LTP is well described and it has been shown that LTP entails also morphological changes, like spine growth (Engert and Bonhoeffer, 1999). The cellular mechanisms leading to these changes and to spine growth are various, but most forms of LTP seem to depend on a rise in the intracellular Ca^{2+} -concentration acting as a second messenger either activating or deactivating various signal cascades. Nevertheless, also its functional counterpart, long term depression (LTD), discovered several years later (Dudek and Bear, 1992) as well as various other cellular processes are triggered by changes of the intracellular Ca^{2+} -concentration. Often even contrary effects, like LTP and LTD, are both triggered somewhat counter-intuitively by an increase in the intracellular Ca^{2+} -concentration (Zucker, 1999a; Yang et al., 1999a).

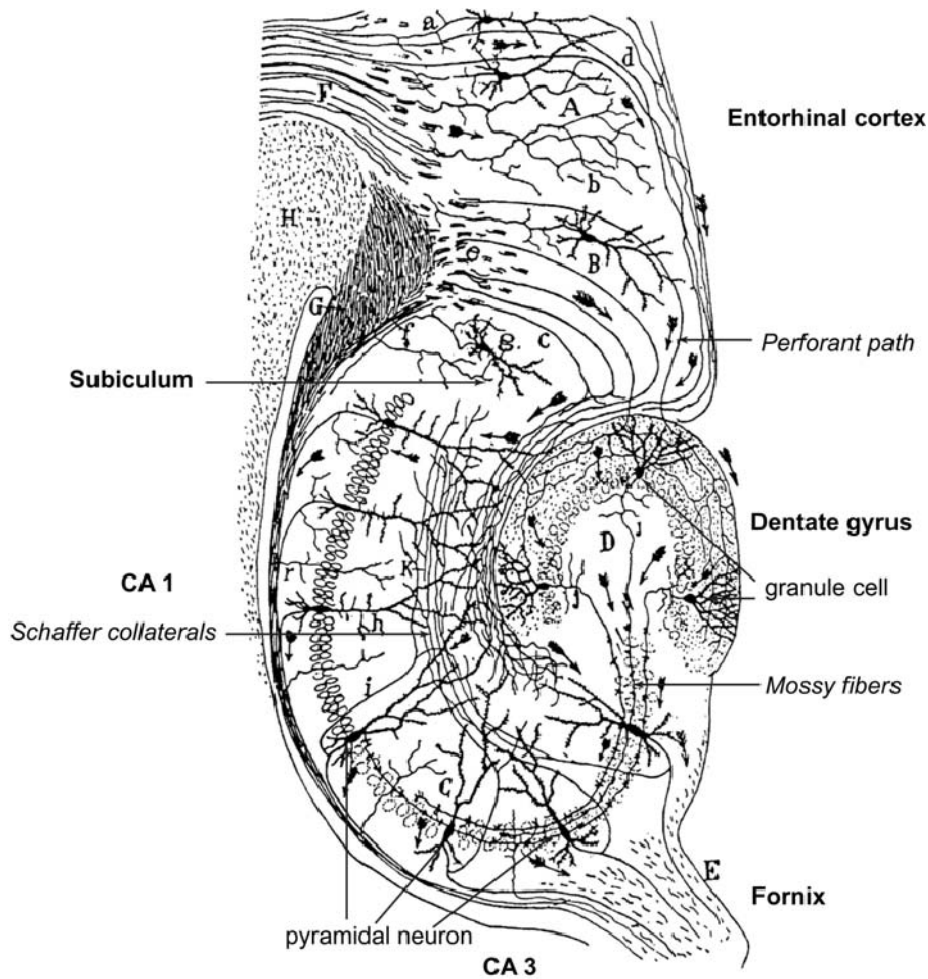


Figure 2-4 Neuronal organization of a hippocampal slice

Transversal slice of a rodent hippocampus showing the neuronal organization and main axonal pathways. CA: Cornu Ammonis. Drawing modified from Ramón y Cajal (Ramón y Cajal, 1911)

2.3 Calcium and Calcium imaging

Ca^{2+} -ions are known to play a pivotal role in regulating various processes not only in neurons but also in many other cell types. As mentioned above, calcium signaling regulates often contrary processes. A well known example is LTP and LTD, both being induced by a rise in the intracellular Ca^{2+} -concentration (Yang et al., 1999b; Zucker, 1999b). An interesting question is why calcium signals are of such outstanding importance in regulating cellular and neuronal processes. At least in part this is due to the large difference in the intracellular and the extracellular

Ca²⁺-concentration. The internal Ca²⁺-concentration of hippocampal pyramidal neurons is around 100 nM while the extracellular concentration is around 2 mM (Nakajima et al., 1993; Maravall et al., 2000a). This difference in concentration of several orders of magnitude and the resulting steep electrochemical gradient cause a heavy driving force for Ca²⁺-ions. Thus, even short openings of single channels in the plasma membrane entail an influx of enough Ca²⁺-ions to cause a large relative change in the local Ca²⁺-concentration (Denk et al., 1996). Synaptic stimulation was estimated to be able to increase the local Ca²⁺-concentration in spines about 100 fold (Yuste et al., 1999) repeated stimulation even up to 500 fold (Petrozzino et al., 1995).

Calcium sensitive enzymes and channels that change their activity upon calcium binding sense the spatially and temporally restricted alterations in the Ca²⁺-concentration. Subsequently, they translate those alterations into a variety of cellular responses covering many aspects from regulating changes in synaptic efficacy (Christie et al., 1996; Harney et al., 2006; Letzkus et al., 2006; Yang et al., 1999b) to regulating and guiding outgrowth and motility of neuronal protrusions (Konur and Ghosh, 2005; Lohmann et al., 2005; Henley and Poo, 2004; Lankford and Letourneau, 1989; Tang et al., 2003; Gomez et al., 1995) or regulating gene transcription (Aizawa et al., 2004; Carrasco et al., 2004; Cohen and Greenberg, 2008). Ca²⁺-transients are often strictly restricted, spatially and temporally, by bound calcium buffers hindering diffusion and fast acting calcium pumps which transport Ca²⁺-ions actively against the electrochemical gradient out of the cell or into intracellular stores like the endoplasmic reticulum.

The combination of high relative changes in the intracellular Ca²⁺-concentration and the variety of cellular processes influenced by these changes are one reason why calcium imaging became a popular tool in research. Another prerequisite was the availability of good dyes reliably reporting changes in the Ca²⁺-concentration under physiological conditions. Today a variety of calcium dyes fulfilling this criterion exists,

not only synthetic ones but also genetically encoded ones (Stosiek et al., 2003; Thomas et al., 2000; Hendel et al., 2008a; Hasan et al., 2004; Heim and Griesbeck, 2004; Mank et al., 2008).

Many synthetic calcium dyes are derivatives of fluorescein, which was discovered 1871 by Adolf von Bayer. Fluorescein is mainly produced by chemical synthesis, but it is also secreted by bacteria like *pseudomonas aeruginosa* (King et al., 1954). Today many derivatives of fluorescein exist, which are often especially tailored for the needs of a specific application. Biological research, for example, often calls for high photostability. One of these photostable derivatives of fluorescein is Oregon Green BAPTA 1 (OGB-1), which was used throughout this study (Figure 2-5).

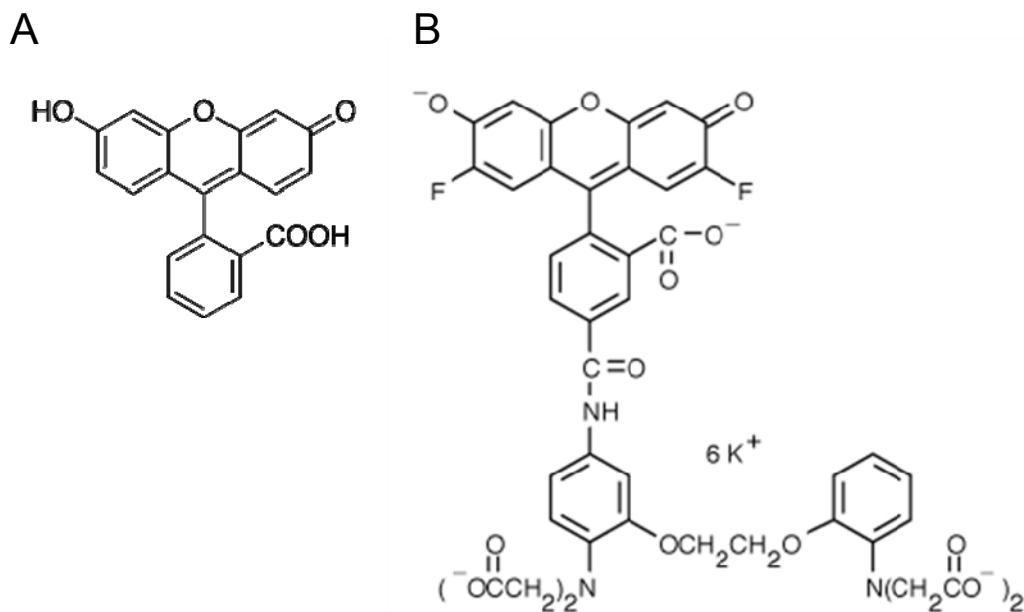


Figure 2-5 Chemical structure of fluorescent dyes

A: Chemical structure of fluorescein (Picture obtained from www.invitrogen.com)

B: Chemical structure of OGB-1 (Picture obtained from www.invitrogen.com)

In contrast to synthetic calcium dyes, genetically encoded calcium dyes are protein structures. Most commonly, they are composed of a calcium

sensing protein, which changes its conformational state upon calcium binding and two differently colored fluorescent proteins. The conformational change induced by calcium binding decreases the distance between the two fluorescent proteins which in turn influences, i.e. increases, the fluorescence resonance energy transfer (FRET) efficacy (Figure 2-6).

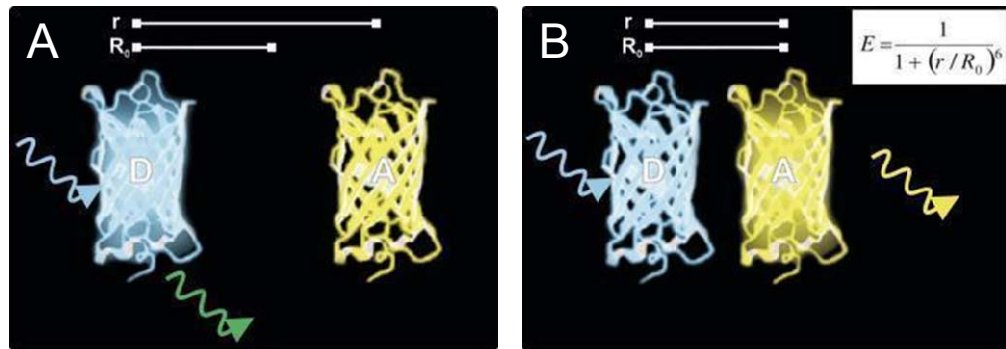


Figure 2-6 FRET – effect

A: At large distances no FRET occurs. Thus only donor wavelength is emitted

B: At closer distances energy is transferred from the donor dye (D) to the acceptor dye (A). Thus, emission at the wavelength of the donor dye decreases, while emission at the wavelength of the acceptor dye increases. (Picture obtained from www.leica-microsystems.com)

The choice of the calcium sensing protein is a crucial factor influencing the effectiveness of genetically encoded calcium indicators (Heim and Griesbeck, 2004). Genetically encoded calcium dyes are being permanently improved and by now a huge variety exists, some of which even allow chronic *in vivo* imaging of calcium dynamics (Mank et al., 2008).

However, using a genetically encoded calcium dye requires expression of the calcium dye in the imaged tissue. Thus it has to be genetically modified, for example by viral transfection (DiCiommo and Bremner, 1998; Kuhlman and Huang, 2008; Narayan and Greif, 2004) or by *in utero* electroporation (Holtmaat et al., 2009; Mank et al., 2008). Alternatively transgenic animals expressing the dye of choice can be used (Hasan et al., 2004; Heim et al., 2007).

To image calcium dynamics using a synthetic dye, the specimen does not need to be genetically modified. Nevertheless, the calcium dye needs to be brought into the cell of interest. Also for synthetic calcium dyes various loading techniques exist, like single cell electroporation (Lang et al., 2006; Nevian and Helmchen, 2007), ballistic techniques using a gene gun (Kettunen et al., 2002; Kettunen et al., 2001) or bolus loading (Murayama et al., 2007; Kreitzer et al., 2000; Stosiek et al., 2003; Garaschuk et al., 2006; Oertner, 2002). These techniques can be used to acutely label either single neurons or a whole population of neurons with the calcium dye. In general the loading techniques for synthetic calcium dyes are easier to handle, especially as there is almost no time delay from loading the cell with the dye to the beginning of the experiment as there is no need to wait for the expression of the dye. Another important advantage of synthetic calcium dyes is their fast kinetics and their high signal to noise ratio. High affinity synthetic calcium dyes like OGB-1, reliably report single action potentials, which is still not possible with genetically encoded calcium dyes (Hendel et al., 2008b).

An important fact to be kept in mind when performing calcium imaging is the interference of the calcium dye with the calcium transients measured. Since calcium dyes act as calcium buffers, they interfere with the spatio-temporal characteristics of the calcium signal (Cornelisse et al., 2007; Regehr and Tank, 1992). Furthermore, even though the fluorescence intensity changes with changing Ca^{2+} -concentration, quantitative measurements of calcium dynamics are challenging, especially when using non ratiometric dyes (Albantakis and Lohmann, 2009; Lohr, 2003; Maravall et al., 2000b).

In neuroscience calcium imaging is mostly used not to study the direct effects of calcium signals upon cellular processes, or to measure the calcium concentration in cells or small cellular compartments, but rather as a reporter for neuronal activity. Ca^{2+} -transients faithfully report not only action potential firing but even single excitatory synaptic events lead to a well detectable postsynaptic Ca^{2+} -transient (Koester and Sakmann, 1998).

Even though voltage sensitive dyes are available, in use and constantly improved (Djurisic et al., 2004; Glover et al., 2008; Palmer and Stuart, 2009; Stuart and Palmer, 2006), in most applications calcium imaging techniques are still advantageous due to their high dynamic range and signal to noise ratio (Grewe and Helmchen, 2009; Cossart et al., 2005). The superior signal to noise ratio of calcium dyes has physical reasons. It is known, for example, that the achievable signal to noise ratio is increasing with the number of photons emitted. Since calcium dyes are distributed throughout the intracellular space, the number of dye molecules is much higher compared to voltage sensitive dyes which need to be within or at least close to the cell membrane to be able to sense the membrane potential. Thus, the achievable number of emitted photons is higher leading to a better signal to noise ratio. The different distribution of calcium sensitive dyes and voltage sensitive dyes in cell leads also to a different distribution in brightness throughout a cell. Voltage sensitive dyes stain membranes, thus the main part of the fluorescence is emitted from neuronal processes, while, when using calcium sensitive dyes, the main part of the fluorescence is emitted by the soma and proximal parts of the dendrites. Even if voltage sensitive dyes are a direct way to measure changes in the membrane potential and in an optimal case one could follow the spread of a single sub threshold synaptic potential from the synapse to the soma, for the purpose of visualizing synaptic activation in developing neurons, calcium imaging was the more promising approach.

2.4 Development of specificity

During the development of the brain a network of billions of individual neurons is formed. To enable this network to function, each neuron needs to connect to the appropriate partners. While in lower animals like *C. elegans* the connection scheme of the 302 neurons building the nervous system is mostly genetically determined (Seifert et al., 2006), the mammalian brain with its billions of neurons requires a combination of various mechanisms to set up a functioning network. Furthermore, the mammalian brain is not only an integrating system triggering a fixed

response behavior upon a given stimulus, but it is able to change and to adapt to changing requirements. One of the main challenges for the mammalian brain is to balance stability and plasticity to guarantee for function throughout lifetime but still allow learning and formation of memories. Plasticity is seen as the basis for learning and memory but additionally it plays an important role during development. Unlike in many lower animals neither the connection schemes nor the numbers of neurons are strictly genetically predetermined but rather also strongly shaped by activity (Cline, 2003). Nevertheless at least the early development of the mammalian brain seems to be predominately controlled by complex genetic programs. These programs range from guiding migrating cells and specifying different cell types in various areas of the brain to directing protrusions to their target region (Goodman and Shatz, 1993; Tessier-Lavigne and Goodman, 1996). All of these genetically controlled steps throughout development are achieved by differential expression and release of molecules triggering different responses in different cells. These steps are essential to build up a rough network which subsequently is to be shaped and adjusted by complex interactions of the genetic prerequisites of cells and their activity patterns (Cline, 2001). However, it should not be assumed that there is a strict order, like first setting up a rough network by genetic means and subsequently tuning and adjusting this network by activity. Rather, it is an interplay with different mechanisms mutually influencing each other (Cline, 2003). The shaping impact of activity enables the network to fine tune and adjust to intrinsic properties of given cells and even compensate for irregularities which inevitable occur in a system made out of billions of single elements. Furthermore, the influence of activity on the wiring diagram provides a link allowing the external environment to exert influence on the development of the network, thus enabling for learning and for the formation of memories. A general rule describing the impact of activity on a nervous system was proposed already end of the 19th century. By then William James wrote in Principles of Psychology that “*if processes 1, 2, 3, 4 have once been aroused together or in immediate*

succession, any subsequent arousal of any one of them (whether from without or within) will tend to arouse the others in the original order" (James Williams, 1890). About 60 years later Donald Hebb postulated a similar idea predicting that if a cell persistently takes part in firing another cell, some changes take place increasing the efficacy of the connection between those two cells (Hebb, 1949). This idea became one of the most studied principles in neuroscience and is by now supported by a large number of investigations. Hebb's law provides a rule explaining how activity of a connected pair influences the fate of its interconnections, namely correlated activity among neurons strengthens their interconnections. Computational models suggest that a map, set up using a combination of molecular cues and Hebbian mechanisms can be more precise, than one set up with molecular cues alone (Yates et al., 2004).

2.5 Spontaneous activity

The activity dependent refinement of the synaptic wiring diagram, mentioned above, has been shown to occur in many mammalian systems already before the onset of sensation. One of the most prominent examples is found in the visual system. Here, the retinal ganglion cells projecting to the optic tectum form a topographic map. This so called retinotopic map is initially generated by molecular guidance cues, but the initial map needs to be refined. This refinement of the retinotopic map has been shown to be activity dependent (Chandrasekaran et al., 2005). Similarly, the segregation by eye of the thalamic input in cortical layer 4, called the ocular dominance columns, is achieved in an activity dependent manner (Katz and Shatz, 1996). Nevertheless, somewhat counter-intuitively a major part of the sharpening of the retinotopic map occurs before the circuit becomes light responsive. But: Not being light responsive does not mean not being active. It has been shown, that retinal ganglion cells are spontaneously active before they become light sensitive and this spontaneous activity spreads wave like across the retina such that neighboring retinal ganglion cells are synchronously active during a short time interval (Meister et al., 1991). That means that a Hebb-like

mechanism can refine the initially crude retinotopic maps before the onset of sensation.

Spontaneous synchronized activity does not only occur in the developing visual system, rather it is a hallmark of developing networks occurring in a wide range of structures and species (Ben Ari, 2001).

In the hippocampus the spontaneous activity occurring during development is best known as giant depolarization potentials (GDPs), but it is also known as early network oscillations, or population bursts (Ben Ari, 2001). GDPs occur in many mammalian species not only *in vitro* but also *in vivo* (Leinekugel et al., 2002; Leinekugel, 2003). GDPs represent large network driven depolarizations occurring between P0 and P10. This period coincides with a period during development in which gamma-aminobutyric acid (GABA), an inhibitory neurotransmitter in the mature hippocampus, is still having a depolarizing effect (Figure 2-7). It has been suggested that the depolarization by GABA plays a central role in the generation of GDPs. Similarly to spontaneous activity, the depolarizing

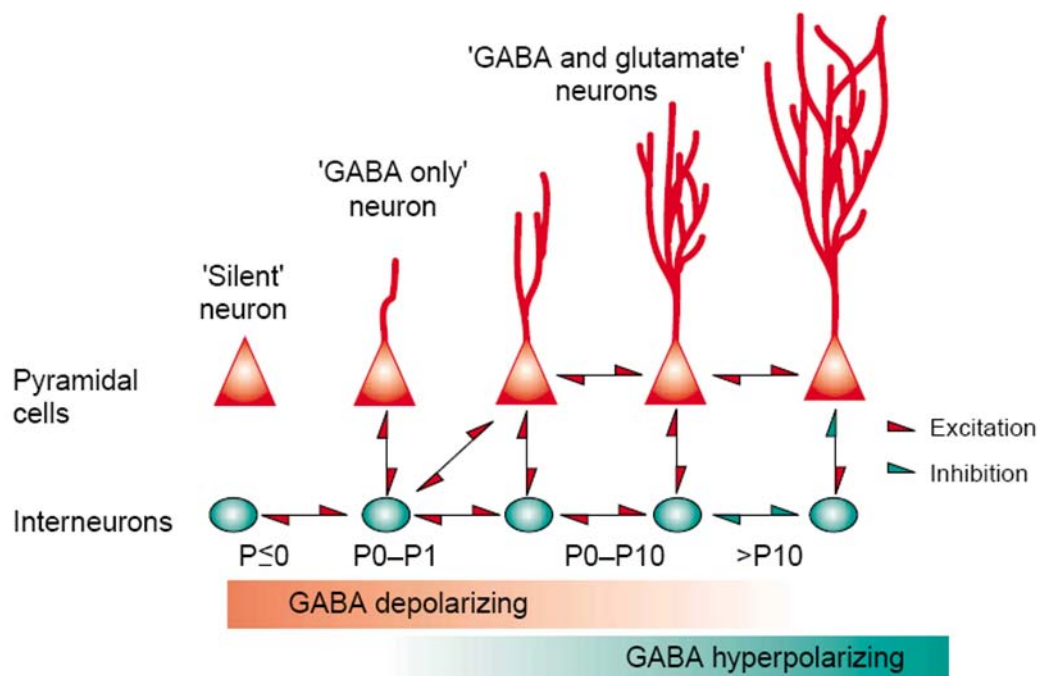


Figure 2-7 Development of the hippocampal circuit in the rat

During the time when GABA is depolarizing, the network generates GDPs. Pyramidal neurons start to receive glutamatergic input around birth (Ben Ari, 2001).

effect of GABA was shown in every species and structure studied (Cherubini et al., 1991a; Leinekugel et al., 1999; Cherubini et al., 1991b).

The depolarizing effect of GABA results from an increased chloride concentration in developing neurons due to different expression patterns of chloride cotransporter systems compared to the mature system (Delpire, 2000; Stein and Nicoll, 2003). The increased chloride concentration leads to a depolarization upon opening of chloride channels by GABA. When the intracellular chloride concentration is reduced, GABA turns inhibitory and the GDPs cease. The function of GDPs seems to be similar to the function of retinal waves in the visual system, as there are indications that they act as coincident detector signals between pre- and postsynaptic activity. This coincidence detection is the result of the facilitation of N-methyl-D-aspartic acid (NMDA) receptor activation by the depolarizing effect of GABA (Kasyanov et al., 2004). Thus, GDPs seem to facilitate a Hebbian mechanism strengthening synapses that connect coactive cells. However, so far little is known about how spontaneous activity shapes the wiring diagram on a subcellular scale. Does activity influence the fate of synapses solely upon the correlation of the connected neurons or also on the level of single synapses? Is there a mechanism strengthening pairs of synapses being often simultaneously active? And if so: Is the location and the relative location of these synapses along the dendritic tree crucial for their fate?

2.6 Dendritic computation

The vast majority of the input picked up by an individual neuron is received by its dendritic tree. Dendritic trees in vertebrates display an extraordinary variety of shapes and sizes as shown in Figure 2-8. Most models treat neurons as points not considering the shape of the dendritic tree nor the subcellular location of synaptic input, even though it is likely that both are of particular importance: *“Generating and maintaining these elaborate structures [the dendrites], which occupy a large proportion of our brains, is energetically costly, implying that their presence is worth this cost”* (Hausser et al., 2000).

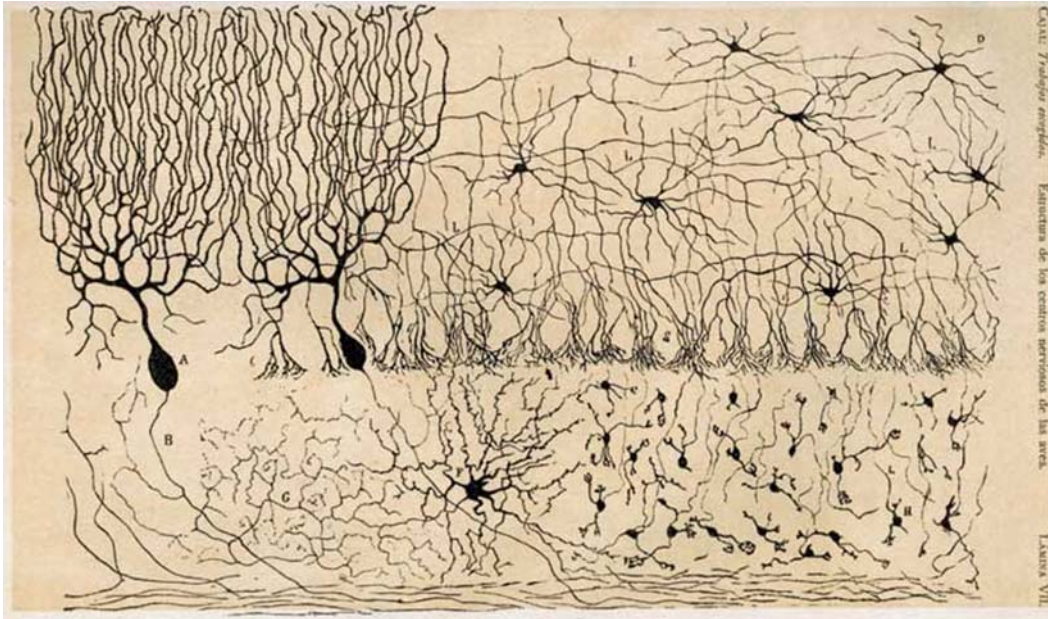


Figure 2-8 Dendritic morphologies

Drawing of different neuronal cell types and their dendritic arborizations; chick cerebellum (Ramón y Cajal, 1888)

In addition, specific neuronal types display a high degree of similarity in dendritic structure and function across different species suggesting an adaptation of the properties of dendrites to the functional requirements of those cells (Hausser et al., 2000). The number of individual synapses impinging onto individual neurons varies widely between different cell types and can be extremely high. For example a single rodent Purkinje cell may receive as many as 150,000 synapses from parallel fibers (Linden, 1994). Furthermore, it has been shown that the position of a synapse along the dendritic tree influences its impact on the cell. Already more than forty years ago scientists realized that electrical signals are attenuated along the dendrite (Rall et al., 1967). This attenuation lowers the impact of distal synapses compared to synapses located more proximal, indicating an interrelation of the morphology of the dendritic tree and the integrative properties of the neuron. But, it has also been shown that dendrites have active properties (Fujita, 1968; Williams and Stuart, 2003) being able to mitigate the impact of attenuation on synaptic inputs, for example by increasing the synaptic conductance with increasing distance from the soma (Stricker et al., 1996; Magee and Cook, 2000).

Another feature of dendrites affecting the time course and amplitude of synaptic potentials is the presence and distribution of voltage gated ion channels. These channels can influence the impact of synaptic currents. Depending on their distribution, the morphology of the dendritic arbor and the time course and amplitude of synaptic input, they may influence synaptic inputs in different areas along the dendritic tree differently (Hausser et al., 2000) and they may even lead to the generation of dendritic spikes. Thus, the dendritic non-linearities provided by the voltage gated ion channels, are not exclusively compensating for the attenuation of the electrical signals, but they are capable of boosting the impact of co-active synapses (Schiller et al., 1997; Golding and Spruston, 1998).

Furthermore, also inhibition is influencing the conductivity of dendritic compartments and by that the spread of backpropagation and forward-propagation (Tsubokawa and Ross, 1996; Pare et al., 1998). The complex interactions of voltage gated ion channels, excitatory and inhibitory synaptic currents and the conductance of the dendritic tree (Figure 2-9) facilitate even flexibility in the compartmentalization of a cell. That means, the compartmentalization depends not only on the developmental state of a cell and the distribution of its ion channels, but also on its state and on the behavioral state of the surrounding network (Hausser et al., 2000). Therefore, the degree of compartmentalization varies not only between different neuronal types but, moreover, it can be dynamically regulated by the state of the network (Hausser et al., 2000).

Despite these variations in the dendritic tree of individual neurons and despite the influence of the dendritic distance on synaptic currents, most models still treat neurons as points and neither the shape of the dendritic tree nor the location of individual synapses along the dendritic tree are taken into consideration.

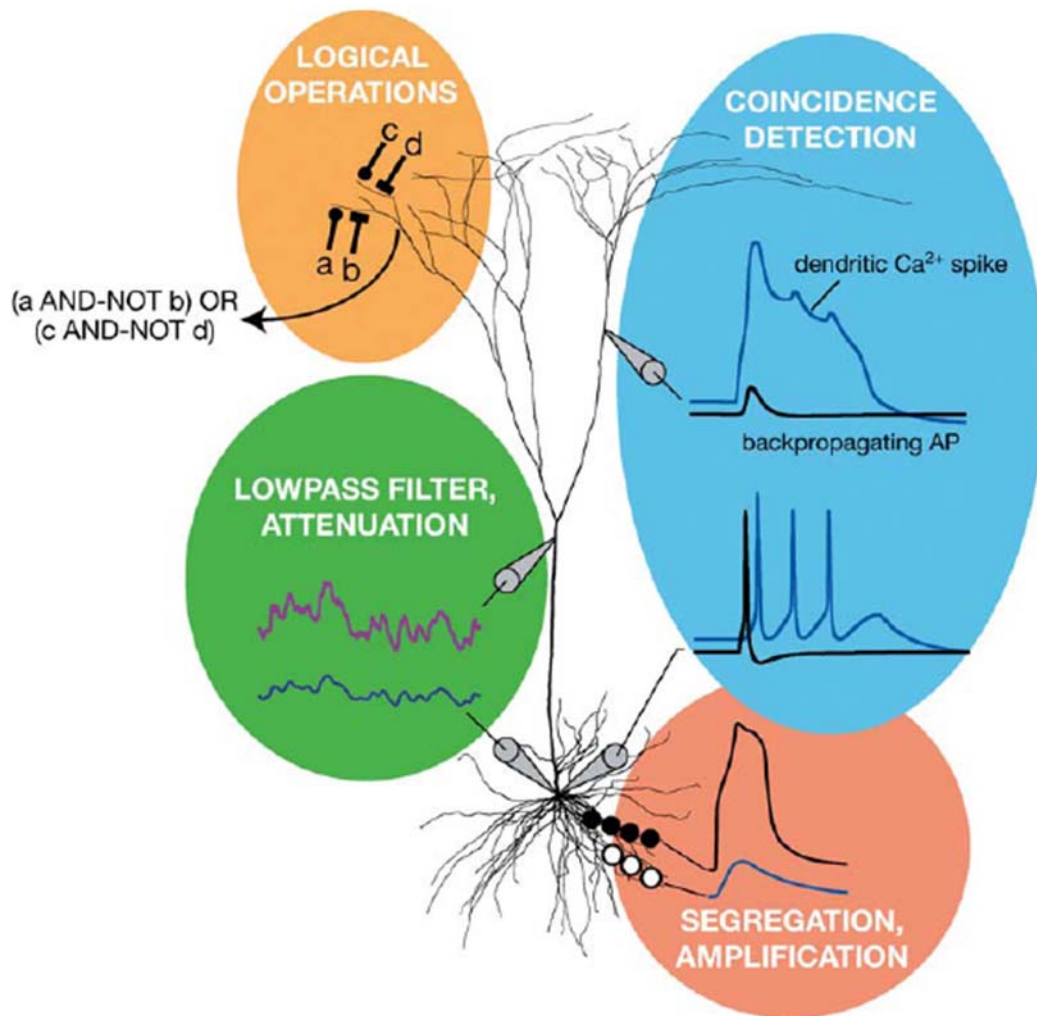


Figure 2-9 Scheme depicting the complex interactions of the integrative properties of dendrites

(London and Hausser, 2005)

However, recently the dendritic nonlinearities and their implications gained increasing attention, especially as it has been shown that they are able to boost the computational power of an individual neuron (Govindarajan et al., 2006; Mel and Schiller, 2004). But mere nonlinearities cannot increase the computational power of a neuron. Since dendritic spikes are triggered by large local depolarizations, they are usually evoked by simultaneous activation of many synapses in close proximity. That means, the similarity of the activation patterns of neighboring synapses and by that the similarity of information transmitted at neighboring synapses, is influencing the impact of the synaptic activations. To evoke dendritic spikes neighboring synapses need to show similar activation patterns. By now, plasticity mechanisms have been discovered favoring potentiation of

coactive synapses in close proximity (Losonczy et al., 2008). Furthermore, a protocol that under control conditions fails to induce LTP is sufficient to trigger LTP in a spine if the neighboring spine was potentiated shortly beforehand (Harvey and Svoboda, 2007).

These findings hint towards a subcellular precision of the synaptic wiring diagram, which should manifest itself in certain activity patterns and thus might be visible by mapping the spontaneous, i.e. not stimulated activity of many synapses onto an individual neuron in space and time. To date, spontaneous synaptic activity has not been visualized with single synapse resolution, thus the spatio-temporal patterns of unstimulated synaptic activity remained largely unknown.

2.7 Objectives of this study

Activity dependent remodeling of the synaptic wiring diagram is known to be an important principle influencing the development of the brain. Despite recent findings demonstrating the importance of the dendritic location on the impact of synapses, little is known about the activity patterns of individual synapses on a subcellular scale. Since spontaneously occurring synaptic activation is a major player in shaping connectivity during development, I set out to describe the subcellular activation patterns evoked by this spontaneous activity in slice cultures of the developing hippocampus. By mapping and describing the spatio-temporal patterns evoked by spontaneous activity I addressed the following questions: How is the input received by an individual neuron distributed across its dendritic arbor? Are there detectable patterns suggesting the existence of plasticity rules that guide synapse formation with subcellular specificity?

The aim of this thesis was to develop a technique to visualize synaptic transmission, if possible at single synapse resolution, and to investigate the patterns of spontaneous synaptic activity in these individual neurons. By combining calcium imaging at a relatively high rate using a cooled CCD-camera with electrophysiological recordings, I found a criterion to discern synaptic from non-synaptic local Ca^{2+} -transients. Subsequently, I focused my attention on the synaptic transients and further investigation of these transients revealed, that they can be used to visualize glutamatergic synaptic transmission. That enabled me to map the distribution of glutamatergic input impinging onto individual pyramidal cells in the developing hippocampus and to investigate the spatio-temporal patterns of synaptic activation evoked by spontaneous activity.

3 MATERIALS AND METHODS

3.1 Materials

All the chemicals and media used in this study are listed in the following tables. If not stated otherwise chemicals were dissolved either in distilled water or dimethyl sulfoxide (DMSO).

3.1.1 Chemicals

Basal Medium Eagle (BME)		Invitrogen
Calcium chloride	CaCl ₂	Merck
D-glucose	C ₆ H ₁₂ O ₆	Merck
DMSO		Sigma
Glutamine	C ₅ H ₁₀ N ₂ O ₃	Invitrogen
Hank's buffered salt solution (HBSS)		
	+MgCl ₂ +CaCl ₂ 10x	Invitrogen

Consisting of:

	mmol
CaCl ₂	12.61
MgCl ₂	4.93
MgSO ₄	4.07
KCl	53.3
KH ₂ PO ₄	4.41
NaCl	1379.31
Na ₂ HPO ₄ x 7 H ₂ O	3.36
D-glucose	55.56

HEPES		Merck
Horse serum		Invitrogen
Kynurenic acid	C ₁₀ H ₇ N ₁ O ₃	Sigma
Magnesium-ATP	Mg-ATP	Sigma
Magnesiumchloride	MgCl ₂	Merck
Magnesiumsulfate	MgSO ₄	Sigma
Monopotassium phosphate	KH ₂ PO ₄	Sigma

Oregon-Green-BAPTA I (OGB-1)		Molecular Probes
Potassium chloride	KCl	Sigma
Potassium gluconate	C ₆ H ₁₁ KO ₇	Merck
Sodium phosphate dibasic	Na ₂ HPO ₄	Sigma
Sodium chloride	NaCl	Merck
Sodium bicarbonate	NaHCO ₃	Merck
Trolox		Sigma

3.1.2 Drugs

D-APV:	competitive NMDA-receptor-antagonist concentration: 50 µmol/l	Biotrend
NBQX:	competitive AMPA-receptor-antagonist concentration: 10 µmol/l	Biotrend
Picrotoxin:	GABA _A - receptor-antagonist concentration: 150 µmol/l	Sigma
TTX:	sodium channel blocker concentration: 0.5 µmol/l	Sigma

3.1.3 Media

Gey's Balanced Salt Solution (GBSS):

Consisting of:

	mmol/l	g/l
CaCl ₂ x 2 H ₂ O	1.50	0,22
KCl	4.96	0,37
KH ₂ PO ₄	0.22	0,03
MgCl ₂ x 6 H ₂ O	1.03	0,21
MgSO ₄ x 7 H ₂ O	0.28	0,07
NaCl	136.89	8,00
NaHCO ₃	2.70	0,227
Na ₂ HPO ₄	0.87	0,12
D-glucose	5.55	1

Preparation medium:

Consisting of:

	mmol/l	g/l
CaCl ₂ x 2 H ₂ O	1.50	0,22
KCl	4.96	0,37
KH ₂ PO ₄	0.22	0,03
MgCl ₂ x 6 H ₂ O	1.03	0,21
MgSO ₄ x 7 H ₂ O	0.28	0,07
NaCl	136.89	8,00
NaHCO ₃	2.70	0,227
Na ₂ HPO ₄	0.87	0,12
D-glucose	61.06	11
Kynurenic acid	1	0.19

pH 7.2; sterile filtered

Culture medium:

- 50% (v/v) BME,
- 25% (v/v) horse serum,
- 25% (v/v) HBSS,
- 1 mmol/l Glutamine,
- 10 g/l D-glucose,

sterile filtered

External solution:

Consisting of:

	mmol/l
CaCl ₂	3.26
MgCl ₂	0.49
MgSO ₄	0.41
KCl	5.33
KH ₂ PO ₄	0.44
NaHCO ₃	4.2
NaCl	137.93
Na ₂ HPO ₄ x 7 H ₂ O	0.336

Material and Methods

D-glucose	5.56
Trolox	0.1

Made by diluting HBSS 10x to 1x with water and additionally adding CaCl₂ 2 mmol, NaHCO₃ 4.17 mmol, Trolox 0.5 M.

Osmolarity adjusted to 320 mOsm.

Internal solution:

Consisting of:

	mmol/l
KCl	12
K-gluconate	130
HEPES	10
Mg-ATP	4
NaCl	8

pH adjusted to 7.2 using KOH.

Osmolarity adjusted to 290 mOsm.

3.1.4 Equipment

Amplifier	MultiClamp 700B	Axon Instruments, Foster City, USA
Digitizer	Digidata 1440A	Axon Instruments, Foster City, USA
Controlling software	P-CLAMP 10	Axon Instruments, Foster City, USA
Fluorescence unit	CoolLED	PrecisExcite, Andover, UK
Camera	Andor iXon+	Andor Technology, Belfast, Northern Ireland

Material and Methods

Controlling software	Andor Solis 4.4	Andor Technology, Belfast, Northern Ireland
Microscope	BX51WI	Olympus Corporation, Tokyo, Japan
Objective	LumPlanFI 40x/0.8 WI	Olympus Corporation, Tokyo, Japan
XY-shifting table	380 FM	Luigs & Neumann, Ratingen, Germany
Micromanipulators	LN-Mini 25	Luigs & Neumann, Ratingen, Germany
Controller unit	SM-5 9	Luigs & Neumann, Ratingen, Germany
Temperature Control	Badcontroller V	Luigs & Neumann, Ratingen, Germany
Puller	Model P-97	Shutter Instrument Co, Novato, USA
Pipettes	GB150TF-8P	Science Products, Hofheim, Germany
pH-meter	PB-11	Sartorius, Göttingen, Germany
Osmometer	Osmomat 030	Gonotec, Berlin, Germany
Balance	AB 204-S	Mettler Toledo, Greifensee, Switzerland
Sonicator	Emmi 5	EMAG AG, Mörfelden- Walldorf, Germany
Stimulus Isolator	A 360	WPI, Sarasota, USA
Incubator	MCO 18 AIC	SANYO Electric Co.,

Material and Methods

		Ltd., Osaka, Japan
Tissue chopper	Mc ILWAIN,	The Mickle Laboratory Engineering Co. LTD. Gomshall, UK
Piezo stepper	P-721.LLQ	Physik Instrumente (PI) GmbH & Co. KG, Karlsruhe, Germany
Piezo controller	E-625.LR	Physik Instrumente (PI) GmbH & Co. KG, Karlsruhe, Germany
Recording chambers	Type I	Workshop of the Max Planck Institute, Martinsried, Germany
Recording chambers	slice mini chamber I	Luigs & Neumann, Ratingen, Germany
Membrane Inserts	0.4 μ m culture plate inserts	Millipore Corporation, Billerica, USA

3.1.5 Programs

Matlab (R2008a)	Version 7.6.0.324 The Mathworks Inc., USA	Toolboxes: Image Processing Signal Processing Statistics
ImageJ	ImageJ 1.40g National Institute of Health, USA	
P-clamp 10	Clampex Version 10.2.012 Multiclamp 700B Commander version	

	2.1.0.13 Molecular Devices	
Andor Solis	Andor Technology, Belfast, Northern Ireland	
Piezo Control	PZT Control Release 3.0.6.1	

3.2 Methods

3.2.1 Cultures

Hippocampal organotypic cultures were prepared from newborn Wistar rats (postnatal days (P) 0–2) according to the method of Stoppini et al. (1991). The animals were decapitated quickly and brains were placed in ice-cold Gey's balanced salt solution (Life Technologies) under sterile conditions. After dissecting the hippocampi (Figure 3-1) transversal slices (400 μ m) were cut using a tissue chopper (McIlwain), placed again in preparation medium and separated. After allowing them to regenerate in

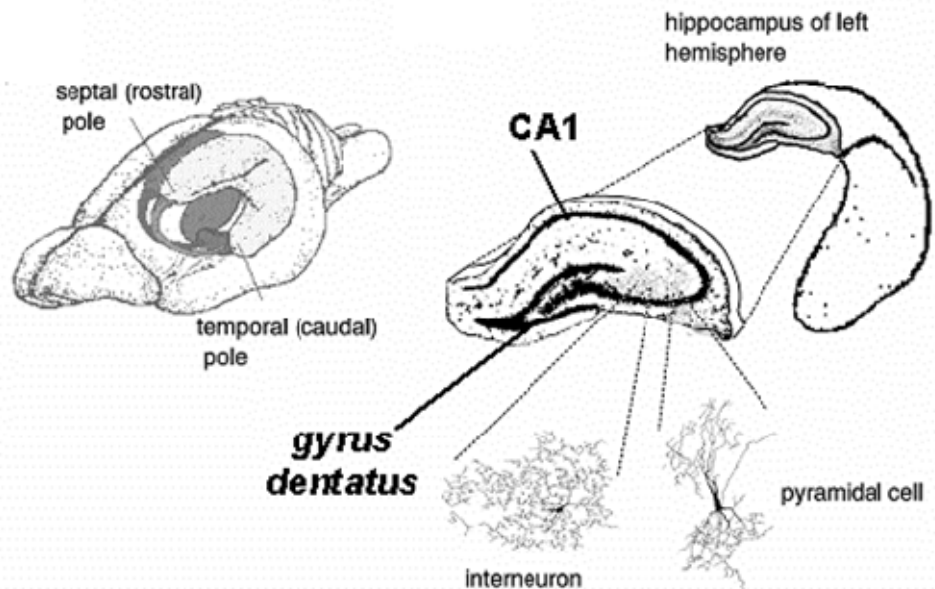


Figure 3-1 The position of the hippocampus in the rodent brain.

Once the entire structure is extracted and sliced, the CA1 and dentate gyrus regions are easily recognizable. Typical pyramidal neurons and interneurons are depicted. Drawing from: <http://www.ecclescorner.org>

the refrigerator for about half an hour they were placed on membrane inserts and incubated with culture medium for 2-4 days.

3.2.2 Patch Clamp Recordings

Experiments were performed after 2-4 days of incubation allowing the slices to regenerate and to adhere to the membrane. The recording chamber was temperature controlled at 35°C and perfused with external solution. Pipettes for patch clamp recordings with a resistance of 3-5 MΩ were pulled using a P97 micropipette puller. Whole-cell patch-clamp recordings from single visually identified CA3-pyramidal neurons were made to record synaptic currents. Pipettes were filled with an internal solution containing 0.033 mmol OGB-1, a calcium dye, to allow visualizing changes in Ca²⁺-concentration within the cell and the entire dendritic tree. Cells were held at a potential of -55 mV, previously shown to be a typical resting membrane potential for developing neurons (Safiulina et al., 2006). Recordings were discarded when the series resistance dropped below 25 MΩ. The recordings started upon a trigger signal given by the camera, which also turned on the fluorescent light. The data was sampled at 10 kHz. The frame trigger signal of the camera was logged as a separate trace in the electrophysiological recording. This allowed exact aligning of the electrophysiological recordings with the data derived from the calcium imaging (see chapter 3.2.7).

A small subset of experiments was carried out in current clamp to measure the relationship between action potential firing and dendritic Ca²⁺-signalling.

3.2.3 Stimulation

For the stimulation experiments a glass pipette filled with external solution was brought in proximity (30 - 100 μm) to the dendrite of the patched cell guided by the fluorescent image obtained from the single filled neuron. Subsequently, stimulation strength was adjusted to reliably evoke synaptic currents in the patched and imaged cell. The duration of the stimulus was 0.5 ms. The trigger signal of the stimulation was recorded as a separate

trace in the electrophysiological recording to mark the time point of each stimulus onset.

3.2.4 Imaging

Patched cells were imaged at the earliest 15 minutes after breaking the cell membrane and going to whole cell configuration to allow the calcium dye to diffuse evenly throughout the entire cell and into the fine dendritic branches. During this time period also the dye that spilled over into the extracellular space before a seal was achieved, dissipated and thus the background brightness was largely reduced when the recordings started. Subsequently images were acquired using a CCD camera mounted on a fluorescence microscope. The camera was cooled to -70°C for low noise imaging at 30 HZ. A region of interest, sized 250 x 250 pixels, containing large dendritic regions but not the soma was chosen and illumination was restricted to that region with the help of the aperture iris diaphragm of the microscope. The images were recorded with 16 bit depth. To increase the signal to noise ratio and to decrease the amount of data images were 4 binned. Thus, the file size of a single image frame was 125 kbyte. Handling the fast accumulating, large amount of data (approximately 3.6 MB/s) required direct streaming onto two fast hard drives (15000 rpm) organized in a RAID 0 array. Organization of the two hard drives in a RAID 0 array almost doubled the writing capabilities of the system and rendered recording times of two minutes and longer possible.

To acquire consecutive frames at different z-planes, a piezo stepper was incorporated between the microscope and the objective. A frame trigger signal given by the camera at the beginning of each frame triggered the movement of the piezo stepper to the next z-position. Three different z-planes separated by 10 μm were recorded, thus a temporal resolution of 10 Hz per cycle was achieved (see Figure 3-2 for a scheme of the setup).

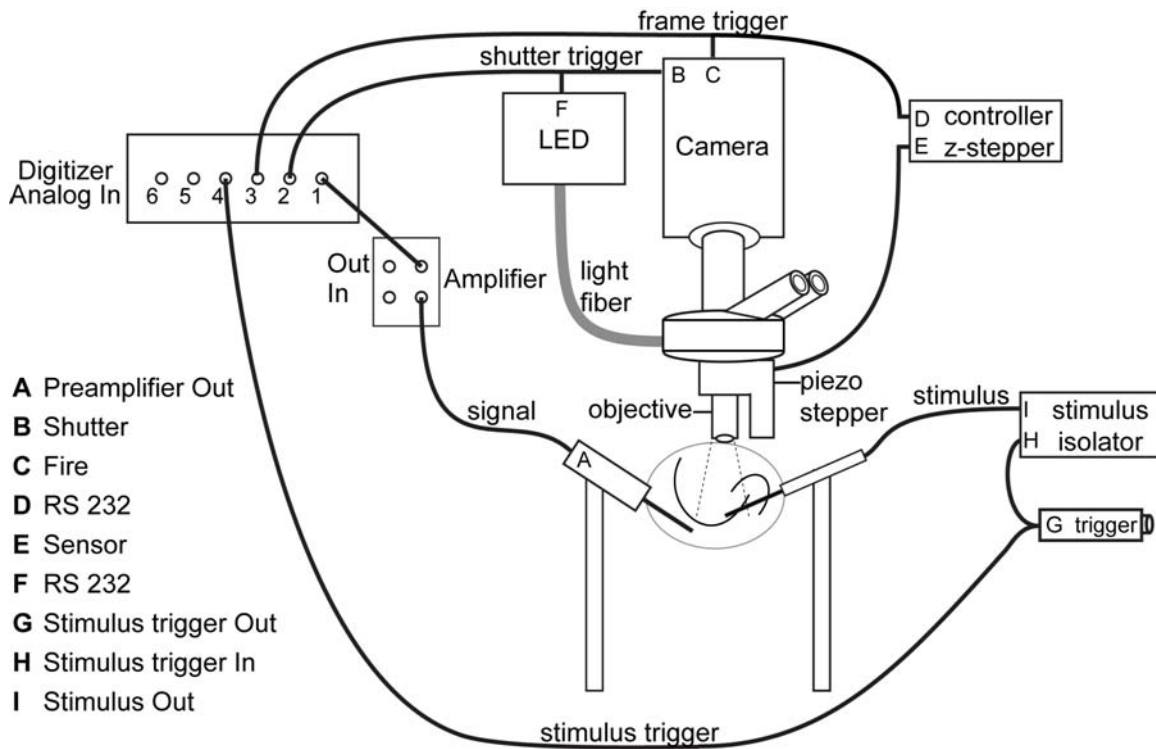


Figure 3-2 Setup for simultaneous electrophysiological recording and Ca^{2+} -imaging

Trigger signals given by the camera at the onset of the recording triggered the illumination by the LED-system and the beginning of the electrophysiological recording.

Trigger signals given by the camera at the beginning of each frame were recorded to align the imaging and the electrophysiological data and additionally they triggered the movement of the piezo stepper to the next position.

3.2.5 Image analysis

Changes in the fluorescence of OGB-1 report for changes in the calcium concentration. To study local Ca^{2+} -transients – locally restricted rises in the intracellular Ca^{2+} -concentration – it was required to detect locally restricted changes in the fluorescence. This analysis was carried out automatically by custom made Matlab software. As a first step in the analysis process, each set of three images recorded at different z-planes was collapsed into one maximum projection image (Figure 3-3). All maximum projection images from one recording were collected in one stack, thus the 4-D image stack (x-y-z-t-stack) was collapsed into a 3-D image stack ($x_{\text{maxproject}}-y_{\text{maxproject}}-t$ -stack) containing all necessary information.

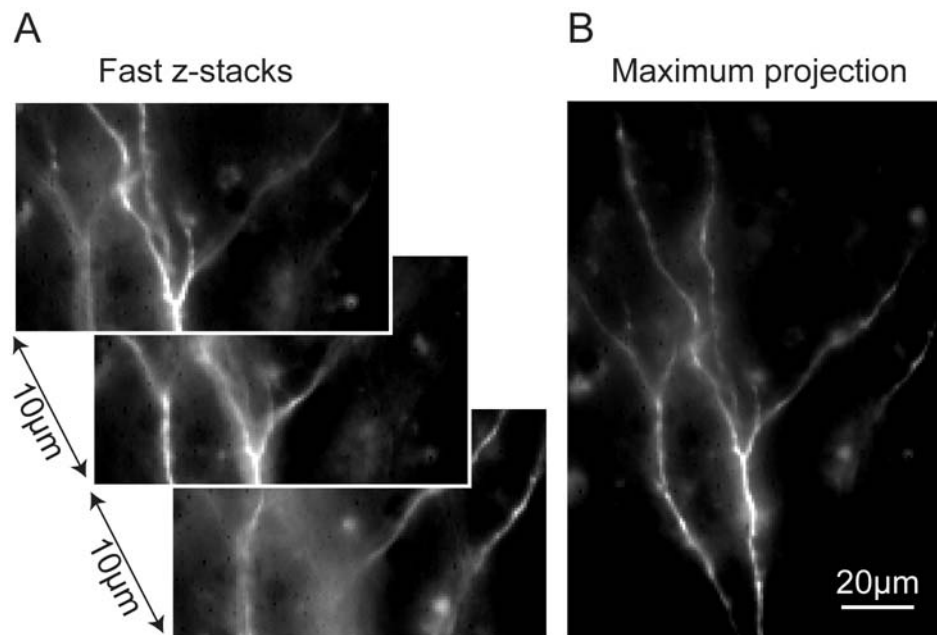


Figure 3-3 Fast z-stepping

A: Single z-planes showing differences in focal planes.

B: Maximum projection of the three z-planes on left side; Note: large parts of the dendrite in the field of view are in focus.

Next, an F_0 image was computed. In this F_0 image the pixel value at each position represented the median of all pixel values over time at exactly this position. The F_0 image was used to generate a $\Delta F/F_0$ stack by subtracting

it from each frame of the stack and dividing the result by F_0 . This $\Delta F/F_0$ stack visualizes changes in fluorescence.

3.2.5.1 Dendrite detection

For various reasons it was required to detect the dendritic regions captured in our recordings: Firstly, only changes in brightness occurring on the detected dendrites were taken as local Ca^{2+} -transients and subsequently analyzed. Secondly, some analysis demanded normalization to the overall length of imaged dendrite, for example the frequency of transients was to be normalized to the length of dendrite.

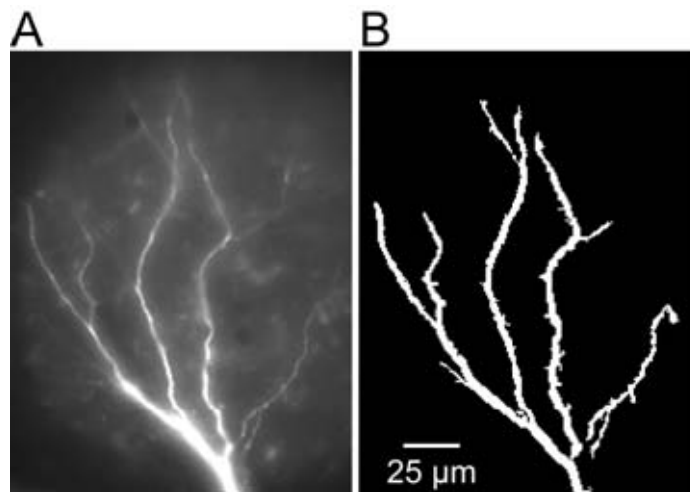


Figure 3-4 Dendrite detection

A: F_0 image - determined as median of the image stack.

B: Detected dendrite after filtering and binarizing the F_0 -image.

To detect dendrites, the F_0 image was tophat filtered using a disk-shaped structure to correct for uneven background brightness and illumination. The radius of the filter structure, 3 pixel, was chosen to be slightly larger than the thickest part of the dendrite. All areas brighter than two times the standard deviation and larger than 200 pixels were marked as dendrites (Figure 3-4) and subsequently only signals being part of the dendritic area were detected (see chapter 3.2.5.2).

3.2.5.2 Detection of local Ca^{2+} -transients

To detect local Ca^{2+} -transients I applied a correlation filter to the $\Delta F/F_0$ representation using a disk-shaped three dimensional filter kernel with a three pixels radius consisting of a series of minus ones, zeros and ones (-1, 0 and +1). The resulting stack, representing the derivative stack, shows changes in fluorescence across three consecutive frames and was used to detect rises in brightness. To exclude rises in brightness of single pixels and very small areas from the detection I eroded the derivative stack with a disk-shaped structure (radius two pixels). Signals were defined as a minimum of 10 connected pixels being part of the previously detected dendrite (see chapter 3.2.5.1) showing a rise in fluorescence of at least 15% ($\Delta F/F_0$) sec^{-1} . Figure 3-5 shows a pseudo line scan and the local Ca^{2+} -transients detected and measured applying this method.

3.2.5.3 Measuring signal properties

To measure the properties of the transients a difference stack was computed by subtracting the average image of the three frames preceding the signal from the following 30 frames. The center of each signal was defined as the position with the largest increase in fluorescence within the signal in the difference stack. To measure extension and duration of the signals, the maximum rise in brightness was determined in the difference stack. Subsequently, the connected area consisting of all pixels brighter

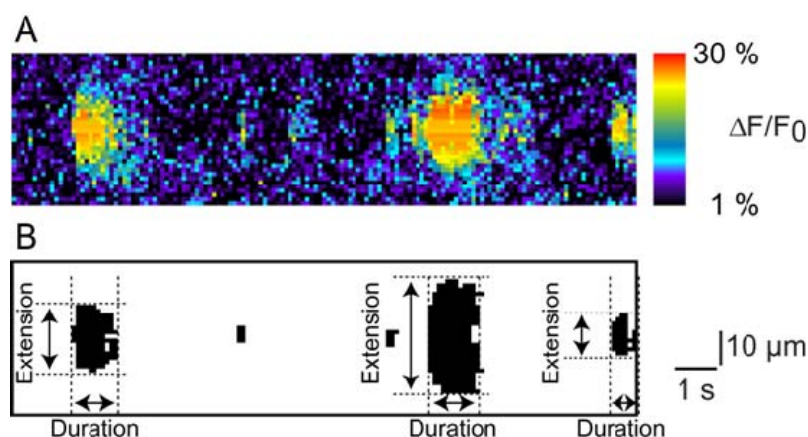


Figure 3-5 Measuring signal properties

A: Pseudo line scan showing Ca^{2+} -transients.

B: Binarized line scan demonstrating detected signals and measured properties.

than 2/3 of this maximum was considered to be part of the signal. Regions falling below this threshold and becoming brighter again were removed from the signal by erosion followed by dilation. This minimized the chance that two subsequent transients were detected as one long lasting one caused by single pixel noise.

3.2.5.4 Spatial alignment of recordings

Small differences in the field of view occurred even though the whole setup was vibration isolated, the slices were weight down with a ring of platinum and in most experiments all recordings were done from the same place without moving the x-y-table. Therefore, prior to defining the sites, it was necessary to align all recordings from a cell to the first recording of this cell. The observed movements were restricted to x-y movements without any rotations or distortions, thus it was sufficient to shift all stacks in x-y-direction to get an optimal overlap of the detected dendrites. This was accomplished by collapsing the detected binarized dendrite into a line and subsequently shifting this line stepwise ± 40 pixel (32 μm) in x-direction and y-direction. For each step the overlap with the collapsed line of the first recording was calculated. The position showing the maximum overlap of the two dendrites was taken as optimal position and for further analysis the entire recording was shifted to meet this position.

3.2.5.5 Defining synaptic and non-synaptic sites

All calcium transients within a distance of $\pm 4 \mu\text{m}$ of a common place along the dendrite were defined as belonging to one site. The center of this site was computed in an iterative way: the center of the first occurring calcium transient was taken and every signal within a distance of $\pm 4 \mu\text{m}$ was assumed to belong to the same site. In the next round the center of the site was defined as the middle of the centers of those calcium transients. Due to the change of the center, some Ca^{2+} -transients were newly assigned to this site while others were too far from the new center to be part of this site. The loop was stopped after twenty iterations and the center of the next calcium transient, which was not yet part of any site, was taken as first estimation of a new site.

The distinction between synaptic and non-synaptic sites was based on the fraction of calcium transients which occurred simultaneously with synaptic events at a given site. As a first step the probability for any calcium transient to be correlated with an electrophysiological event by chance was calculated by dividing the number of frames during which at least one synaptic current was detected by the total number of frames.

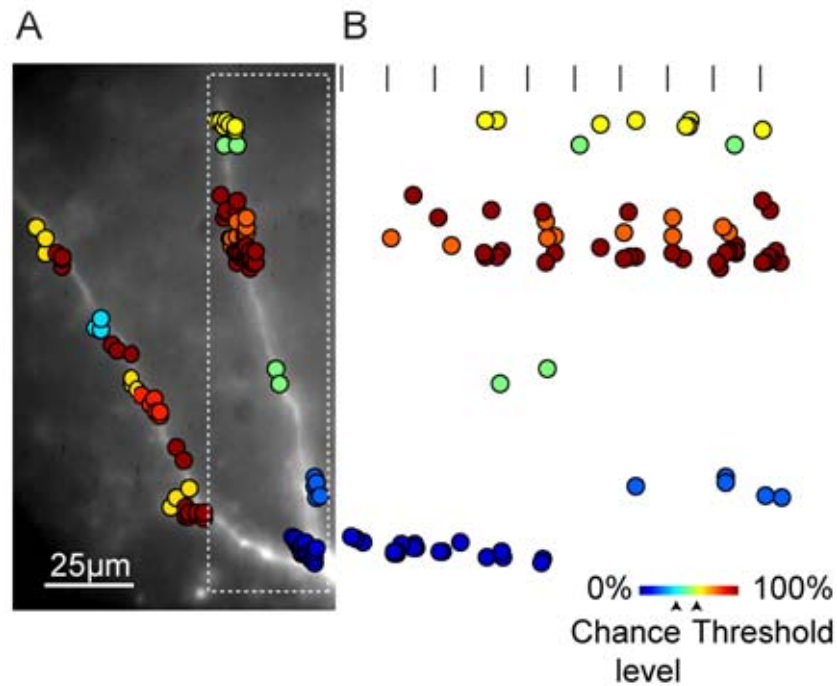


Figure 3-6 Sites of local Ca^{2+} -transients

A: Ca^{2+} -transients (dots) projected onto the dendrite, grouped and dedicated to sites; the color of the dots codes for the percentage of correlated Ca^{2+} -transients at each site.

B: Occurrence of Ca^{2+} -transients (dots) in time (x-axis); vertical lines represent onsets of recordings; recording time was two minutes.

Subsequently, the percentage of correlated calcium transients at each site was computed (Figure 3-6). Sites were assigned to be synaptic if the correlation of calcium transients and electrophysiological events exceeded the chance level 1.5 times.

Cells with an electrophysiological activity level exceeding 60% the imaging frequency were excluded from the analysis, since this high level of activity rendered a distinction between synaptic sites and non-synaptic sites based upon the fraction of correlated transients impossible.

3.2.5.6 Manual detection of local Ca^{2+} -transients

For manual analysis of local Ca^{2+} -transients image stacks were imported in ImageJ to derive pseudo line scans. Pseudo line scans carry the spatial and brightness information of the pixels along the region of interest in the y-axis while the information of each point in time is carried on the x-axis (Figure 3-5 A). To generate pseudo line scans a region of interest (line) was drawn along each dendritic branch and the function “Reslice” plotted the pseudo line scan of the region of interest.

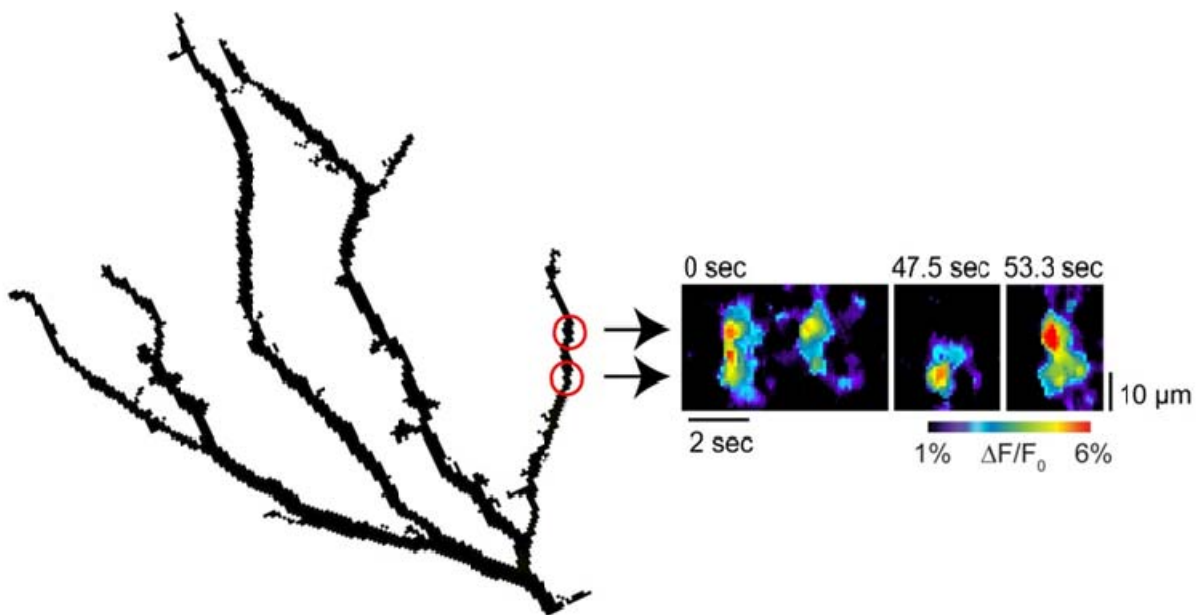


Figure 3-7 Manual detection of local Ca^{2+} -transients

Two synaptic sites (red circles) projected onto the respective dendrite and parts of a pseudo line scan of these sites showing local Ca^{2+} -transients.

Synaptic positions, as detected by the Matlab program, were marked in these pseudo line scans and verified by eye (Figure 3-7). Subsequently, signals were detected by eye for each synaptic site separately. Afterwards the complete linescans, containing multiple synaptic sites, were reinspected to exclude those Ca^{2+} -transients which could not unambiguously be assigned to a specific synapse. This procedure allowed analyzing the activation pattern of a given synapse blindly to the activity

patterns of the neighboring synapses, yet permitted to exclude wrongly detected Ca^{2+} -transients.

3.2.5.7 Measuring distances between synapses

For calculating the shortest distance between all sites along the dendrite a binarized model of the dendrite was created semi-automatically by averaging the detected dendrites (see chapter 3.2.5.1) of all recordings taken from an individual cell and collapsing those detected dendrites into a line. Subsequently, individual pixels were manually added and removed respectively to avoid breaks and loops in the dendritic arbor. Next, the distance along the dendrite between all neighboring points of interest was computed. Points of interest (knots) were branching points, end points or sites of interest, like synapses. Finally, a matrix showing the shortest distance between all pairs of knots was generated using the Floyd-Warshall-Algorithm.

3.2.5.8 Correlation between synapses

As a measure of the correlation between two synapses, the probability for one synapse to fire given that the other one fires was computed. Specifically, the number of simultaneous activations of both synapses was divided by the total number of activations per synapse. Subsequently, the average correlation for each pair of synapses was computed (Figure 3-8).

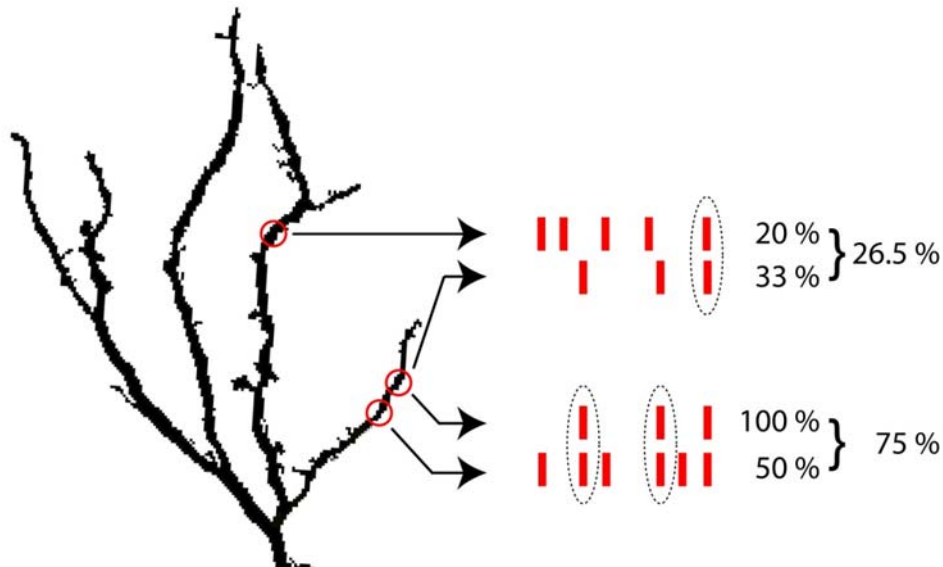


Figure 3-8 Inter-synapse correlation

Scheme depicting calculation of correlation between synaptic pairs: red vertical lines symbolize individual activations of each synapse (red circle); the number of co-activations for each synaptic pair is counted and divided by the number of single activations of each of the two partners separately.

3.2.5.9 Analyzing the number of synapses per axon onto a single dendrite

Investigating activation patterns of neighboring synapses, I considered whether neighboring synapses can possibly be formed by a single axon. Thus, to check if individual axons make multiple synapses onto one and the same dendrite, previously published anatomical data obtained in the same culture system investigated throughout this study was analyzed (Lohmann and Bonhoeffer, 2008). The axons were fluorescently labeled via bolus loading with Oregon Green, while dendrites were fluorescently labeled by single cell electroporation with OGB-1 and Alexa 594. High magnification z-stacks were recorded with a confocal microscope. In these stacks, dendrites were displayed in red (Alexa 594), while axons were displayed in green (Oregon Green). All sites having an overlap of the two colors within a single z-plane, thus sites displaying yellow pixels, were referred to as putative synapses.

3.2.6 Electrophysiological analysis

Analysis of the electrophysiological recordings was done in Matlab. Mainly custom made programs were used, enabling completely automated analysis. To import electrophysiological traces recorded in P-Clamp 10 the program *import_abf* written by *John Bender* in and for Matlab was used. This program is freeware and available at <http://webscripts.softpedia.com/script/Scientific-Engineering-Ruby>.

3.2.6.1 Elimination of current-fluctuations caused by the piezo stepper

The movement of the piezo stepper caused small waves in the extra cellular solution. Depending on the type of the recording chamber used, these waves introduced periodic fluctuations in the recorded current. Prior to further analysis, these fluctuations needed to be corrected for. Since a Fourier-transformation revealed that their frequency components were quite similar to the frequency components of synaptic events (data not shown), a different approach than frequency filtering was chosen. For each recording the fluctuation for a whole cycle of the piezo stepper was estimated by averaging the fluctuations per cycle throughout the recording. To get the best possible overlay of those fluctuation cycles, the single cycles were aligned prior to averaging them by taking the peaks of each cycle as landmark. Subsequently, a current trace the same length as the raw recording was generated by concatenating repetitions of the averaged fluctuation cycle. Finally, this trace was subtracted from the recorded current. In the corrected current trace, which was cleared from the periodic current fluctuations (Figure 3-9), synaptic events could be detected as described in chapter 3.2.6.2.

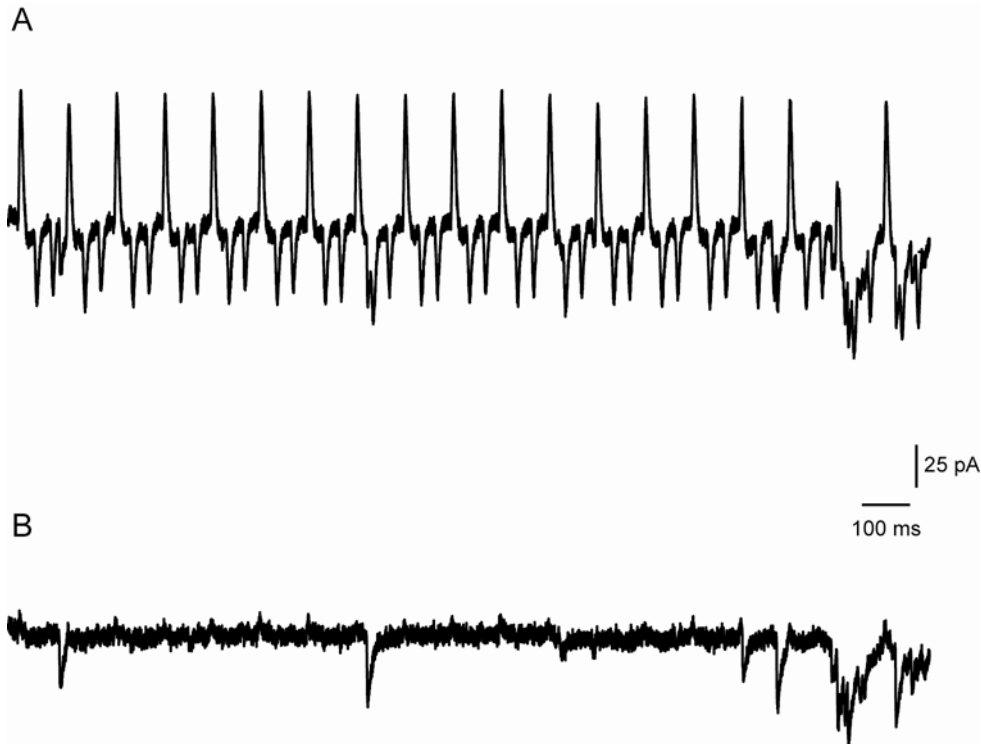


Figure 3-9 Removing current fluctuations induced by the fast z-stepping

A: Raw current trace of an electrophysiological recording with fast z-stepping.

B: Current trace after subtracting the periodic fluctuations induced by the piezo stepper.

However, these fluctuations occurred solely when using the recording chambers produced by the workshop of the MPI-Martinsried. When using the temperature controlled slice mini chambers I from Luigs & Neumann no periodic current fluctuations were observed, thus no correction was needed.

3.2.6.2 Detecting electrophysiological events

For the detection of spontaneous electrophysiological events a similar procedure as described in chapter 3.2.5.2 was used. Firstly, the data was filtered by averaging 50 consecutive data points of the measured current. Subsequently, the onsets of the signals were detected in a convolved trace of this average filtered current trace (filter kernel: -1, 0, 1). Due to the chosen filter kernel this convolved trace reflects the derivative in time of the average filtered current trace. The threshold for signal detection was depending on the noise level. To estimate the noise level I assumed that fluctuations between 0 and 2 pA/ms in the derivative trace (moderate

changes in measured current towards zero) were mainly due to noise in the recording. In contrast, synaptic inward currents are represented as large, negative values in the derivative trace. The threshold for signal detection was set to 3.5 times this noise level. To distinguish between single synaptic inputs and bursts of synchronous activity I defined that bursts consist of at least four transients within 100 ms.

3.2.7 Temporal alignment of datasets

To precisely register the electrophysiological and the optical recordings in time I logged the frame trigger signal given by the camera at the beginning of every frame as a separate trace in the electrophysiological recording. Automated counting of these trigger signals in Matlab allowed to exactly determine the beginning of every single frame of the calcium imaging in the electrophysiological trace and vice versa. The single trigger events were detected by binarizing the trace using an adequate threshold and subsequently taking the onset of every frame trigger signal as the beginning of each frame (Figure 3-10).

This method turned out to be easy to handle and more accurate than triggering solely the beginning of the recording, as it automatically corrects small time shifts occurring when recording large amounts of fast accumulating data with two independent computers. Reasons for those time-shifts are, for example, small delays caused by computing and saving the large amount of data from each imaging stack (1.3 GB per recording).

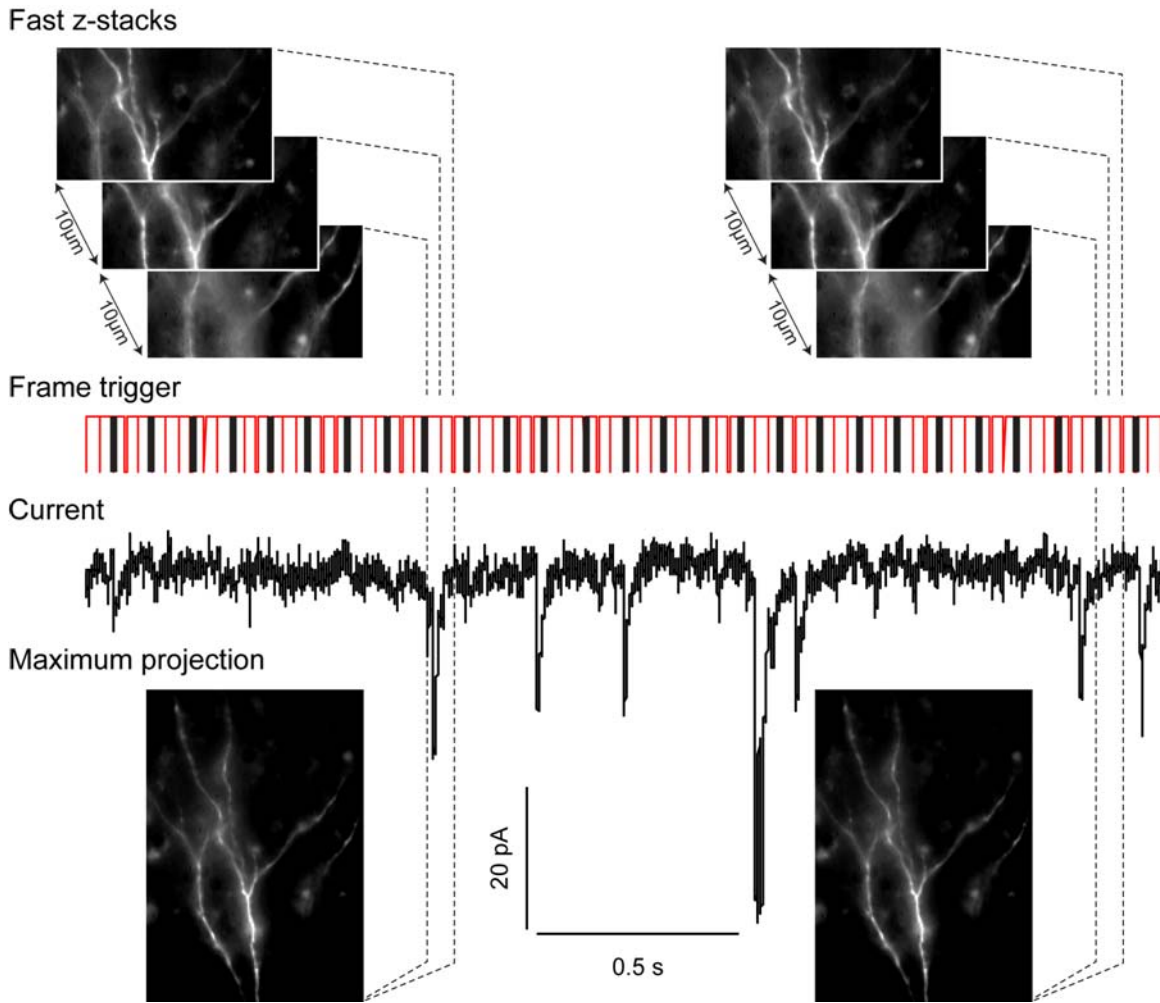


Figure 3-10 Scheme depicting the aligning principle

Every third frame trigger signal is marked in black as it tags the beginning of a new cycle of the piezo stepper.

4 RESULTS

This study focuses on the spatio-temporal patterns of spontaneous synaptic activity. As electrophysiological methods alone do not provide any information on the sub-cellular location of the recorded synaptic activation, I combined electrophysiological recordings with high speed calcium imaging to bridge this gap. Combining these two techniques I set out to visualize spontaneous synaptic activity in pyramidal neurons of the CA3 region in developing hippocampal slice cultures.

4.1 Electrophysiological recordings

The electrophysiological recordings showed spontaneously occurring synaptic currents, which could be assigned to two distinct groups: single current peaks and bursts of synaptic activity. Single current peaks represent most likely unitary synaptic events. These unitary synaptic events are characterized by clearly detectable individual peaks. In contrast, bursts of synaptic activity reflect synchronous synaptic input at many synapses at the same time (Leinekugel et al., 1995). They are therefore characterized by an accumulation of multiple individual current peaks. Single current peaks occurred at a rate of 1.8 ± 0.62 Hz (mean \pm s.d. per cell) and bursts of activity occurred at a rate of 11.5 ± 10.8 min⁻¹ (n = 15 cells).

4.2 Ca²⁺-transients

4.2.1 Global Ca²⁺-transients

Pyramidal cells of the CA3 region of the developing hippocampus stained with a calcium sensitive dye by electroporation show frequent increases in fluorescence in the entire dendritic tree (Lang et al., 2006). These global Ca²⁺-transients reflect action potential firing evoked by giant depolarization potentials, a well-known phenomenon shaping the developing hippocampus (Leinekugel et al., 1998; Leinekugel et al., 1995; Ben Ari, 2001).

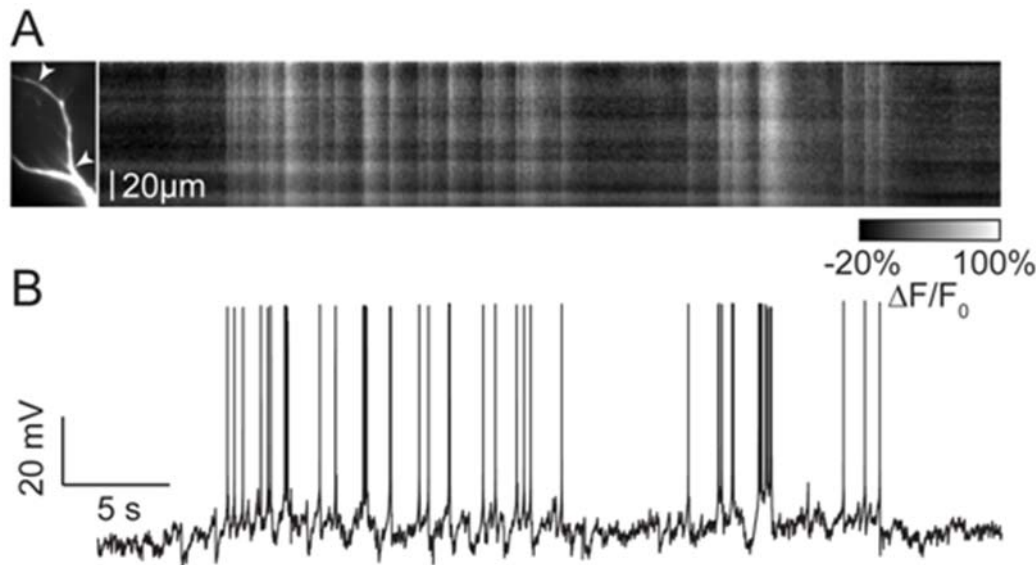


Figure 4-1 Global Ca²⁺-transients

A: Left side shows the dendritic region imaged. Right side: pseudo line scan with global Ca²⁺-transients. The dendritic area of the pseudo line scan is depicted on the left side by the arrowheads.

B: Voltage trace showing single and multiple action potentials.

A small set of experiments (n = 13) performed in current clamp demonstrated that global Ca²⁺-transients reliably reflected firing of single or multiple action potentials (Figure 4-1). When normalizing the amplitude of the global Ca²⁺-transients to the average fluorescence increase evoked by a single action potential (Figure 4-2) it becomes obvious that the fluorescence of global Ca²⁺-transients scales with the number of action potentials evoking these global Ca²⁺-transients.

Therefore, global Ca²⁺-transients can be used to estimate the number of action potentials a given cell fires. Nevertheless, with increasing levels

of activity the calcium dye will increasingly saturate, thus,

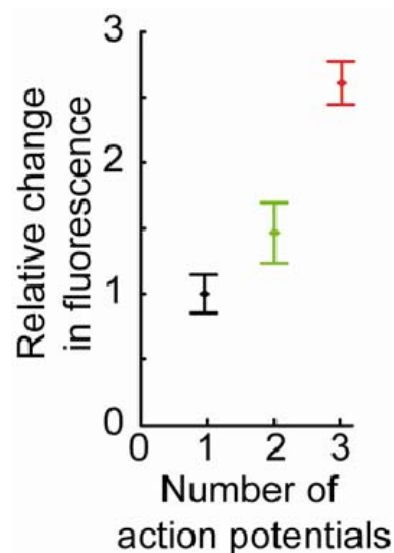


Figure 4-2 Global Ca²⁺-transients and spike rate

Relative change in fluorescence scales with the number of action potentials evoking the global Ca²⁺-transients.

dependent on the activity level of the imaged cell, more elaborate methods to deduce the spiking rate from the imaging data might be required (Yaksi and Friedrich, 2006).

However, most experiments throughout this study were performed in voltage clamped cells to suppress the initiation of action potential firing and the occurrence of global calcium transients. Under current clamp conditions many local Ca^{2+} -transients are masked by global calcium transients of back propagating action potentials. Thus preventing spiking of the imaged cell and thus occurrence of global Ca^{2+} -transients unmasked these local Ca^{2+} -transients.

4.2.2 Local Ca^{2+} -transients and their correlation with synaptic currents

Local Ca^{2+} -transients occurred at a frequency of $68.0 \pm 43.8 \text{ min}^{-1} \text{ mm}^{-1}$ dendrite (mean \pm s.d.) and approximately 50% of these transients were correlated with synaptic currents. To investigate whether these local Ca^{2+} -transients were accidentally correlated with synaptic currents, or whether more local Ca^{2+} -transients are correlated than one would expect, given the activity levels, I plotted a histogram showing the time differences between the electrophysiological events and the local Ca^{2+} -transients (Figure 4-3; $n = 11$ cells).

This plot (Figure 4-3 A) shows a clear peak at zero demonstrating that the correlation between Ca^{2+} -transients and electrophysiological events was not incidental but systematic. The peak is completely absent in a similar histogram which was computed using a reversed time axis of the Ca^{2+} -recordings but not of the electrophysiological events. This histogram serves as a control (Figure 4-3, panel A inset).

Since I was interested in finding out which receptor would possibly be responsible for the correlated local Ca^{2+} -transients, I blocked ionotropic glutamate receptors using NBQX and APV. This reduced activity in the neurons but did not completely abolish it, neither calcium signaling, nor synaptic transmission (Figure 4-3, panel B). Nevertheless, the remaining Ca^{2+} -transients were not correlated in time with synaptic currents anymore.

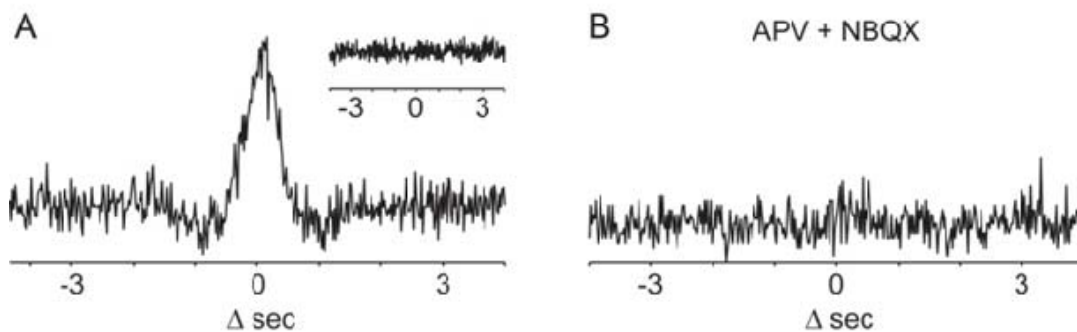


Figure 4-3 Histogram of time differences between local Ca^{2+} -transients and synaptic currents

A: Histogram of time differences between the onsets of calcium transients and electrophysiological events shows a high prevalence of co-occurrence. Inset shows histogram calculated with reversed time points of calcium transients as a control; here no peak exists.

B: The histogram of time differences in the presence of the glutamate receptor antagonists APV and NBQX does not show a detectable peak.

4.2.3 Stimulated Ca^{2+} -transients

In order to corroborate the synaptic origin of the subset of local Ca^{2+} -transients, experiments were performed in which current was injected close to the imaged region in order to stimulate axons in the proximity of the imaged cell (see chapter 3.2.3). The connectivity in the hippocampus at this stage of development is rather low (Malinow, 1991; Sorra and Harris, 1993; Pavlidis and Madison, 1999) leading to a low rate of successful electrical stimulations. The fact that stimulated synapses needed to be within the field of view of the camera lowered the success rate even more.

However, in successful experiments Ca^{2+} -transients which were correlated with synaptic currents could be triggered repeatedly at the same site by applying current injections (Figure 4-4). Since the depolarization induced by the current injection is decreasing with distance from the site of stimulation, direct depolarization of the dendrite should be most likely to occur close to the stimulation electrode. However, in none of the cells, the stimulated site was at the dendrite closest to the stimulation electrode, indicating that the observed Ca^{2+} -transients were evoked by presynaptic release events rather than by direct depolarization. The duration (1.6 ± 1.0 s) and extension ($17.6 \pm 13.8 \mu\text{m}$) of the stimulated transients were indistinguishable from the duration and extension of spontaneously occurring correlated Ca^{2+} -transients (duration: 1.3 ± 1.0 s; extension: $20.9 \pm 19.8 \mu\text{m}$). In none of these experiments stimulation triggered local Ca^{2+} -transients at more than one site ($n = 3$ cells).

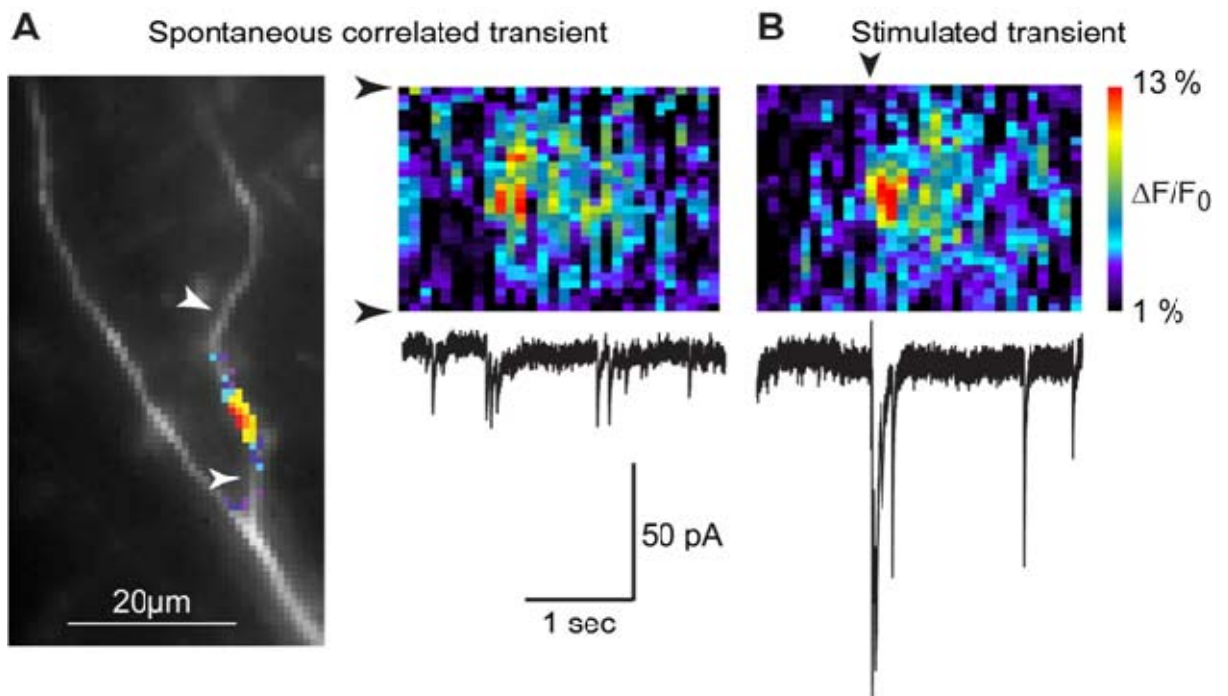


Figure 4-4 Spontaneous and stimulated local Ca^{2+} -transients

A: Left side : Local Ca^{2+} -transient superimposed onto its dendritic location. Right side: Spontaneous correlated Ca^{2+} -transient shown as pseudo line scan with the corresponding current trace below.

B: Stimulated Ca^{2+} -transient with the corresponding current trace below; The arrowhead is depicting the time point of stimulation

4.2.4 Local Ca^{2+} -transients as reporters of glutamatergic transmission

As Ca^{2+} -transients tended to be highly correlated with synaptic currents at some places but rather uncorrelated at others, I assigned the observed Ca^{2+} -transients to sites, computed the correlation of each site and subsequently distinguished between synaptic and non-synaptic sites (see chapter 3.2.5.5).

In presence of NBQX and APV, which block ionotropic glutamate receptors, no local Ca^{2+} -transients could be observed at synaptic sites. In contrast, non-synaptic sites remained active in the presence of the glutamate receptor antagonists. Thus, Ca^{2+} -transients at synaptic sites dependent on glutamate transmission while those at non-synaptic sites do not (Figure 4-4; n = 11 cells).

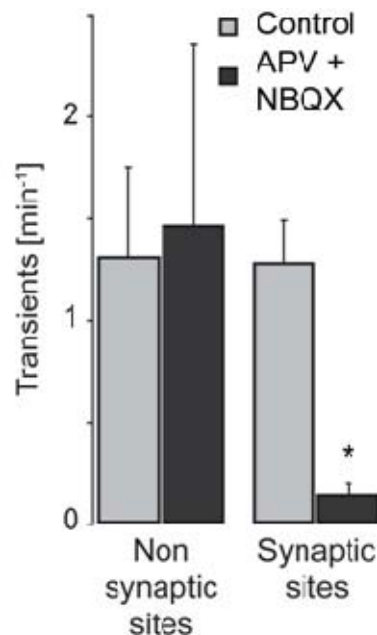


Figure 4-5 Synaptic sites show glutamate receptor activation

Ca^{2+} -transients at non-synaptic sites (left bars) are not blocked by APV and NBQX while at synaptic sites (right bars) the frequency of Ca^{2+} -transients is strongly reduced in presence of APV and NBQX.

In a different set of experiments TTX was used to block voltage gated sodium channels and, therefore, exclude effects caused by the reduction of activity in the entire slice due to the application of a drug. TTX prevents propagation of activity through the network by blocking spread of excitation along the axons. Thus, release of transmitter is no longer controlled by Ca^{2+} -influx triggered by action potential firing, but it is caused solely by spontaneous fusions of single vesicles with the presynaptic plasma membrane. Postsynaptically, in the presence of TTX miniature synaptic currents reflecting activation of postsynaptic receptors due to spontaneous quantal release from vesicles at the presynaptic terminals can be observed (Brown et al., 1979). Therefore, transmitter release in presence of TTX is not influenced by the activity of the network and observed effects of, for example additionally applied drugs, can be assumed to be direct effects, which are not brought about by changes in the network.

In the experiments presented here miniature synaptic currents occurred at a rate of 1.34 ± 0.42 Hz. Miniature synaptic currents with a minimum size of 5 pA were detected; their average amplitude was 25.9 ± 19.3 pA (Figure 4-6; n = 26 recordings).

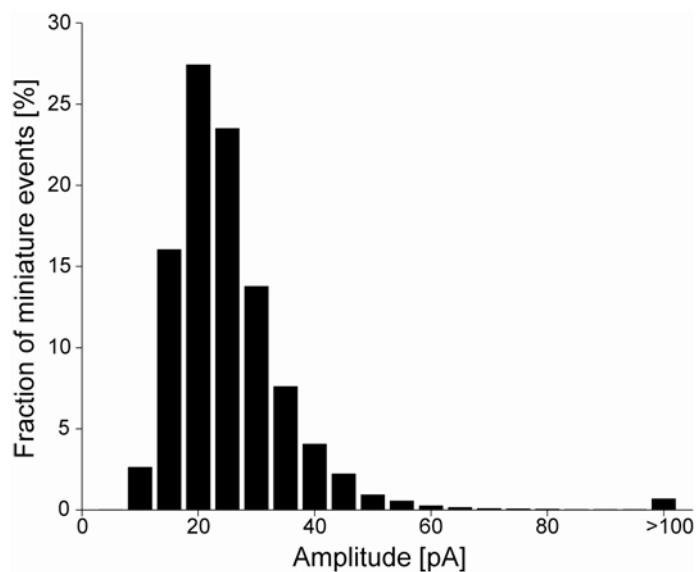


Figure 4-6 Histogram of the amplitude of miniature EPSCs

During treatment with TTX, local Ca^{2+} -transients were observed at synaptic as well as at non-synaptic sites. To boost the frequency of miniature synaptic events latrotoxin, which increases presynaptic transmitter release (Deak et al., 2009) was added to the recording solution. After recording miniature synaptic currents and Ca^{2+} -transients in the presence of TTX and latrotoxin, NBQX and APV were washed in to additionally block ionotropic glutamate receptors. Even though miniature synaptic currents and local Ca^{2+} -transients at non-synaptic sites could still be observed in the presence of the glutamate receptor antagonists, Ca^{2+} -transients at synaptic sites were completely abolished ($n = 6$ cells).

4.2.5 Properties of synaptic and non-synaptic Ca^{2+} -transients

Comparing the properties of Ca^{2+} -transients at synaptic and non-synaptic sites revealed a significant difference in their average duration and extension. Specifically, synaptic Ca^{2+} -transients were longer lasting and more extended (1.35 ± 0.25 s; 23.4 ± 1.8 μm) than non-synaptic transients (0.88 ± 0.12 s; 16.2 ± 1.2 μm) as observed in 11 cells. Also the amplitude

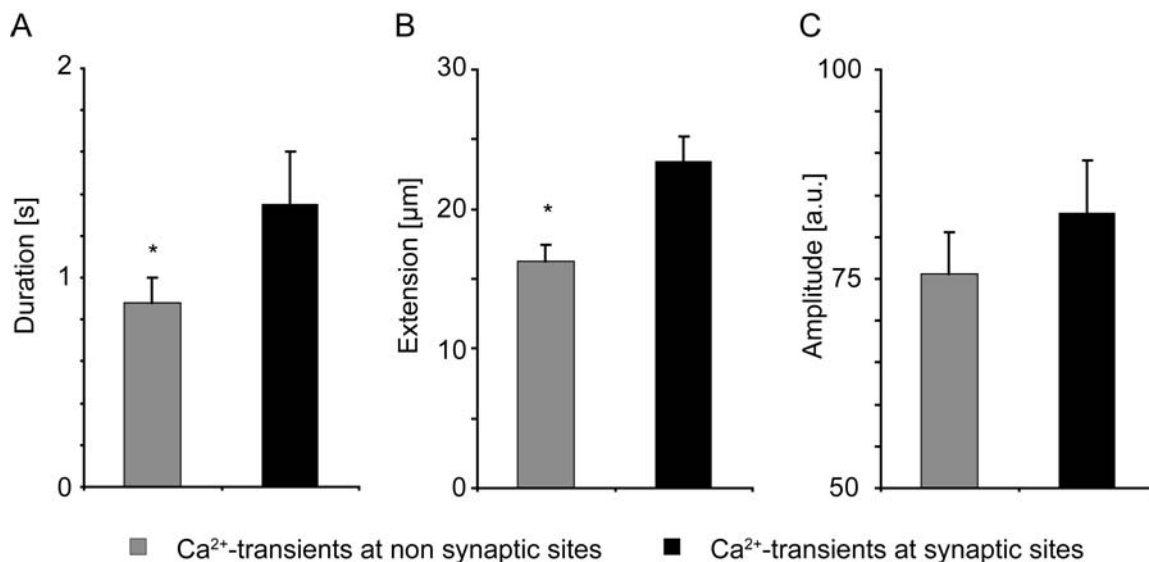


Figure 4-7 Properties of Ca^{2+} -transients at synaptic and at non-synaptic sites

A: Duration of Ca^{2+} -transients occurring at synaptic and non-synaptic sites.

B: Extension of Ca^{2+} -transients occurring at synaptic and non-synaptic sites.

C: Amplitude of Ca^{2+} -transients occurring at synaptic sites and non-synaptic sites.

of calcium transients at synaptic sites tended to be higher than the amplitude of those occurring at non-synaptic sites, but this difference was not significant.

Nevertheless, due to the relative large standard deviation, the small magnitude of the difference in duration and extension did not allow classifying sites into synaptic and non-synaptic ones merely on the basis of the imaging data. Plotting the properties of the detected Ca^{2+} -transients, duration, extension and amplitude in a 3 dimensional graph did not reveal any obvious clustering in different groups of Ca^{2+} -transients (not shown).

4.3 Developmental changes

It has been shown that glutamatergic synapses in the hippocampus of rats are mainly built in the first two weeks after birth (Hsia et al., 1998a). That means, during this period of time the amount of glutamatergic transmission in the hippocampus is constantly increasing. Furthermore, various other properties of neurons change within the first two postnatal weeks, for example the intracellular concentration of chloride and by that the effect of GABA signaling (chapter 2.5). Thus, I decided to visualize synaptic activity in hippocampal slice cultures prepared of older rats (P7-8) to investigate if the changing properties of hippocampal neurons influence the properties of the local Ca^{2+} -transients.

In slices prepared from P7-8 rats the frequency of synaptic currents as well as the frequency of synaptic local Ca^{2+} -transients was about four fold increased ($n = 12$) compared to slices of rats prepared at P2-3. Plotting the properties of the observed local Ca^{2+} -transients revealed, for example, that the duration of the Ca^{2+} -transients at synaptic and at non-synaptic sites changed during development (Figure 4-8). Specifically, local Ca^{2+} -transients at synaptic sites were longer lasting in slices of P 2-3 rats than in slices of P7-8 rats. In contrast, local Ca^{2+} -transients at non-synaptic sites were shorter lasting in the slices of younger rats (P2-3).

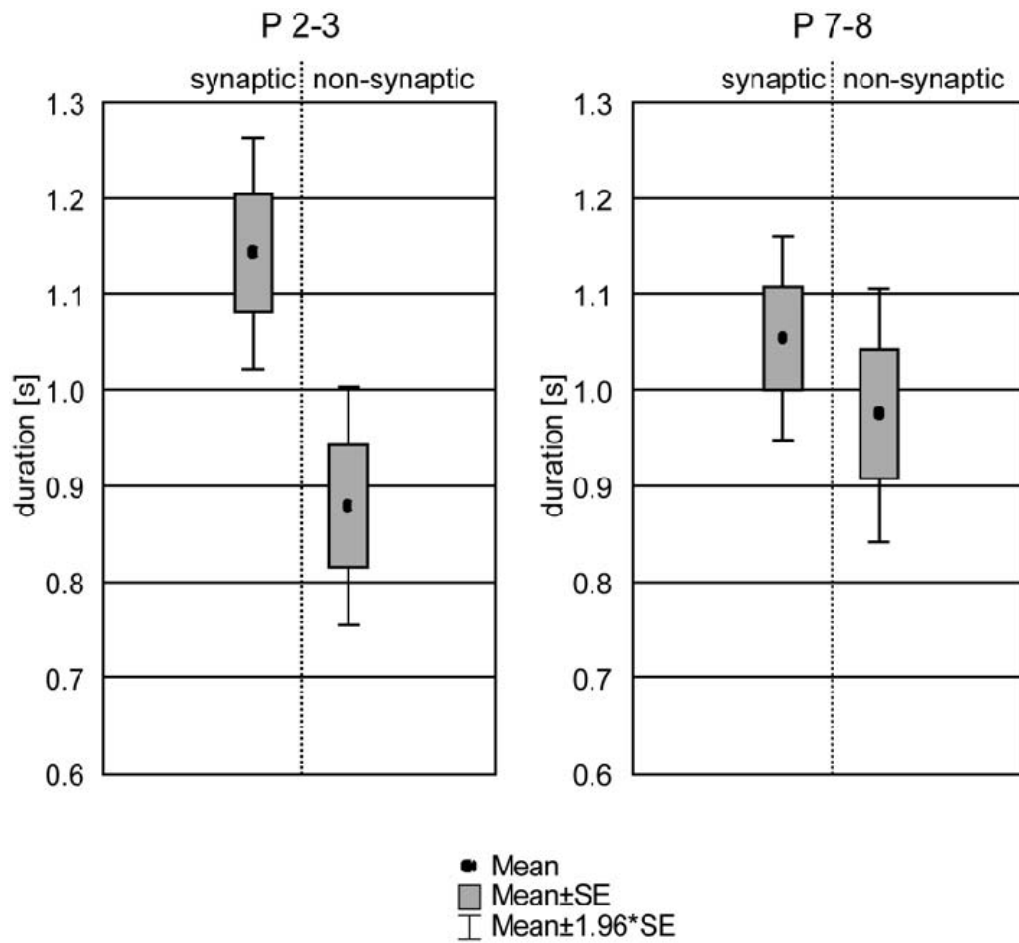


Figure 4-8 Duration of synaptic and non-synaptic transients at different developmental stages

Duration of synaptic versus non-synaptic Ca^{2+} -transients of slices of rats sliced at postnatal day 2-3 compared to slices prepared at postnatal day 7-8

4.4 Mapping synaptic inputs in individual neurons

In order to increase the proportion of dendrites being in the focus plane, the imaged volume was increased by recording from three consecutive z-planes separated by 10 μm . The information gained from each stack of three z-planes was combined in one maximum projection for analysis (see chapter 3.2.5). This technique allowed overcoming the restriction to a single focal plane, which had at the given setup a depth of approximately 10 μm . Acquiring images from three different z-planes at a frequency of 30 Hz resulted in gathering information from a focal volume with a depth of about 30 μm at a sampling rate of 10 Hz. Handling the large amount of

data acquired at high rates demanded a computer capable of streaming the imaging data directly onto hard drives (see chapter 4.2.4).

Imaging for several minutes at three to four different locations was sufficient to map the synaptic inputs of the major parts of the dendritic tree of individual neurons. Seven CA3 pyramidal cells of seven different slices were mapped. Prior further analysis, I compared the fraction of synaptic local Ca^{2+} -transients of the total number of local Ca^{2+} -transients close by the soma and distally to test, whether classification of synaptic and non-synaptic sites was compromised in more distal parts of the dendrites. Such an impaired classification could be the result of attenuation and thus a less reliable detection of distally evoked synaptic currents. However, the fraction of synaptic Ca^{2+} -transients was similar (or even higher) in distal dendrites compared to proximal dendrites (proximal: $< 200 \mu\text{m}$ from the soma $59 \pm 9 \%$; distal: $> 200 \mu\text{m}$ from the soma $74 \pm 17 \%$; $P = 0.06$; not significant).

The obtained topographic maps of synaptic activation clearly show that synaptic Ca^{2+} -transients were detected throughout the dendritic arbor, in all regions of the basal dendrites as well as from the most proximal parts of the apical dendrites to the most distal tips. However, the density of synaptic input appeared to be rather high in the basal dendrites close to the soma, and in the most proximal parts of the apical dendrites, while synaptic activity in the most distal parts of the apical dendrites seemed to be low (Figure 4-9).

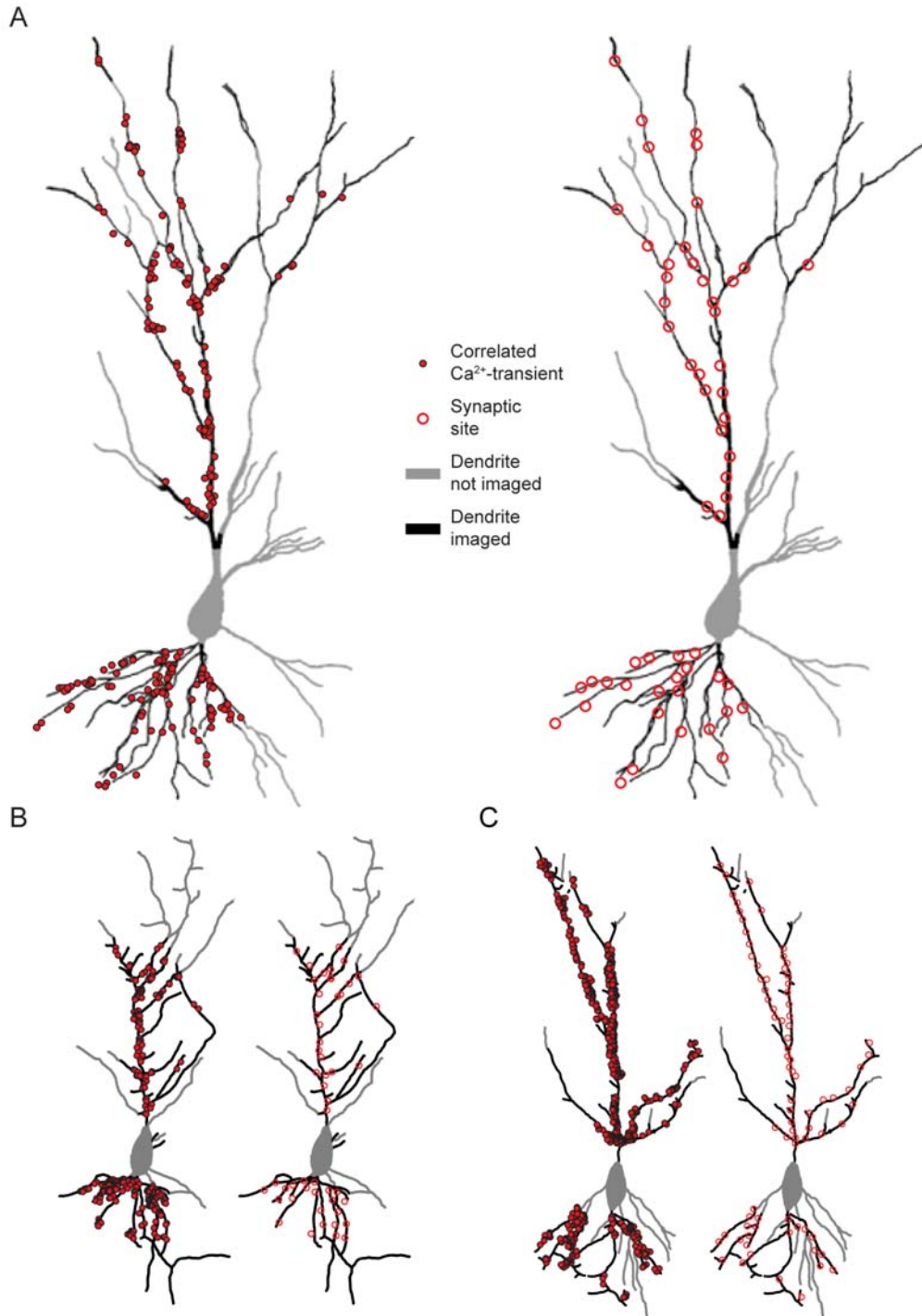


Figure 4-9 Mapping the synaptome

A-C: Individual mapped CA3 pyramidal cells; in each case the left side shows calcium transients (red dots) that coincided with synaptic currents, superimposed on a reconstructed cell; the right side shows synaptic sites (red circles) of the same cell. Black parts of the dendrites represent imaged areas while grey parts represent areas that were not imaged. For reconstruction of the cells a high resolution z-stack was taken at the end of the experiment.

Comparing maps of various individual neurons required a new way of representing the data gathered from these differently shaped neurons. Thus, to summarize the recorded maps of synaptic activation a representation inspired by the Sholl diagram (Sholl, 1953) was designed, a functional Sholl diagram. In a classical, structural Sholl diagram the number of intersections between the dendrite and concentric circles around the soma is plotted against the distance from the soma. In contrast to the structural Sholl diagram, the functional Sholl diagram shows synaptic activity instead of structural complexity as a function of the distance from the soma. Here, synaptic activity means either the frequency of synaptic activations or the frequency normalized to the length of dendrite, i.e. synaptic activations per min and mm. This way of representing the data allowed comparing data gathered from many individual and thus differently shaped neurons (Figure 4-10; n = 7 cells).

The structural and the functional Sholl diagrams differ in some aspects. For example, structurally the analyzed CA3 pyramidal neurons showed only a low amount of branching in apical regions close to the soma, but the synaptic input impinging onto this area was rather high. In general the synaptic input was highest in the basal dendrite. But, since the basal dendrites were also highly branched, the density of input, i.e. the synaptic activations per min and mm dendrite, was not higher in the basal dendrites than in the most proximal apical dendrites. Also the apical region spanning roughly from 100 μm to 170 μm from the soma displayed a density of synaptic input comparable to the basal dendrites. Furthermore, the functional Sholl diagrams revealed that activity is lower in the most distal parts of the apical dendrites, i.e. regions further away from the soma than 200 μm , than in more proximal parts of the apical dendrites, or in the basal dendrites (Figure 4-10). This was not surprising because it could be seen in the maps of synaptic activation described above.

Results

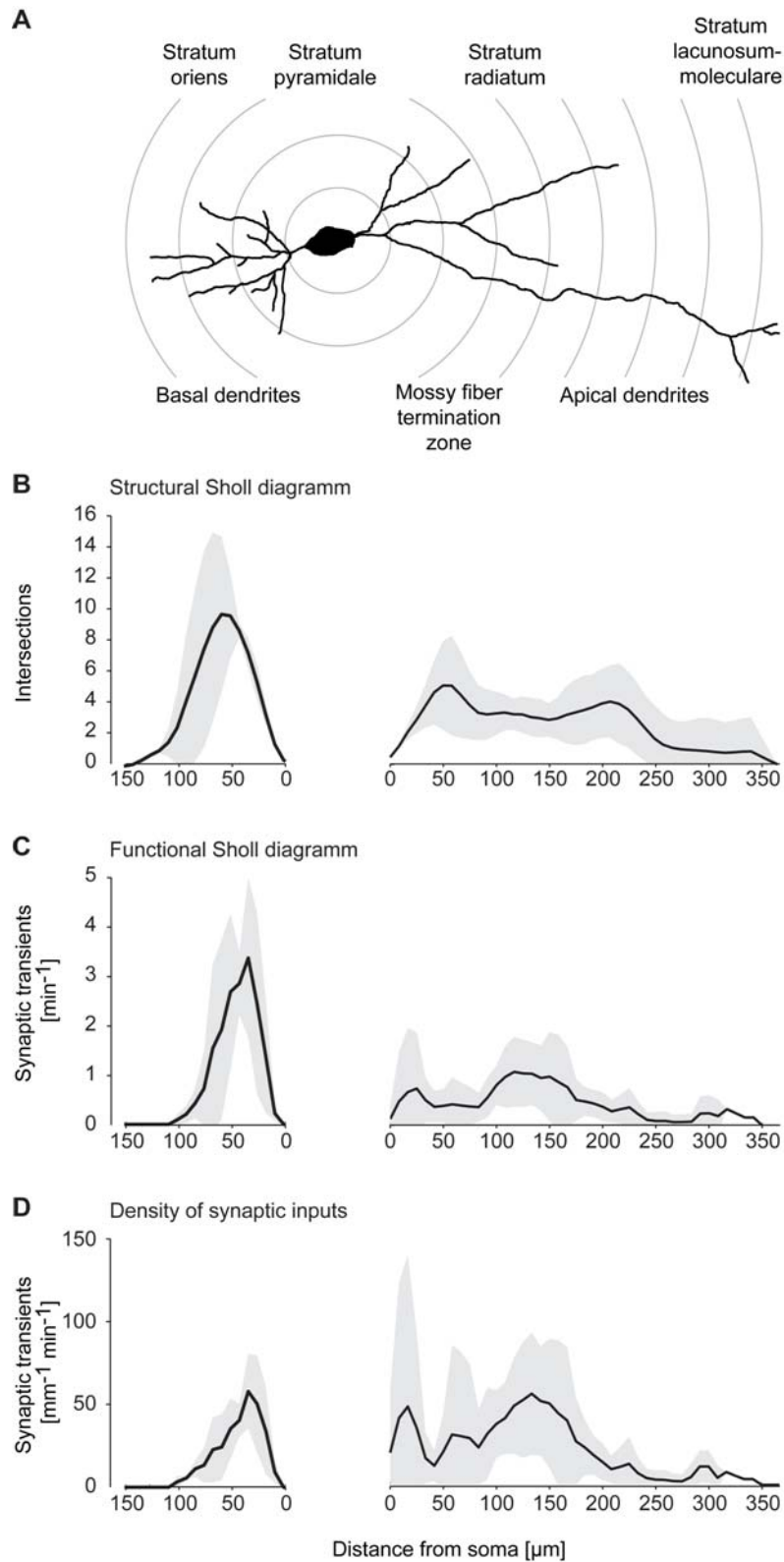


Figure 4-10 Structural and functional Sholl diagrams

A: Example pyramidal neuron.

B: Structural Sholl diagram: numbers of intersections between dendrites and imaginary circles at increasing distances from the soma. (black lines show average of seven and three pyramidal cells for the apical and basal arborizations, respectively; grey areas represent mean \pm s.d.).

C: Functional Sholl diagram derived from the cells in A: synaptic transients per minute at increasing distances from the soma.

D: Density of synaptic inputs: similar to C but normalized to the length of dendrite at each distance.

4.5 Activation-patterns during bursts of synaptic activation

In most brain areas, amongst them the hippocampus, spontaneous activity, i.e. activity independent of sensory input, plays an important role during development (Ben-Ari et al., 1989a; Kasyanov et al., 2004; Mohajerani and Cherubini, 2006; Sipila et al., 2006). In the hippocampus this spontaneous activity is known as giant depolarization potentials (GDPs). GDPs appear in voltage-clamp recordings of a single neuron as bursts of synaptic activity (Leinekugel et al., 1995; Ben-Ari et al., 1989b), which reflect the simultaneous activation of many synapses within a very short time window.

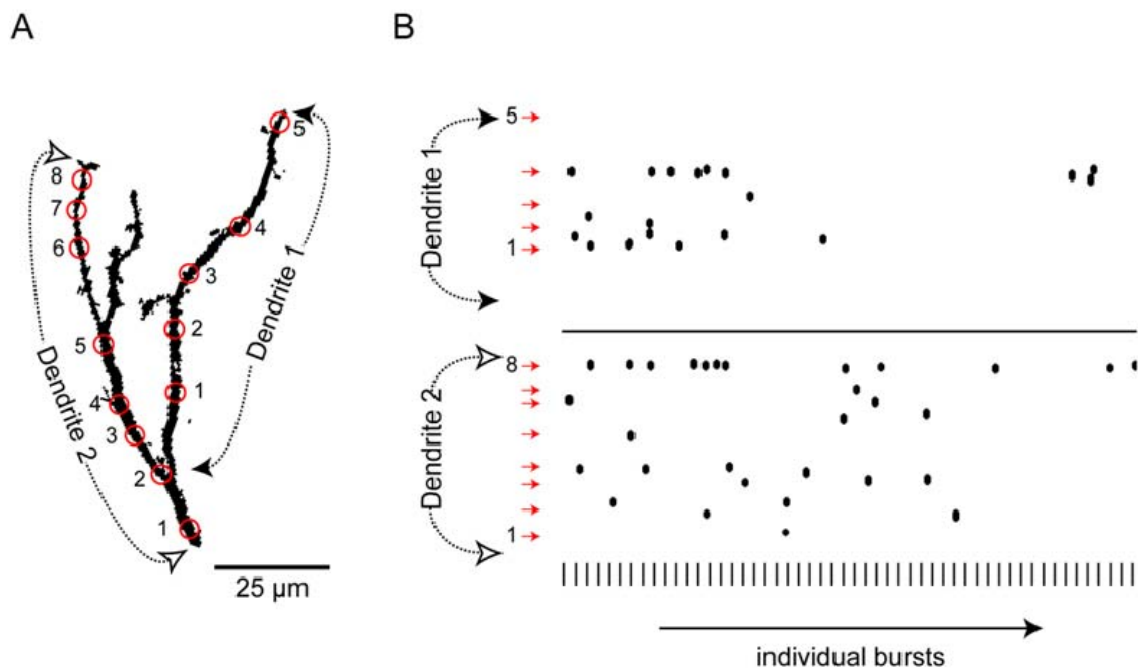


Figure 4-11 Synaptic activity pattern during successive bursts

A: The arrowheads depict the endpoints of the dendritic branches labeled as dendrite 1 and dendrite 2 represented in B. Red circles mark the positions of the synapses.

B: Synaptic activity pattern during 53 successive bursts. Dots represent active synaptic sites during each burst. Individual bursts are represented on the x-axis. Red arrows mark the positions of the synapses shown in A.

Investigating the spatio-temporal patterns of synaptic activation, I analyzed the glutamatergic synapses contributing to successive bursts. On average individual synapses were active during 2.8 ± 1.0 % of the bursts. To address whether recurrent patterns of synaptic activations can be found, different ways of representing the activity patterns during bursts were used. For example, plots were created which show the activity of

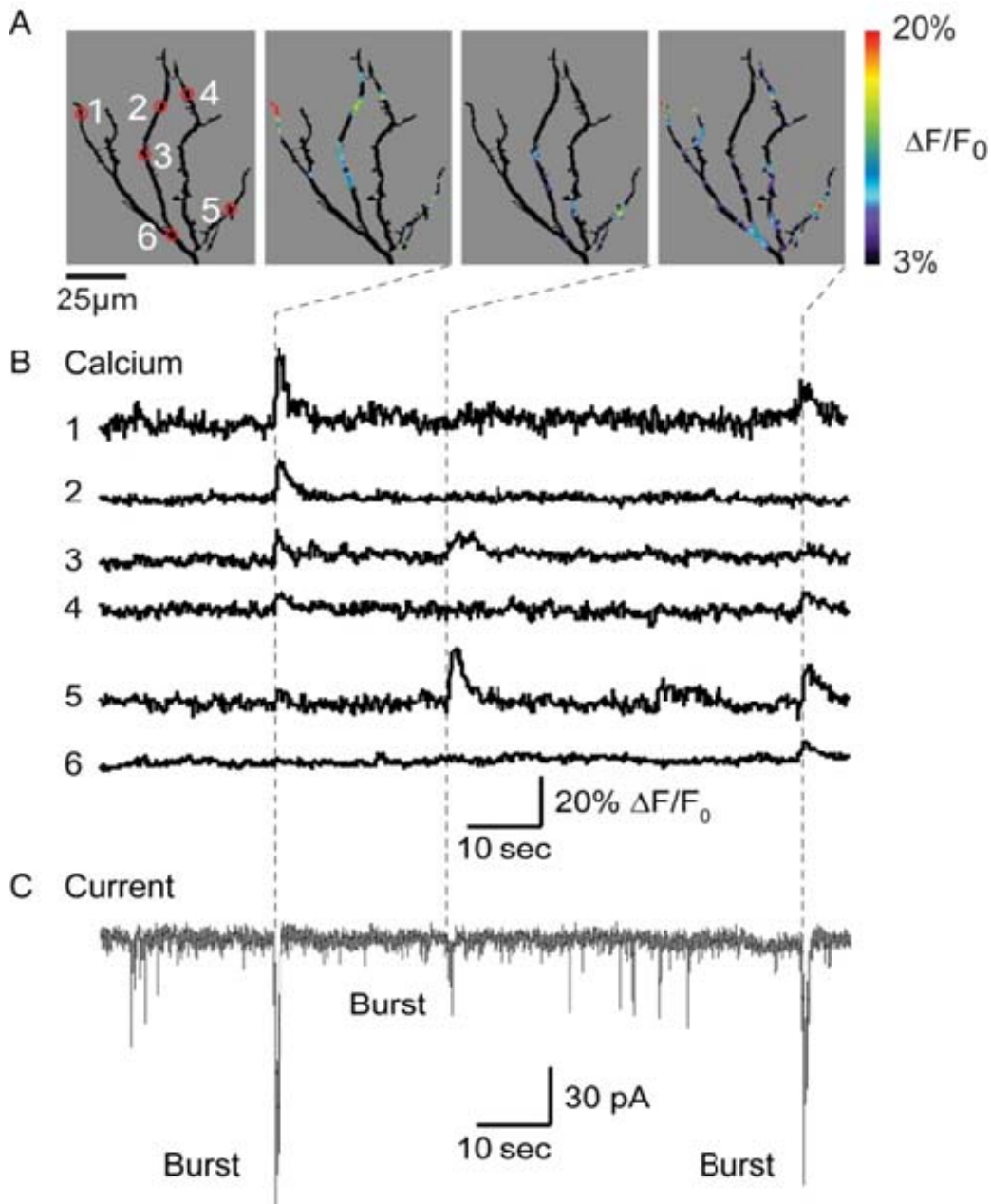


Figure 4-12 Activation patterns of individual synapses during consecutive bursts

A: Synaptic sites (left) and calcium activity patterns during three consecutive bursts.

B: Calcium activity at the six synaptic sites shown in A in $\Delta F/F_0$.

C: Current trace: time points of bursts are depicted by dotted lines.

each synaptic site during successive bursts (Figure 4-11). Subsequently, those representations were carefully analyzed by eye to find possible patterns of activation.

However, I did not find any recurrent synaptic activation pattern. Even between similar bursts with respect to amplitude and duration the contributing set of synapses varied (Figure 4-12).

4.6 Correlated activation of individual pairs of synapses

It has been suggested that dendrites do not only act as passive structures, which receive synaptic inputs and pass the information to the soma, but that stretches of dendrites are also able to compute the received synaptic input and subsequently transmit modifications of this input (Losonczy and Magee, 2006; Nevian et al., 2007; Polsky et al., 2004). For example, strong depolarization of dendritic stretches due to simultaneous activation of many synapses can trigger dendritic spikes, i.e. large regenerative depolarization events initiated in dendrites (Schiller et al., 1997; Golding and Spruston, 1998). These dendritic spikes exert a high impact on the membrane potential at the soma and the axon hillock and are, therefore, more likely to evoke an action potential than normal synaptic currents. The generation of a dendritic spike can be seen as a computation performed solely by the dendrite. Thus, an individual neuron might comprise of several more or less independent computational units. This could increase the computational power of a single neuron tremendously (Govindarajan et al., 2006; Mel and Schiller, 2004). The mechanisms described so far would boost only the output of two or more synchronously active synapses at one stretch of dendrite, thus they require a subcellular precision of synaptic wiring. The subcellular precision of the wiring diagram should be apparent by mapping the patterns evoked by spontaneous activity. To address whether correlation between two given synapses is linked to the relative location of these synapses, I computed the percentage of correlated firing of each pair of synapses. This percentage of correlated firing was subsequently set in relation to spatial aspects concerning the

relative location of those two synapses, like distance between the synapses along the dendrite or difference in vertical distance from the soma.

4.6.1 Correlation vs. vertical distance from the soma

Most axons cross the dendritic arbor of CA3-pyramidal-cells in an almost orthogonal angle (Andersen et al., 2007). Assuming that neighboring synapses might carry related information, I Investigated whether two synapses at the same vertical distance from the soma might be more often simultaneously active than synapses located at different vertical locations.

Since, the cells were imaged in a defined orientation, namely the apical dendrite perpendicular to the x-axis, the vertical distance from the soma was reflected in the vertical position within the image, i.e. in the y-dimension. Hence, to address whether synapses at similar vertical position are more likely to be simultaneously active, I plotted the correlation of each pair of synapses against their difference in the y-dimension. Even though there was a tendency of synapses located at the same vertical distance from the soma to fire more often in concert, this tendency was not significant (Figure 4-13).

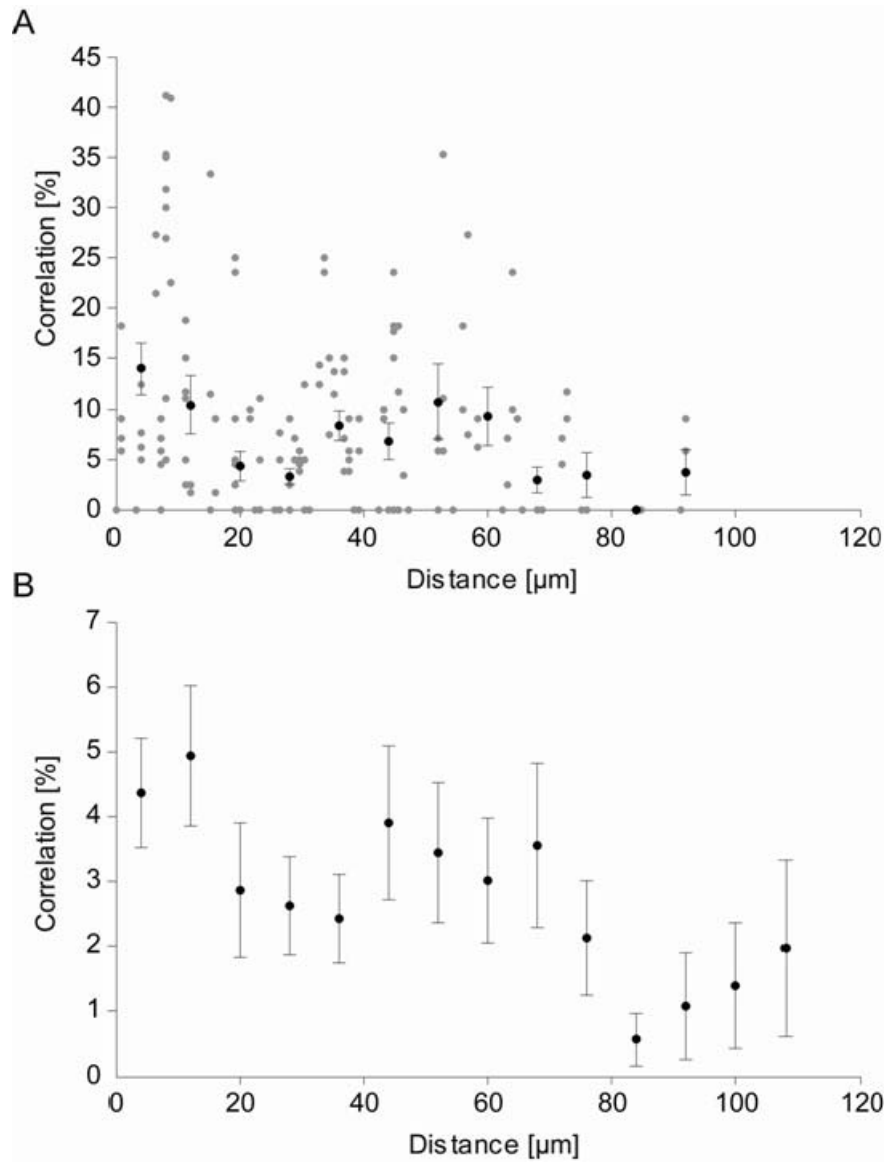


Figure 4-13 Correlation of pairs of synapses against their vertical distance

A: Manual analysis of a single cell.

B: Automated analysis of 10 cells

4.6.2 Correlation vs. inter-synapse-distance

It has already been shown that simultaneous activation of many synapses within a short distance can lead to an amplification of the inputs (Schiller et al., 1997; Golding and Spruston, 1998). Thus, neighboring synapses having a high probability of being synchronously activated are more likely to fire the neuron. Hebb postulated that synapses contributing in firing a neuron are likely to be strengthened rather than eliminated (Hebb, 1949). If Hebb's postulate is applicable to the cells investigated here, there should be a tendency to strengthen neighboring synapses having a high correlation. An increased probability for strengthening neighboring synapses if they are simultaneously active would lead to an increased probability of neighboring synapses being coactive. To test this assumption across the set of synapses of an individual neuron I compared the activation patterns of all pairs of synapses and the distance between them along the dendrite. However, prior investigating the activation patterns of neighboring synapses, it was necessary to ensure that the activation patterns of two synapses at close range can reliably be assigned to the respective synapses.

To determine whether the activation patterns of two synapses can be clearly visualized and assigned to the respective synapses I analyzed activations of synaptic pairs lying close by one another. Figure 4-14 shows that it can be clearly distinguished between synchronous activation and single activation of either synapse even at synapses with an inter-synaptic distance of 8 μm .

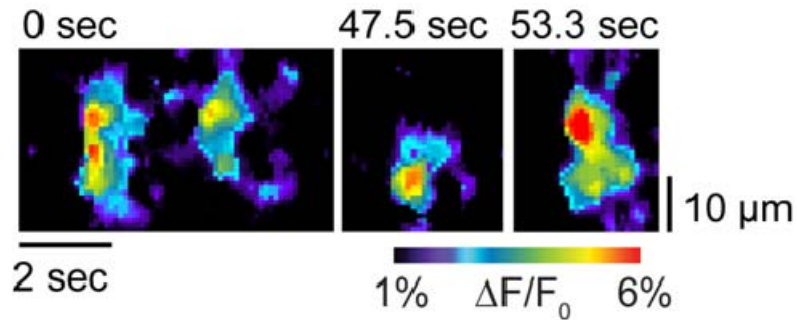


Figure 4-14 Synaptic activations at two neighboring synapses

Activation patterns of two synapses within 8 μm . Note: simultaneous and individual activation are clearly distinguishable.

After verifying that the activity at neighboring sites can clearly be assigned to one of the sites I investigated the interrelation of activation patterns and distance. Plotting the correlation of all pairs of synapses against their distance (Figure 4-15) revealed, that synapses being in close proximity are more often activated simultaneously than synapses being farther apart from one another. This result was not only seen in a single manually analyzed cell in which 14 synapses (91 pairs) were visualized (Figure 4-15 A), but also in the set of 10 automatically analyzed cells (Figure 4-15 B). Specifically, synapses with an inter synapse distance of less than 16 μm fired significantly more often in concert than synapses being farther apart from each other (Figure 4-15 B). Plotting the distance of all pairs of synapses against the likelihood of each pair being activated with 200-300 ms delay revealed that the observed relationship was restricted to a very narrow time window, since there was no interrelation of this delayed-correlation and distance (Figure 4-15 C).

Results

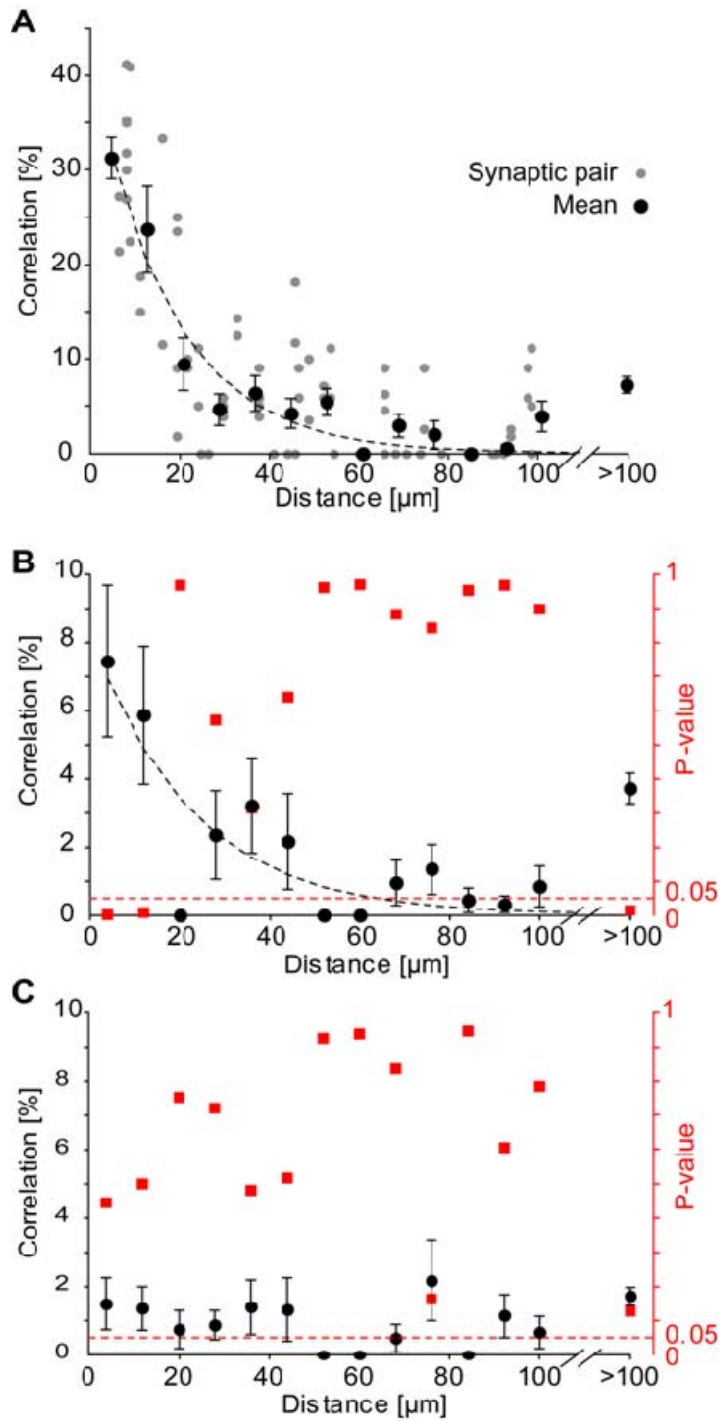


Figure 4-15 Correlation of pairs of synapses against their distance along the dendrite

A: Manual analysis of a single cell.

B: Automated analysis of 10 cells.

C: Automated analysis of 10 cells / time difference 200-300 ms

4.6.2.1 Analyzed synapses between stained axons and dendrites

To test whether the distance dependence of correlation is due to single axons making multiple synapses onto a single stretch of dendrite, I analyzed the synapses made by individual axons (see chapter 3.2.5.9). In seven high magnification z-stacks of hippocampal slices in which axons and dendrites were fluorescently labeled, the synapses of more than two hundred stained axons were analyzed. The axons formed 43 putative synapses with a fluorescently labeled dendrite but not a single axon formed more than one synapse onto an individual stretch of dendrite.

5 DISCUSSION

Many brain areas, including the hippocampus, show spontaneously occurring synaptic activity during development (Blankenship and Feller, 2010; Khazipov and Luhmann, 2006; O'Donovan, 1999; Wong, 1999). This spontaneous synaptic activity shapes the developing network by influencing the fate of newly formed synaptic connections (Hua and Smith, 2004; Huberman et al., 2008; Katz and Shatz, 1996). But also in the adult brain the major part of activity is spontaneous activity (Thivierge, 2009). Recently it has been proposed that the fate of synapses depends not only on correlated firing patterns of entire neurons, but also on the spatio-temporal patterns of firing of individual dendritic segments (Govindarajan et al., 2006; Mehta, 2004; Poirazi and Mel, 2001). Nevertheless, so far little is known about the spatial aspects of synaptic function on a sub cellular level (Chklovskii et al., 2004), since the functional development of synapses has mostly been studied using electrophysiological methods. Electrophysiological recordings provide a valuable tool to detect synaptic activity at high temporal resolution, but do not provide any information on the sub cellular distribution of spontaneous synaptic activity. They are therefore on their own not suitable to study spatio-temporal patterns of synaptic function. But, to investigate the spatial arrangement of activated synapses and specifically a potential interdependence of the activity and the development at neighboring synapses, it is necessary to map synaptic activity on the dendritic tree of developing neurons with single synapse precision.

The aim of this study was to describe spatio-temporal-patterns of spontaneous synaptic activity in developing hippocampal slice cultures. To visualize synaptic activity with sufficient temporal and spatial resolution, a new approach was chosen. Combining electrophysiological methods with calcium imaging at a relative high rate, I was able to show that a subset of local Ca^{2+} -transients is a reliable reporter for glutamatergic transmission and that these synaptic local Ca^{2+} -transients can be used to visualize

synaptic transmission with subcellular precision. The reconstruction of a major part of the synaptic input along the dendritic tree of an individual hippocampal pyramidal neuron, lead to what, to my knowledge, is the first mapping of a neurons “synaptome”. Finally, by correlating spatial and temporal aspects of spontaneous synaptic transmission I could show that synapses lying close by one another are activated in concert more often than synapses being farther apart from each other.

5.1 A subset of local Ca^{2+} -transients is linked to glutamatergic transmission

After establishing a method to simultaneously perform calcium imaging and patch-clamp-recordings and reliably and precisely align the two acquired datasets in time (see chapter 0), I showed that a major part of all local Ca^{2+} -transients coincided with synaptic currents (see chapter 4.2.2). To exclude that this coincidence is accidental, I plotted a histogram of time differences (Figure 4-3). The peak at zero in this histogram showed that more local Ca^{2+} -transients and synaptic currents are correlated in time than one would expect if this correlation was just the by chance correlation. One major advantage of such a histogram is that the overall activity level affects all time differences equally. Even very high activity levels leading to a high probability of accidental correlation would not lead to a peak like that seen in Figure 4-3. The graph with reversed time axis of the onsets of local Ca^{2+} -transients (inset Figure 4-3) serves as a control on the one hand side and is on the other hand illustrating the mentioned effect. Furthermore, since there is no peak in the graph with the reversed time axis, similar periodicities in the occurrence of local Ca^{2+} -transients and electrophysiological events can be excluded to cause the peak in Figure 4-3.

The broadness of the peak (± 0.5 s) and the symmetrical shape of the graph are due to the long duration of the bursts of synaptic input that occur in developing hippocampal slices. During the entire duration of bursts many individual synapses are activated but also many

electrophysiological events are detected. Thus, the histogram shows a large proportion of electrophysiological events preceding local Ca^{2+} -transients but it also shows a large proportion of local Ca^{2+} -transients preceding electrophysiological events.

The synaptic Ca^{2+} -transients are probably evoked by a series of events starting with the binding of a transmitter to a postsynaptic receptor. The activation of the postsynaptic receptor entails a depolarization of the postsynaptic membrane, which in turn results in opening of voltage-gated calcium channels and thus leads to an influx of Ca^{2+} -ions. The increasing concentration of Ca^{2+} -ions finally enhances the fluorescence efficacy of the calcium dye. This series of events could be expected to cause some delay from the synaptic activation to the occurrence and detection of the local Ca^{2+} -transients. However, even though it is a series of many events, the delay would be in the range of milliseconds, thus it was not detectable with the imaging settings described here.

Also exactly the opposite, namely a delay of the electrophysiological events compared to the local Ca^{2+} -transients caused by the time it takes the current to reach the soma, is not patent in the graph. This is not surprising, as the conduction velocity is estimated to be in the range of 0.12 m/s and faster than 1 m/s (Kawaguchi and Fukunishi, 1998; Stuart et al., 1993). Therefore, even synaptic currents evoked far out in the dendritic tree need only a very short time to reach the soma or the axon hillock. Assuming a speed of 0.12 m/s, a signal needs less than 10 ms (8.33 ms) for a distance 1 mm. The recorded field of view with the settings used is 208 μm x 208 μm . Since for this analysis the most basal apical dendrites are taken the maximal distance is less than 200 μm . This would lead to a maximum travelling time of less than 2 ms within the field of view which is far below the temporal resolution of the imaging settings used (imaging frequency 10 Hz). Even for recordings far out in the tips of the dendrites the maximal distance is probably less than 500 μm , meaning that even here the time it takes for the electrophysiological signal to reach the soma is far below the temporal resolution of the imaging.

As a next step, I investigated the dependence of the correlated local Ca^{2+} -transients on activation of ionotropic glutamate receptors. Blocking ionotropic glutamate receptors with APV and NBQX completely eliminated the peak in the histogram (Figure 4-3). Nevertheless, synaptic currents and local Ca^{2+} -transients still occurred, although at a lowered rate. That means a systematic correlation between these events would still be visible in the histogram plot.

This result clearly shows the existence of a subset of local Ca^{2+} -transients, which not only systematically coincided with synaptic currents, but also depended on glutamate receptor activation.

5.2 Stimulated Ca^{2+} -transients

To confirm the synaptic origin of the correlated local Ca^{2+} -transients, I set out to stimulate local Ca^{2+} -transients by presynaptic stimulation. Various techniques could be used to stimulate axons that make contact onto the imaged cells. The two most common ones are patching of a connected cell and stimulation by extracellular current injection. I chose to stimulate by extracellular current injection in close distance to the imaged dendrite, since for the purpose of this investigation, this approach had various advantages compared to paired patching: First, placing an extracellular stimulation electrode close to the imaged cell is easier and faster to accomplish than patch clamping of a second cell in the same slice. Second, extracellular stimulation leads to stimulation of not only a single axon but a bunch of axons, thus increasing the chance that one of those is contacting the imaged cell within the recorded field of view. This is an important factor since the connectivity in hippocampal slices at this age is low (Pavlidis and Madison, 1999; Sorra and Harris, 1993; Malinow, 1991). This low connectivity would render finding and patching connected pairs of cells unlikely. Especially as patching a connected pair would not be sufficient. Additionally, the stimulated synapse connecting those two neurons would have to be within the field of view of the camera.

Extracellular stimulation does, in general, not stimulate a single or a predefined subset of axons but this was also not required to confirm the synaptic origin of the correlated local Ca^{2+} -transients. To exclude stimulation of the entire network, the stimulation strength was adjusted to just reliably trigger a synaptic current in the patched cell. Too strong stimulation was to be avoided, since it could evoke local Ca^{2+} -transients by directly depolarizing a part of the dendrite of the imaged cell, especially as the stimulation electrode was placed in close proximity to the recorded and imaged cell. Thus, stimulation strength needed to be adapted to a level at which direct stimulation could be excluded.

As shown in chapter 4.2.3 local Ca^{2+} -transients could be triggered by extracellular current injections. This proof of principle was a necessary element in the chain of evidence indicating the synaptic origin of correlated local Ca^{2+} -transients. Importantly, in those experiments stimulation triggered synaptic currents and local Ca^{2+} -transients instantaneously, thus rendering it unlikely that the stimulation caused the Ca^{2+} -transients indirectly by secondary effects due to the excitation of the entire network. Furthermore, repeated stimulation in individual cells triggered local Ca^{2+} -transients repeatedly and reliably at the very same sites, rendering an accidental coincidence unlikely. It can be excluded that direct stimulation of the imaged dendrite triggered the Ca^{2+} -transients since the observed stimulated Ca^{2+} -transients never occurred at the part of the dendritic tree closest to the stimulation electrode. Moreover, the stimulated Ca^{2+} -transients resembled the spontaneous occurring ones in terms of duration and extension, indicating that the same mechanisms (activation of ionotropic glutamate receptors) may be involved in triggering these transients. Altogether and despite the low number of successfully stimulated cells, the information gained by the stimulation experiments seems sufficient to confirm the synaptic origin of the correlated local Ca^{2+} -transients.

5.3 Ca²⁺-transients as reporter of glutamatergic transmission

Not all local Ca²⁺-transients report synaptic activity, some are also triggered by other events, like BDNF signaling (Lang et al., 2007) or by Ins(1,4,5)P₃, which triggers Ca²⁺-release from intracellular stores (Nakamura et al., 1999). Therefore, to utilize local Ca²⁺-transients as reporter of synaptic activity it was required to distinguish between synaptic and non-synaptic local Ca²⁺-transients. Assuming that synaptic and non-synaptic transients occur at different sites each Ca²⁺-transient was assigned to a site along the dendrite. Subsequently, the synaptic character of each site was determined based on the fraction of local Ca²⁺-transients being correlated with synaptic currents at this site. As threshold for assigning a site to be synaptic a correlation of at least 1.5 times the by chance correlation was chosen (chapter 3.2.5.5).

Blocking ionotropic glutamate receptors by APV and NBQX did not lower the rate of local Ca²⁺-transients at non-synaptic sites but almost completely silenced synaptic sites (Figure 4-5) This demonstrates the capability to selectively discriminate between synaptic and non-synaptic sites upon the fraction of local Ca²⁺-transients being correlated with synaptic currents. Furthermore, any imprecision in assigning local Ca²⁺-transients to sites would hinder the clear separation into synaptic, i.e. glutamate receptor dependent, and non-synaptic sites, not affected by APV and NBQX. Thus, the combination of the almost complete absence of local Ca²⁺-transients at synaptic sites and the unchanged activity at non-synaptic sites in presence of APV and NBQX also confirmed the chosen way to assign individual local Ca²⁺-transients to their respective sites and to distinguish between individual sites.

APV and NBQX in the extracellular solution affect not only the imaged cell, but also influence the activity of the entire slice. That means the observed effect of APV and NBQX was not necessarily caused by direct blocking of the imaged synaptic sites. Also a reduction of the activity of the entire slice

could entail a reduced activity at the imaged sites. However, this possibility could be excluded in a different set of recordings, in which voltage gated sodium channels were blocked using TTX. TTX treatment prevents cells from spiking, thus remaining transmitter release is caused by spontaneous fusion of individual presynaptic vesicles with the presynaptic membrane (Brown et al., 1979). The frequency of the spontaneous vesicle fusions can be increased by latrotoxin (Deak et al., 2009). In recordings in the presence of TTX and latrotoxin synaptic currents as well as local Ca^{2+} -transients at synaptic and at non-synaptic sites could be observed. Yet, when additionally ionotropic glutamate receptors were blocked by NBQX and APV, sites previously described as synaptic sites did not reveal local Ca^{2+} -transients any longer. Nevertheless, local Ca^{2+} -transients at non-synaptic sites as well as synaptic currents, most likely reflecting GABAergic currents, were still observed.

Given that synaptic sites were almost completely silenced in the presence of APV and NBQX while non-synaptic sites continued firing without significant changes in frequency, the technique presented enables to visualize synaptic transmission. More precisely, it enables to visualize the purely excitatory, glutamatergic part of transmission without further need of pharmaceutical identification.

As mentioned, local Ca^{2+} -transients are caused by various events, thus they can be clustered in different groups. These groups might differ in their properties like duration, extension and amplitude. In this study only synaptic and non-synaptic local Ca^{2+} -transients were discerned, but the non-synaptic local Ca^{2+} -transients are a rather heterogeneous group as indicated by a large variation in their appearance. This suggests that non-synaptic transients are enclosing different subgroups of Ca^{2+} -transients. Although, discerning between the subgroups of non-synaptic local Ca^{2+} -transients might be interesting for further studies, it was beyond the scope of this thesis, which focuses on investigating synaptic activation patterns.

Yet, to distinguish between synaptic and non-synaptic transients merely upon the imaging data might be of great interest. This would allow monitoring synaptic activity in cells without the requirement of simultaneous patching the imaged cells, which could be advantageous for many applications. It would, for example, facilitate conducting long lasting experiments, since patch clamp recordings are difficult to maintain over longer periods of time. The comparison of the properties of local Ca^{2+} -transients at synaptic versus non-synaptic sites showed that these two subsets of local Ca^{2+} -transients indeed significantly differed in duration and extension (Figure 4-7). Unfortunately, a closer investigation revealed that the magnitude of the difference in relation to the standard deviation was too small to allow a classification of individual sites merely upon the imaging data. Hence, for future studies it might be worth investigating different approaches to gauge duration, extension and amplitude of the detected local Ca^{2+} -transients. Using different ways of filtering the imaging data as well as further enhancing the imaging quality might facilitate and improve an exact and faithful measurement of these properties. But also analyzing various other parameters of the signals, like rise time or decay time or normalizing each signal to the diameter of the stretch of dendrite of its site might help separating the different groups of local Ca^{2+} -transients.

An alternative and complete different approach would be to distinguish between synaptic and non-synaptic sites upon the correlation between sites. During bursts of activity many local Ca^{2+} -transients occurred synchronously. The sites at which those transients occurred were exclusively synaptic sites. Since synchronous activation of many non-synaptic sites was not observed, synaptic sites could be detected as those sites that are activated simultaneously with other sites. It remains to be shown, how many of the synaptic sites can be detected with this local-local correlation method and if this method works in slices of different developmental stages, but nevertheless this seems to be a promising approach.

5.4 Developmental changes

Visualizing synaptic inputs in pyramidal neurons in hippocampal slices from older rats (P7-8) revealed an increased frequency and density of synaptic Ca^{2+} -transients (chapter 4.3). This most likely reflects the increasing number of synapses and the increasing frequency of synaptic activation due to the formation of glutamatergic synapses during the first postnatal weeks, which has been described previously (Hsia et al., 1998b; Ben Ari, 2001). The density of synaptic inputs at this developmental stage is already at the spatial resolution limit of the setup used. Furthermore, in even later stages of development also the temporal resolution of the used imaging settings would probably not allow distinguishing between synaptic and non-synaptic local Ca^{2+} -transients upon the fraction of correlated local Ca^{2+} -transients. The frequency of synaptic activation in those slices would probably exceed the frame rate and thus most Ca^{2+} -transients would appear to be correlated. Thus, a separation of synaptic and non synaptic sites upon the correlation of the site with synaptic currents would be rendered the impossible. However, these problems could be overcome by various approaches.

To reach a spatial and temporal resolution sufficient to reliably visualize synaptic activity in adult slices, different imaging approaches should be taken into consideration. For instance, fast two-photon microscopy could provide the high spatial and high temporal resolution needed if only a few selected spots of interest, like synapses, or a few lines along the dendrite of interest are scanned (Helmchen and Denk, 2005; Denk et al., 1994; Denk et al., 1996; Denk et al., 1990). This approach would require a scanning microscope, i.e. a two-photon microscope, capable of fast scanning along arbitrary lines in x-y-z-dimension. One problem when scanning only along defined lines is that small movements of the dendrite or the entire cell could resemble local Ca^{2+} -transients in the imaging data. This would impair the signal detection as those movements can hardly be distinguished from local Ca^{2+} -transients. To overcome this problem the two-photon setup should ideally allow recording two emitted wavelength

simultaneously thus being capable of ratiometric imaging. This would allow imaging cells stained with two different dyes, being one a calcium sensitive dye, like for example, Oregon Green BAPTA 1, and the other a calcium insensitive dye, like Alexa Fluo 594. Since these two dyes could be excited simultaneously by a two-photon laser and the emitted wavelengths could be separated and imaged simultaneously using appropriate filter sets in two independent emission pathways, this approach would enable imaging both dyes without lowering the temporal resolution. Movements of the imaged slice or dendrite would affect both datasets equally, thus using an F_0 deduced from the calcium insensitive imaging (Alexa Fluo 594) could help to detect the movements and thereby improve the signal detection (Svoboda and Yasuda, 2006; Helmchen, 2005; Oertner, 2002; Grewe and Helmchen, 2009).

But also with conventional fluorescence microscopy the spatial resolution can be increased, for example by reducing the binning. But, reducing the binning reduces the signal to noise ratio and thus, impairs the signal detection. This impairment could be mitigated by either using more light, which would lead to increased phototoxicity, or by using objectives with a higher numerical aperture, which would decrease the focal volume. Additionally, increasing the spatial resolution would tremendously increase the amount of data recorded. Doubling the spatial resolution would result in quadrupling the amount of data, making handling and analysis of the acquired data demanding. Furthermore, the approach to discern synaptic and non-synaptic sites upon the correlation of the local Ca^{2+} -transients with synaptic currents at each site in mature slices, would additionally require an increased temporal resolution as mentioned above. This could be achieved by reducing the exposure time, which would in turn decrease the imaging quality and increase the amount of data recorded. In addition to these disadvantages, the possible increase in temporal resolution with the described experimental setup is limited and would most probably not be sufficient to map synaptic inputs in slices of adult rats. But, different approaches of discerning synaptic and non-synaptic sites could be used as already mentioned in chapter 4.3. For those approaches the temporal

resolution would not have to be increased, but nevertheless, they would require a setup providing sufficient spatial resolution to clearly separate individual sites. As discussed in chapter 5.3 synaptic and non synaptic local Ca^{2+} -transients might be distinguishable merely upon the imaging data. If one succeeds in finding criteria to clearly separate synaptic and non-synaptic local Ca^{2+} -transients in slices of young rats one still would need to show that these criteria remain unchanged in the more mature slices. But, as it is shown in Figure 4-7, the magnitude of the difference in duration of synaptic and non-synaptic transients is already decreased at slices of P7-8 rats. At the first glance this could indicate an impaired distinction, but this indication may be misleading for several reasons. Firstly, cells with too high electrophysiological activity were excluded from the analysis (see chapter 3.2.5.5). Secondly, an impaired distinction due to high electrophysiological activity would result in non-synaptic sites to be assigned to be synaptic, since some local Ca^{2+} -transients would accidentally appear to be correlated due to the high fraction of frames in which synaptic currents are detected. Thus, high levels of electrophysiological activity would indeed decrease the average duration of the synaptic events, since the non-synaptic events were on average shorter lasting. But, it seems unlikely, that only a certain sub-population of the non-synaptic sites, for example, those displaying short lasting Ca^{2+} -transients, would be assigned to be synaptic. Consequently the duration of the non-synaptic events would not necessarily be changed or increased. Thirdly, neither the standard deviation of the synaptic transients nor the standard deviation of the non-synaptic transients was dramatically changed, which would be expected if an impaired distinction would be responsible for the changed properties. Taken together, the reduced magnitude of difference in duration of synaptic and non-synaptic events seems to reflect a real change in the properties of the transients and not an impaired distinction of sites. That means in turn, that properties that reliably discern synaptic and non-synaptic sites at a given age, do not necessarily discern sites at different stages of development as they may change during development.

Most promising to reliably distinguish between synaptic and non-synaptic sites in slices with high electrophysiological activity is, in my eyes, an approach that takes use of the correlation between synaptic sites, as described in chapter 5.3. But, also prior using this approach it would need to be shown that it works in later stages of development.

5.5 Mapping synaptic inputs in individual neurons

Having established local Ca^{2+} -transients as indicator of synaptic transmission, I mapped active synapses across large parts of the dendritic tree of individual neurons. The fast z-stepping as described in chapter 3.2.4 was a necessary prerequisite, which allowed gathering comprehensive data of large parts of the dendritic tree within the field of view. Nevertheless, the whole dendritic arborization of a pyramidal cell was larger than the field of view thus making imaging sessions at different locations along the dendritic tree of a single neuron and subsequent assembling of the acquired data inevitable.

Mapping large parts of the dendritic arborization of individual CA3 pyramidal neurons illustrated that synaptic local Ca^{2+} -transients were detectable across the entire dendritic tree. However, the density of synaptic input seemed to be lower in regions more distal than close by the soma leading to the concern that classification of sites could be impaired by attenuation of the electrical currents originating at sites farther apart from the recording site - the soma. This attenuation could in principle lead to a reduced detection efficacy of small synaptic currents of distal synapses (Djurisic et al., 2004; Henze et al., 1996) and therefore to an increased probability of wrongly assigning a distal site to be non-synaptic. However, the ratio between synaptic and non synaptic local Ca^{2+} -transients was not reduced in distal dendrites compared to proximal dendrites making an impaired classification of sites unlikely (see chapter 4.4).

To summarize and view the data gathered from mapping individual neurons, I chose to represent it in a diagram, similar to a conventional

Sholl diagram (Figure 4-10). This allowed analyzing data gathered from many individual neurons despite their different geometries (Sholl, 1953). While a conventional Sholl diagram represents the structural complexity of a cell against the distance from the soma, the functional Sholl diagram reflects the synaptic input received at a given distance of the soma.

Comparing a conventional Sholl diagram with the functional Sholl diagrams revealed that the structural complexity of a given area differed widely from its functional significance in terms of synaptic inputs. Specifically, the number of dendritic branches at the most proximal parts of the apical dendrites was found to be low, but the synaptic activity in this area was high in relative terms (normalized to the length of dendrite) as well as in absolute terms (frequency of synaptic activations). This area corresponds in parts still to the pyramidal cell layer and in parts to the *stratum lucidum*. In *stratum lucidum* mossy fibers pass through the CA3 region and are known to form synapses onto pyramidal neurons. It has been shown, that in the hippocampus of rats mossy fibers start extending into the CA3 region at very early stages of development (Dailey et al., 1994). Already in the first postnatal week immature contacts between mossy fibers and CA3 pyramidal neurons are formed (Stirling and Bliss, 1978). But, even though potentials evoked by mossy fibers can be recorded in CA3 pyramidal neurons already at P2 (Bliss et al., 1974), the well known giant synapses, connecting mossy fibers and CA3 pyramidal neurons in the adult hippocampus, start to emerge only in the second week after birth (Dailey et al., 1994; Stirling and Bliss, 1978). Thus, it is likely that at least a part of the observed synaptic activity in this area represented activation of immature synapses of mossy fibers.

Another area that revealed high levels of activity is the area spanning from 100 μm - 170 μm distance of the soma. This area represents the *stratum radiatum*, thus it contains mostly associational connections between CA3 neurons. In this area also the Schaffer collateral connections are located, but Schaffer collaterals are fibers connecting CA3 neurons to CA1

neurons (Amaral and Lavenex, 2007), thus, they should not contribute in firing CA3 neurons.

The absolute frequency of synaptic input in the basal dendrites was higher than in any part of the apical dendrite. However, in this area, which is called the *stratum oriens*, there was also a large number of dendritic branches. Thus, the density of synaptic input was similar to the active regions of the apical dendrites described before. Dendrites in *stratum oriens*, receive input mainly from CA3 to CA3 associational connections, although it has been shown that at least in slice cultures mossy fibers can terminate in this region (Robain et al., 1994).

The frequency and density of the input at distances of 200 μm and more was low. This might be due to the fact that the slices were not yet mature and thus the dendrites were still growing. Thus, that region of the dendrites was relatively young and maybe not yet as densely innervated as the older parts of the dendritic tree.

It is intriguing, that the structural complexity of the dendritic arborization in different regions of an individual cell did not correlate with the amount of input impinging onto these parts. However, the data gathered and presented here reflects only one stage of development. The functional Sholl diagrams of more mature slices or of slices from adult rats remain to be investigated. It would be interesting to map synaptic activity in slices of different developmental stages and compare the resulting functional and structural Sholl diagrams. Subsequently, one could relate the changing activation patterns with the developmental events that have been shown to occur in each developmental stage. However, mapping the synaptic activation patterns of later developmental stages requires a different approach as mentioned in chapter 5.4.

Another interesting question would be to study differences between slice cultures, acute slices and the *in vivo* situation. For example, it has been shown that pyramidal neurons in the CA3 region in slice cultures are not as densely packed as they are *in vivo* (Robain et al., 1994) and also the localization of the mossy fibers has been shown to be less extended *in*

in vivo than in cultured slices (Robain et al., 1994). Nevertheless, so far little is known about differences in the synaptic activation patterns in slice cultures, acute slices and *in vivo*. Here, the isolation of slice cultures from external inputs should be reflected in the functional Sholl diagram, and this isolation from external inputs might also influence the fate of existing connections. Furthermore, in the *in vivo* situation there is also a high connectivity between the hippocampi in the two hemispheres, which does not exist in slice cultures or in acute slices, which is also missing in slice cultures and in acute slices. That means, differences in the functional Sholl diagram between the *in vivo* situation and the *in vitro* situation are to be expected, but to what extent this differences influence the entire wiring diagram remains speculative and has to be investigated.

It is important to keep in mind that the maps of synaptic activation do not allow any prediction about the impact of a certain region on firing action potentials. The maps of synaptic activation are a descriptive representation of the frequency and density of synaptic input impinging onto the dendritic arbor of cell in different regions. The influence on the membrane potential at the soma of the cell exerted by each synaptic activation depends on a variety of factors. Aside from the distance from the soma, also the existence, the number, and the distribution of voltage gated ion channels and many other factors may shape the actual impact of an individual synaptic activation and thus its probability in firing the neuron.

5.6 Synaptic patterns during bursts of synaptic activation

Spontaneous activity propagating through the developing brain is a major factor shaping the initial synaptic wiring diagram in many brain areas, amongst them the hippocampus (Ben-Ari et al., 1989a; Kasyanov et al., 2004; Mohajerani and Cherubini, 2006; Sipila et al., 2006). In the hippocampus this spontaneous activity is mostly referred to as giant depolarization potentials (GDPs). In voltage clamp recordings they are

reflected by huge synaptic currents caused by barrages of synaptic input impinging on the recorded cell within a very short time window. Since I was interested in temporal-spatial-patterns of synaptic activity, I analyzed the activated synapses during successive bursts. However, no repetitive patterns of synaptic activation could be found. Different representations of the synaptic activation pattern during successive bursts (Figure 4-11) were created and examined by colleagues of mine as well as by myself to search for the occurrence of recurrent patterns of activations. Unfortunately, no reoccurring motif and no pattern describing the activations during successive bursts could be found. As shown (Figure 4-12), even bursts with similar amplitude and time course reflect activations of different sets of synapses.

However, this does not necessarily mean that the synaptic activation patterns during successive bursts are completely random. Various reasons might hinder spotting patterns of synaptic activation. First of all, recordings represent only a relative short time slot. Thus, also all chosen representations, which were used to search for patterns of activation, can only display this short period of time. This complicates the detection of a potential periodicity in synaptic activation. Secondly, even though analysis was done completely automatically to guarantee reliability and objectivity, there are still variations in the reliability of signal detection, for example due to changes in the imaging quality. These variations may affect consecutive recordings or even consecutive images unequally thus leading to a variance in the analysis, which in turn could make the recognition of a pattern more difficult. However, most important is the fact that only patterns that are specifically searched for can be found, making the detection of complicated and uncommon patterns unlikely. Short lasting often repeated motifs are easier to detect than complicated long lasting ones that occur only infrequently. Different approaches can be chosen to search for patterns. It seems promising to take advantage of our inherited ability to categorize and to recognize all sorts of patterns. This ability was crucial for the surviving of our ancestors, as it allowed identification of certain patterns being a sign for food or warning of danger.

Consequently, there must have been an evolutionary pressure enhancing our mental sorting mechanisms. But, to find the occurring motifs, it is essential to find a representation of the data revealing the underlying patterns. For this purpose, uncommon representations like representing each synaptic site by a defined tone pitch and subsequently listening to the “melody” of bursts might be useful. A first attempt in this direction was rather unsuccessful but this can be due to the fact that synapses were not represented as harmonic tones but rather as arbitrary noises.

5.7 Correlated activation of individual pairs of synapses

5.7.1 Correlation vs. vertical distance from the soma

According to the postulate of Hebb, synapses that persistently take part in firing a neuron should be strengthened (Hebb, 1949). To take part in firing a neuron the electrical signals generated by synaptic activation are to reach the initial segment of the axon, the axon hillock, to depolarize it above a certain threshold to finally evoke an action potential, which in turn triggers transmitter release in presynaptic terminals (Stuart et al., 1997). Multiple signals arriving at the same point in time at the axon hillock add up and are, therefore, more likely to reach the threshold for evoking an action potential (Agmon-Snir and Segev, 1993). Thus inputs being correlated at the initial segment of the soma should be more likely to be stabilized or strengthened. Axons pass the dendrites of CA 3 pyramidal neurons in an almost orthogonal angle. Thus, it seemed likely that neighboring axons make contact at the same distance from the soma. Assuming that neighboring axons carry similar information this could lead to an increased likelihood of synchronous synaptic activation at similar vertical distances from the soma. However, neither pairs of synapses at the same vertical distance from the soma nor pairs of synapses at the same distance from the soma along the dendrite revealed a significant higher likelihood to be activated in concert than any random pair of

synapses (Figure 4-13). However, the low connectivity of the hippocampus in this stage of development which entails a low probability of neighboring axons to make contact with one and the same CA3 pyramidal neuron might also hinder such a correlation to occur.

5.7.2 Correlation vs. inter-synapse-distance

It has been proposed already in 1967 that dendrites shape the synaptic current (Rall et al., 1967). This shaping of the synaptic current already implies that synaptic currents originating in different regions of the dendritic tree have different impact on the cell body and thus different probabilities to contribute in firing the neuron. Furthermore, recent publications suggest that dendrites act not only as passive cable like structures, but as active, information integrating units (Hausser and Mel, 2003; Hausser et al., 2000). These non-linearities may serve various requirements. In some cells they seem to simply compensate for the different attenuation of currents evoked at different distances from the soma (Stricker et al., 1996; Magee and Cook, 2000). However, recent studies suggest that parts of dendrites may also act as computational units. For example it has been shown that dendrites are capable of amplifying synaptic currents depending on the size of the current and the context of the synaptic activation, like activity at neighboring synapses (Johnston et al., 1996). This is proposed as a mechanism boosting the computational power and information storage capacity (Poirazi and Mel, 2001) by increasing the number of computational units within the system. However, non-linear integration in itself is not sufficient to affect the computational power. Another prerequisite to boost the computational power is a wiring scheme with a precision exceeding just cellular resolution. Only the combination of those two properties would allow single dendrites or parts of dendrites to be individual computational units and thus would multiply the number of computational units, which in turn would lead to an enhancement of the computational capacity of an individual neuron and thus the neuronal network as an entire (Govindarajan et al., 2006; Mel and Schiller, 2004). The idea that parts of

a single neuron and not the entire neuron might serve as smallest computational units has previously been proposed mainly on theoretical grounds (Poirazi and Mel, 2001). By now it has also been shown that plasticity mechanisms exist which could lead to a subcellular wiring precision (Engert and Bonhoeffer, 1997; Harvey and Svoboda, 2007). Some of those plasticity mechanisms seem to favor the potentiation of synapses along a dendrite being relatively often coactivated, thus preferentially connecting those axons to a common stretch of dendrite which share similar patterns of activation (Govindarajan et al., 2006; Mehta, 2004; Poirazi and Mel, 2001). Since the above described approach enables visualization of spontaneous synaptic activity, it seemed likely that a closer investigation of the patterns of co-activations of synapses could reveal the outcome of such a local plasticity rule.

Investigation of the interrelation of correlation and distance of pairs of synapses revealed that synapses being in close neighborhood tend to fire more often in concert than synapses being farther apart from each other (Figure 4-15). This phenomenon was seen in the set of 10 completely automatically analyzed cells, but also in a single cell in which synaptic local Ca^{2+} -transients were detected manually (see also chapter 3.2.5.6). Specifically, synaptic pairs in close neighborhood (0-8 μm and 8-16 μm) were significantly more often activated simultaneously than synapses being farther apart from each other. In contrast, activation of pairs of synapses at a specific delay of 200-300 ms showed no interrelation with distance, indicating that the time window for strengthening by co activation is short, more precisely less than 200 ms.

The remaining question is which mechanism caused neighboring synapses to be more often activated than synapses being farther apart from each other. The effect could for example be caused by individual axons making multiple synapses in very close distance. However, this seems highly unlikely for a couple of reasons:

Firstly, the connectivity in the hippocampus at this stage of development is extremely low, and even at later developmental stages axons form only

one to five synapses with a pyramidal cell and rarely more than one functional bouton with an individual dendrite (Pavlidis and Madison, 1999; Sorra and Harris, 1993).

Secondly, in none of the stimulation experiments (chapter 4.2.3) pre-synaptic stimulation caused synaptic local Ca^{2+} -transients at two synaptic sites at a distance of 20 μm or less.

Thirdly, analysis of anatomical data (Lohmann and Bonhoeffer, 2008) revealed that the stained axons (more than 200) passed dendrites of pyramidal cells in an almost orthogonal angle and not in a single case one axon formed more than one synapse onto an individual dendrite within 16 μm (chapter 4.6.2.1).

Thus, a different mechanism seems to cause the interrelation of distance and correlation of synapses. As mentioned above, plasticity mechanisms have been shown to exist which strengthen neighboring synapses that display similar activity patterns (Govindarajan et al., 2006; Mehta, 2004; Poirazi and Mel, 2001). Such an increased likelihood for being strengthened and stabilized if correlated with one's neighbors could be sufficient to entail the here observed effect and therefore to provide a basis for setting up a wiring diagram at subcellular resolution. Thus, these mechanisms seem to be the most likely explanation. Moreover the range estimated for such a local plasticity rule – around 10 μm (Harvey and Svoboda, 2007) - is similar to the distance for an increased likelihood of simultaneous activation of synapses found in this study.

6 CONCLUSION AND OUTLOOK

In my thesis I developed a technique to visualize active glutamatergic synapses in developing CA3 pyramidal neurons. This technique allows mapping the synaptic input in large parts of the dendritic tree of individual neurons with single synapse precision. Even though calcium imaging is known to report for synaptic activity in spiny (Denk et al., 1996; Zito et al., 2009; Murphy et al., 1994) as well as in non spiny dendrites (Goldberg et al., 2003; Murthy et al., 2000), until now the synaptic activity impinging onto individual neurons has never been mapped with single synapse precision and thus, the spatio-temporal patterns of synapse activation are poorly investigated.

By mapping the synaptic activity of large parts of the dendritic tree and investigating the occurring spatio-temporal patterns I described a local activity pattern, namely an increased probability of neighboring synapses to be active in concert (Figure 6-1). The existence of such a local activity pattern shows that the synaptic wiring diagram has a subcellular specificity. This specificity is a prerequisite to enable parts of the dendritic tree to be independent computational units, which has been shown to tremendously increase the computational power of a single neuron and of the entire network (Poirazi and Mel, 2001). To my knowledge, this is the first time that patterns of spontaneous synaptic activity are visualized with single synapse precision. Consequently, it is also the first direct indication that in the synaptic wiring diagram synapses carrying similar input patterns are preferably connected in close proximity to one another, which might be the result of a local plasticity mechanism that has been described previously.

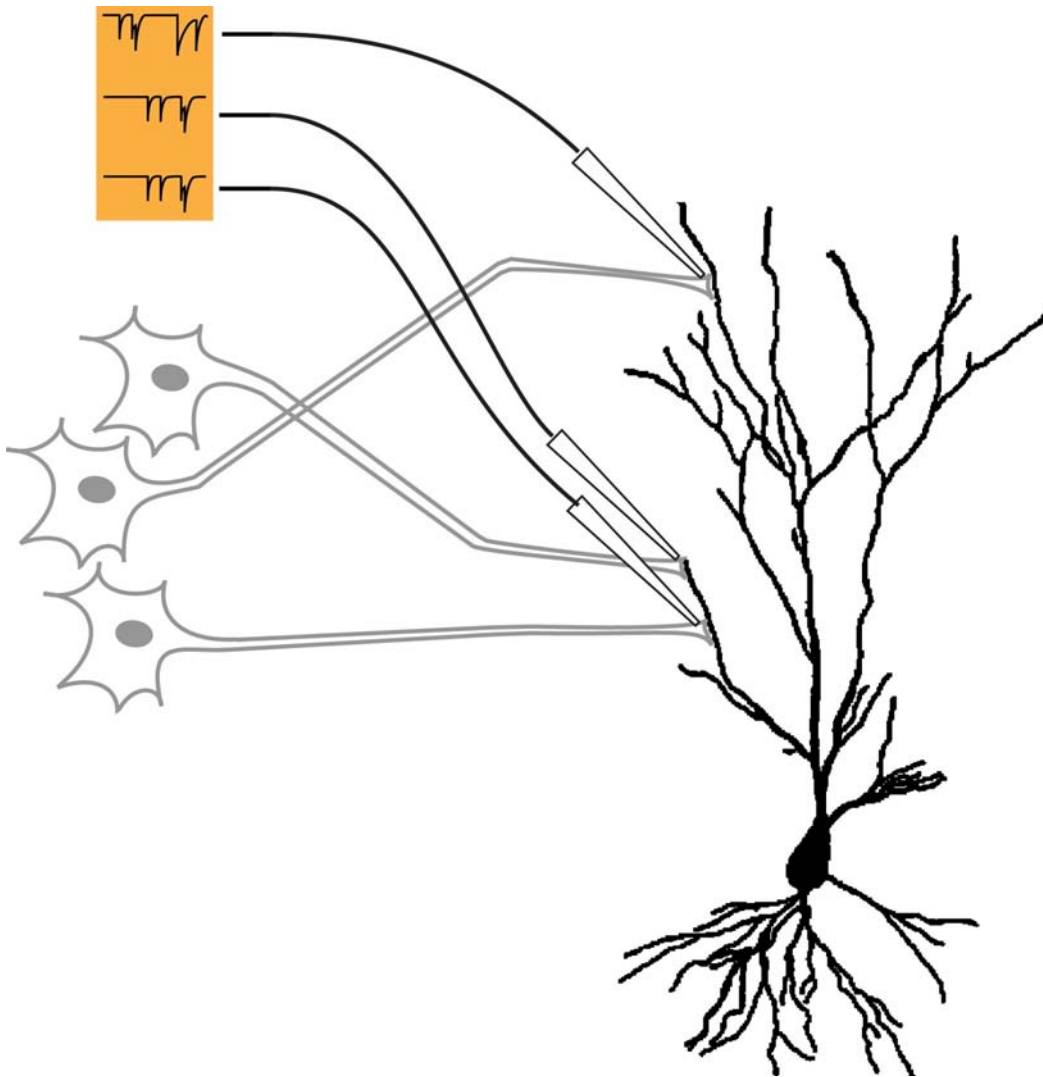


Figure 6-1 Scheme of subcellular wiring diagram

Orange area shows electrical activity measured at shown positions.

Note: Axons showing correlated activity are preferably connected in close neighborhood.

In future studies it would be interesting to investigate if similar spatio-temporal patterns can be found in different regions of the brain during development and might possibly even be a hallmark of the developing mammalian brain. On the other hand, if they occur only in certain areas of the brain, this would raise the question in which areas and why.

The combination of techniques described in this thesis, namely simultaneously imaging the Ca^{2+} -concentration and performing

electrophysiological recordings, is not only applicable to study spontaneous activity, but could also be used to visualize stimulated synaptic activity. By doing so, one could, for example, map the distribution of synaptic inputs of different axons onto an individual postsynaptic neuron. If the data is analyzed in real time, one could also pair stimulations with spontaneous activity of neighboring synapses and investigate whether the potentiation of synapses is facilitated when two neighboring sites are activated simultaneously.

It would be challenging to adapt the technique to visualize synaptic activity to the needs and limitations of *in vivo* imaging. For *in vivo* applications one would preferably choose an imaging approach without the requirement of simultaneously patching the imaged cell. As a criterion for defining synaptic sites one could, for example, take the correlation between sites as described in chapter 5.3. Visualizing synaptic activity *in vivo* would, for example, allow investigating the activation patterns triggered by sensory input, like visual stimuli. Subsequent comparison of the activation patterns evoked by sensory stimuli and the activation patterns evoked by spontaneous activity could allow deducing the “images” created by spontaneous activity. Furthermore, if spontaneous activity is indeed a major factor shaping the wiring diagram, spontaneously coactive axons should carry related information when transmitting sensory stimuli. For example, in topographically organized areas of the brain one might expect axons of neurons in neighboring receptive fields to be often simultaneously active. This might be reflected in the spontaneous activity shaping the wiring diagram. Thus, when mapping the synaptic input evoked by sensory stimulation of neighboring receptive fields, I would expect to see a similar local activation pattern like described in this thesis.

Another question to address is how functionality is maintained over time in such a complex and plastic network like the mammalian brain. Are there synapses that do not show plasticity at all or do certain spontaneously occurring activity patterns strengthen “important” synapses or prevent them from getting depressed or eliminated?

Less challenging but, to my mind, not less interesting would be adapting the imaging technique to the requirements of the increased synapse density of more mature slices and investigating the activity patterns at different developmental stages. In this line, one might want to know whether in the adult brain adjacent synapses are more often synchronously active than synapses being farther apart from each other. Furthermore, it would be interesting to compare the functional Sholl diagram developed in this thesis with the structural Sholl diagram in mature systems. Is there a relation between the structural complexity and the synaptic activity in mature dendrites? On the long run, visualizing synaptic activity with single synapse precision might allow to map not only the synaptic activity but also the functional significance of a region, i.e. its impact on firing the cell.

To my mind, visualizing synaptic activity and mapping the synaptic input of individual neurons is an important requirement, which might help deciphering the complex computations performed by individual neurons or even parts of a neuron. For example imaging calcium dynamics of electroporated cells at very high rates without performing electrophysiological recordings, might facilitate to map the synaptic input and simultaneously allow the cell for firing action potentials. Such an approach could allow, for example, the identification of those synapses that regularly contribute in firing a cell. Subsequently, one could investigate whether those synapses are strengthened over time. But also studying the compositions of synaptic activations that entail spiking of the neuron would be interesting. For example, visualizing excitatory and inhibitory synaptic activations simultaneously and correlating them to the output of the neuron could allow decrypting the various interactions of excitation, inhibition, attenuation and conductivity within the dendritic tree. Decoding these interactions is necessary in order to predict the output of an individual neuron upon a given input which would be a big step towards understanding how individual neurons process information. Figuring out how the individual elements of the brain process information is a necessary prerequisite to understand the function of the brain,

However, this is still a far way to go and it requires analyzing huge amounts of data, which is facilitated by modern computers. The current rapid progress in computer science and the accompanying improvements in available and affordable storage and computing systems allow acquiring huge amounts of data in short periods of time and subsequent handling and analysis of this of data. Complicated algorithms requiring immense computational power can be performed by relative standard computers and thus by normally equipped laboratories to an increasing extent. This is a necessary prerequisite to gain further insight into the mammalian brain with its estimated 10^{14} synaptic connections. Faster and more powerful computer systems in combination with more sophisticated methods of analysis will facilitate deciphering the complex interaction of structural and functional changes during development and during learning and memory formation, thus, eventually we might become able to understand how a brain works and become aware of the differences between species in perception, information processing and memory formation.

7 BIBLIOGRAPHY

Agmon-Snir H, Segev I (1993) Signal delay and input synchronization in passive dendritic structures. *J Neurophysiol* 70:2066-2085.

Aizawa H, Hu SC, Bobb K, Balakrishnan K, Ince G, Gurevich I, Cowan M, Ghosh A (2004) Dendrite development regulated by CREST, a calcium-regulated transcriptional activator. *Science* 303:197-202.

Albantakis L, Lohmann C (2009) A simple method for quantitative calcium imaging in unperturbed developing neurons. *J Neurosci Meth* 184:206-212.

Amaral DG (1993) Emerging principles of intrinsic hippocampal organization. *Curr Opin Neurobiol* 3:225-229.

Amaral DG, Lavenex P (2007) Hippocampal Neuroanatomy. In: *The Hippocampus Book* (Andersen P, Morris R, Amaral DG, Bliss TV, O'Keefe J, eds), pp 37-114. New York: Oxford.

Andersen P, Morris R, Amaral DG, Bliss TV, O'Keefe J (2007) The Hippocampal Formation. In: *The Hippocampus Book* (Andersen P, Morris R, Amaral DG, Bliss TV, O'Keefe J, eds), pp 9-36. New York: Oxford.

Andersen P, Trommald M, Jensen V (1994) Low synaptic convergence of CA3 collaterals on CA1 pyramidal cells suggests few release sites. *Adv Second Messenger Phosphoprotein Res* 29:340-351.

Ben Ari Y (2001) Developing networks play a similar melody. *Trends Neurosci* 24:353-360.

Ben-Ari Y, Cherubini E, Corradetti R, Galarsa J-L (1989a) Giant synaptic potentials in immature rat CA3 hippocampal neurones. *J Physiol (Lond)* 416:303-325.

Ben-Ari Y, Cherubini E, Corradetti R, Galarsa J-L (1989b) Giant synaptic potentials in immature rat CA3 hippocampal neurones. *J Physiol (Lond)* 416:303-325.

Biederer T, Sara Y, Mozhayeva M, Atasoy D, Liu X, Kavalali ET, Sudhof TC (2002) SynCAM, a synaptic adhesion molecule that drives synapse assembly. *Science* 297:1525-1531.

Blankenship AG, Feller MB (2010) Mechanisms underlying spontaneous patterned activity in developing neural circuits. *Nat Rev Neurosci* 11:18-29.

Bliss TV, Chung SH, Stirling RV (1974) Proceedings: Structural and functional development of the mossy fibre system in the hippocampus of the post-natal rat. *J Physiol* 239:92P-94P.

Bliss TVP, Lomo T (1973) Long-lasting potentiation of synaptic transmission in the dentate area of the anaesthetized rabbit following stimulation of the perforant path. *J Physiol (Lond)* 232:331-356.

Bibliography

Bolshakov VY, Siegelbaum SA (1995) Regulation of hippocampal transmitter release during development and long-term potentiation. *Science* 269:1730-1734.

Brown TH, Wong RK, Prince DA (1979) Spontaneous miniature synaptic potentials in hippocampal neurons. *Brain Res* 177:194-199.

Carrasco MA, Jaimovich E, Kemmerling U, Hidalgo C (2004) Signal transduction and gene expression regulated by calcium release from internal stores in excitable cells. *Biol Res* 37:701-712.

Chandrasekaran AR, Plas DT, Gonzalez E, Crair MC (2005) Evidence for an instructive role of retinal activity in retinotopic map refinement in the superior colliculus of the mouse. *J Neurosci* 25:6929-6938.

Chavis P, Westbrook G (2001) Integrins mediate functional pre- and postsynaptic maturation at a hippocampal synapse. *Nature* 411:317-321.

Cherubini E, Gaiarsa JL, Ben-Ari Y (1991a) GABA: an excitatory transmitter in early postnatal life. *Trends Neurosci* 14:515-519.

Cherubini E, Gaiarsa JL, Ben-Ari Y (1991b) GABA: an excitatory transmitter in early postnatal life. *Trends Neurosci* 14:515-519.

Chklovskii DB, Mel BW, Svoboda K (2004) Cortical rewiring and information storage. *Nature* 431:782-788.

Christie BR, Magee JC, Johnston D (1996) Dendritic calcium channels and hippocampal long-term depression. *Hippocampus* 6:17-23.

Cline H (2003) Sperry and Hebb: oil and vinegar? *Trends Neurosci* 26:655-661.

Cline HT (2001) Dendritic arbor development and synaptogenesis. *Curr Opin Neurobiol* 11:118-126.

Cohen S, Greenberg ME (2008) Communication Between the Synapse and Nucleus in Neuronal Development, Plasticity, and Disease. *Annu Rev Cell Dev Biol*.

Cohen-Cory S (2002) The developing synapse: construction and modulation of synaptic structures and circuits. *Science* 298:770-776.

Cornelisse LN, van Elburg RA, Meredith RM, Yuste R, Mansvelder HD (2007) High speed two-photon imaging of calcium dynamics in dendritic spines: consequences for spine calcium kinetics and buffer capacity. *PLoS ONE* 2:e1073.

Cossart R, Ikegaya Y, Yuste R (2005) Calcium imaging of cortical networks dynamics. *Cell Calcium* 37:451-457.

Cowan WM, Kandel ER (2001) A Brief History of Synapses and Synaptic Transmission. In: *Synapses* (Sudhof TC, Stevens CF, eds), pp 1-89. New York: The Johns Hopkins University Press.

Dailey ME, Buchanan J, Bergles DE, Smith SJ (1994) Mossy fiber growth and synaptogenesis in rat hippocampal slices in vitro. *J Neurosci* 14:1060-1078.

- Deak F, Liu X, Khvotchev M, Li G, Kavalali ET, Sugita S, Sudhof TC (2009) α -Latrotoxin Stimulates a Novel Pathway of Ca^{2+} -Dependent Synaptic Exocytosis Independent of the Classical Synaptic Fusion Machinery. *J Neurosci* 29:8639-8648.
- Delpire E (2000) Cation-Chloride Cotransporters in Neuronal Communication. *News Physiol Sci* 15:309-312.
- Denk W, Delaney KR, Gelperin A, Kleinfeld D, Strowbridge BW, Tank DW, Yuste R (1994) Anatomical and functional imaging of neurons using 2-photon laser scanning microscopy. *J Neurosci Meth* 54:151-162.
- Denk W, Strickler JH, Webb WW (1990) Two-photon laser scanning fluorescence microscopy. *Science* 248:73-76.
- Denk W, Yuste R, Svoboda K, Tank DW (1996) Imaging calcium dynamics in dendritic spines. *Curr Opin Neurobiol* 6:372-378.
- DiCiommo DP, Bremner R (1998) Rapid, high level protein production using DNA-based semliki forest virus vectors. *J Biol Chem* 273:18060-18066.
- Djurisic M, Antic S, Chen WR, Zecevic D (2004) Voltage Imaging from Dendrites of Mitral Cells: EPSP Attenuation and Spike Trigger Zones. *J Neurosci* 24:6703-6714.
- Dudek SM, Bear MF (1992) Homosynaptic long-term depression in area CA1 of hippocampus and effects of N-methyl-D-aspartate receptor blockade. *Proc Natl Acad Sci U S A* 89:4363-4367.
- Engert F, Bonhoeffer T (1997) Synapse specificity of long-term potentiation breaks down at short distances. *Nature* 388:279-284.
- Engert F, Bonhoeffer T (1999) Dendritic spine changes associated with hippocampal long-term synaptic plasticity. *Nature* 399:66-70.
- Fujita Y (1968) Activity of dendrites of single Purkinje cells and its relationship to so-called inactivation response in rabbit cerebellum. *J Neurophysiol* 31:131-141.
- Gahwiler BH (1981) Organotypic monolayer cultures of nervous tissue. *J Neurosci Methods* 4:329-342.
- Gahwiler BH, Capogna M, Debanne D, McKinney RA, Thompson SM (1997) Organotypic slice cultures: a technique has come of age. *Trends Neurosci* 20:471-477.
- Garaschuk O, Milos RI, Konnerth A (2006) Targeted bulk-loading of fluorescent indicators for two-photon brain imaging in vivo. *Nat Protoc* 1:380-386.
- Gilbert PE, Brushfield AM (2009) The role of the CA3 hippocampal subregion in spatial memory: a process oriented behavioral assessment. *Prog Neuropsychopharmacol Biol Psychiatry* 33:774-781.
- Glover JC, Sato K, Sato YM (2008) Using voltage-sensitive dye recording to image the functional development of neuronal circuits in vertebrate embryos. *Dev Neurobiol* ..

Bibliography

- Goldberg JH, Tamas G, Aronov D, Yuste R (2003) Calcium microdomains in aspiny dendrites. *Neuron* 40:807-821.
- Golding NL, Spruston N (1998) Dendritic sodium spikes are variable triggers of axonal action potentials in hippocampal CA1 pyramidal neurons. *Neuron* 21:1189-1200.
- Gomez TM, Snow DM, Letourneau PC (1995) Characterization of spontaneous calcium transients in nerve growth cones and their effect on growth cone migration. *Neuron* 14:1233-1246.
- Goodman CS, Shatz CJ (1993) Developmental mechanisms that generate precise patterns of neuronal connectivity. *Cell* 72:77-98.
- Govindarajan A, Kelleher RJ, Tonegawa S (2006) A clustered plasticity model of long-term memory engrams. *Nat Rev Neurosci* 7:575-583.
- Grewe BF, Helmchen F (2009) Optical probing of neuronal ensemble activity. *Curr Opin Neurobiol* In Press, Corrected Proof.
- Hall ZW, Sanes JR (1993) Synaptic structure and development: the neuromuscular junction. *Cell* 72 Suppl:99-121.
- Harney SC, Rowan M, Anwyl R (2006) Long-Term Depression of NMDA Receptor-Mediated Synaptic Transmission Is Dependent on Activation of Metabotropic Glutamate Receptors and Is Altered to Long-Term Potentiation by Low Intracellular Calcium Buffering. *J Neurosci* 26:1128-1132.
- Harvey CD, Svoboda K (2007) Locally dynamic synaptic learning rules in pyramidal neuron dendrites. *Nature* 450:1195-1200.
- Hasan MT, Friedrich RW, Euler T, Larkum ME, Giese GG, Both M, Duebel J, Waters J, Bujard H, Griesbeck O, Tsien RY, Nagai T, Miyawaki A, Denk W (2004) Functional Fluorescent Ca(2+) Indicator Proteins in Transgenic Mice under TET Control. *PLoS Biol* 2:E163.
- Hausser M, Spruston N, Stuart GJ (2000) Diversity and dynamics of dendritic signaling [In Process Citation]. *Science* 290:739-744.
- Hausser M, Mel B (2003) Dendrites: bug or feature? *Curr Opin Neurobiol* 13:372-383.
- Hebb DO (1949) *The Organization of Behavior: A Neuropsychological Theory*. New York: Wiley.
- Heim N, Griesbeck O (2004) Genetically encoded indicators of cellular calcium dynamics based on troponin C and green fluorescent protein. *J Biol Chem*.
- Heim N, Garaschuk O, Friedrich MW, Mank M, Milos RI, Kovalchuk Y, Konnerth A, Griesbeck O (2007) Improved calcium imaging in transgenic mice expressing a troponin C-based biosensor. *Nat Meth* 4:127-129.
- Helmchen F (2005) Calibration of fluorescent calcium indicators. In: *Imaging in neuroscience and development* (Yuste R, Konnerth A, eds), pp 253-263. Cold Spring Harbor, New York: Cold Spring Harbor Laboratory Press.

- Helmchen F, Denk W (2005) Deep tissue two-photon microscopy. *Nat Methods* 2:932-940.
- Hendel T, Mank M, Schnell B, Griesbeck O, Borst A, Reiff DF (2008a) Fluorescence Changes of Genetic Calcium Indicators and OGB-1 Correlated with Neural Activity and Calcium In Vivo and In Vitro. *J Neurosci* 28:7399-7411.
- Hendel T, Mank M, Schnell B, Griesbeck O, Borst A, Reiff DF (2008b) Fluorescence Changes of Genetic Calcium Indicators and OGB-1 Correlated with Neural Activity and Calcium In Vivo and In Vitro. *Journal of Neuroscience* 28:7399-7411.
- Henley J, Poo MM (2004) Guiding neuronal growth cones using Ca²⁺ signals. *Trends Cell Biol* 14:320-330.
- Henze DA, Cameron WE, Barrionuevo G (1996) Dendritic morphology and its effects on the amplitude and rise-time of synaptic signals in hippocampal CA3 pyramidal cells. *J Comp Neurol* 369:331-344.
- Holtmaat A, Bonhoeffer T, Chow DK, Chuckowree J, De P, V, Hofer SB, Hubener M, Keck T, Knott G, Lee WC, Mostany R, Mrsic-Flogel TD, Nedivi E, Portera-Cailliau C, Svoboda K, Trachtenberg JT, Wilbrecht L (2009) Long-term, high-resolution imaging in the mouse neocortex through a chronic cranial window. *Nat Protoc* 4:1128-1144.
- Hsia AY, Malenka RC, Nicoll RA (1998a) Development of excitatory circuitry in the hippocampus. *J Neurophysiol* 79:2013-2024.
- Hsia AY, Malenka RC, Nicoll RA (1998b) Development of excitatory circuitry in the hippocampus. *J Neurophysiol* 79:2013-2024.
- Hua JY, Smith SJ (2004) Neural activity and the dynamics of central nervous system development. *Nat Neurosci* 7:327-332.
- Huberman AD, Feller MB, Chapman B (2008) Mechanisms Underlying Development of Visual Maps and Receptive Fields. *Annu Rev Neurosci* 31:479-509.
- Jacobs LF, Gaulin SJ, Sherry DF, Hoffman GE (1990) Evolution of spatial cognition: sex-specific patterns of spatial behavior predict hippocampal size. *Proc Natl Acad Sci U S A* 87:6349-6352.
- James Williams (1890) *The Functions of the Brain*. In: *Principles of psychology* (James Williams, ed), New York: Holt.
- Johnston D, Magee JC, Colbert CM, Christie BR (1996) Active properties of neuronal dendrites. *Annu Rev Neurosci* 19:165-186.
- Karczmar AG (1996) The Otto Loewi Lecture. Loewi's discovery and the XXI century. *Prog Brain Res* 109:1-27, xvii.
- Kasyanov AM, Safiulina VF, Voronin LL, Cherubini E (2004) GABA-mediated giant depolarizing potentials as coincidence detectors for enhancing synaptic efficacy in the developing hippocampus. *Proc Natl Acad Sci U S A* 101:3967-3972.

Bibliography

- Katz LC, Shatz CJ (1996) Synaptic activity and the construction of cortical circuits. *Science* 274:1133-1138.
- Kawaguchi H, Fukunishi K (1998) Dendrite classification in rat hippocampal neurons according to signal propagation properties. Observation by multichannel optical recording in cultured neuronal networks. *Exp Brain Res* 122:378-392.
- Kettunen P, Demas J, Lohmann C, Gong YD, Wong ROL, Gan WB (2001) Rapid loading of calcium indicators by particle mediated ballistic delivery. *Soc Neurosci Abstr*.
- Kettunen P, Demas J, Lohmann C, Kasthuri N, Gong Y, Wong R, Gan W (2002) Imaging calcium dynamics in the nervous system by means of ballistic delivery of indicators. *J Neurosci Meth* 119:37-43.
- Khazipov R, Luhmann HJ (2006) Early patterns of electrical activity in the developing cerebral cortex of humans and rodents. *Trends in Neurosciences* 29:414-418.
- King EO, WARD MK, RANEY DE (1954) Two simple media for the demonstration of pyocyanin and fluorescein. *J Lab Clin Med* 44:301-307.
- Knierim JJ (2009) Imagining the possibilities: ripples, routes, and reactivation. *Neuron* 63:421-423.
- Koester HJ, Sakmann B (1998) Calcium dynamics in single spines during coincident pre- and postsynaptic activity depend on relative timing of back-propagating action potentials and subthreshold excitatory postsynaptic potentials. *Proc Natl Acad Sci U S A* 95:9596-9601.
- Konur S, Ghosh A (2005) Calcium signaling and the control of dendritic development. *Neuron* 46:401-405.
- Kreitzer AC, Gee KR, Archer EA, Regehr WG (2000) Monitoring presynaptic calcium dynamics in projection fibers by in vivo loading of a novel calcium indicator. *Neuron* 27:25-32.
- Kuhlman SJ, Huang ZJ (2008) High-resolution labeling and functional manipulation of specific neuron types in mouse brain by Cre-activated viral gene expression. *PLoS ONE* 3:e2005.
- Lang SB, Bonhoeffer T, Lohmann C (2006) Simultaneous imaging of morphological plasticity and calcium dynamics in dendrites. *Nature Protocols* 1:1859-1864.
- Lang SB, Stein V, Bonhoeffer T, Lohmann C (2007) Endogenous brain-derived neurotrophic factor triggers fast calcium transients at synapses in developing dendrites. *J Neurosci* 27:1097-1105.
- Lankford KL, Letourneau PC (1989) Evidence that calcium may control neurite outgrowth by regulating the stability of actin filaments. *J Cell Biol* 109:1229-1243.
- Leinekugel X (2003) Developmental patterns and plasticities: the hippocampal model. *J Physiol Paris* 97:27-37.

- Leinekugel X, Khalilov I, Benari Y, Khazipov R (1998) Giant depolarizing potentials: the septal pole of the hippocampus paces the activity of the developing intact septohippocampal complex in vitro. *J Neurosci* 18:6349-6357.
- Leinekugel X, Khalilov I, McLean H, Caillard O, Gaiarsa JL, Ben-Ari Y, Khazipov R (1999) GABA is the principal fast-acting excitatory transmitter in the neonatal brain. *Adv Neurol* 79:189-201.
- Leinekugel X, Khazipov R, Cannon R, Hirase H, Ben-Ari Y, Buzsaki G (2002) Correlated bursts of activity in the neonatal hippocampus in vivo. *Science* 296:2049-2052.
- Leinekugel X, Tseeb V, Ben-Ari Y, Bregestovski P (1995) Synaptic GABA_A activation induces Ca²⁺ rise in pyramidal cells and interneurons from rat neonatal hippocampal slices. *J Physiol* 487 (Pt 2):319-329.
- Letzkus JJ, Kampa BM, Stuart GJ (2006) Learning Rules for Spike Timing-Dependent Plasticity Depend on Dendritic Synapse Location. *J Neurosci* 26:10420-10429.
- Lichtman JW, Colman H (2000) Synapse elimination and indelible memory. *Neuron* 25:269-278.
- Linden DJ (1994) Long-Term Synaptic Depression in the Mammalian Brain. *Neuron* 12:457-472.
- Lohmann C, Bonhoeffer T (2008) A role for local calcium signaling in rapid synaptic partner selection by dendritic filopodia. *Neuron* 59:253-260.
- Lohmann C, Finski A, Bonhoeffer T (2005) Local calcium transients regulate the spontaneous motility of dendritic filopodia. *Nat Neurosci* 8:305-312.
- Lohr C (2003) Monitoring neuronal calcium signalling using a new method for ratiometric confocal calcium imaging. *Cell Calcium* 34:295-303.
- London M, Häusser M (2005) DENDRITIC COMPUTATION. *Annu Rev Neurosci* 28:503-532.
- Losonczy A, Magee JC (2006) Integrative Properties of Radial Oblique Dendrites in Hippocampal CA1 Pyramidal Neurons. *Neuron* 50:291-307.
- Losonczy A, Makara JK, Magee JC (2008) Compartmentalized dendritic plasticity and input feature storage in neurons. *Nature* 452:436-441.
- Magee JC, Cook EP (2000) Somatic EPSP amplitude is independent of synapse location in hippocampal pyramidal neurons. *Nat Neurosci* 3:895-903.
- Maguire EA, Nannery R, Spiers HJ (2006a) Navigation around London by a taxi driver with bilateral hippocampal lesions. *Brain* 129:2894-2907.
- Maguire EA, Woollett K, Spiers HJ (2006b) London taxi drivers and bus drivers: a structural MRI and neuropsychological analysis. *Hippocampus* 16:1091-1101.
- Malinow R (1991) Transmission between pairs of hippocampal slice neurons: quantal levels, oscillations, and LTP. *Science* 252:722-724.

Bibliography

- Mank M, Santos AF, Direnberger S, Mrcic-Flogel TD, Hofer SB, Stein V, Hendel T, Reiff DF, Levelt C, Borst A, Bonhoeffer T, Hubener M, Griesbeck O (2008) A genetically encoded calcium indicator for chronic in vivo two-photon imaging. *Nat Meth* 5:805-811.
- Maravall M, Mainen ZF, Sabatini BL, Svoboda K (2000a) Estimating intracellular calcium concentrations and buffering without wavelength ratioing. *Biophys J* 78:2655-2667.
- Maravall M, Mainen ZF, Sabatini BL, Svoboda K (2000b) Estimating intracellular calcium concentrations and buffering without wavelength ratioing. *Biophys J* 78:2655-2667.
- Mehta MR (2004) Cooperative LTP can map memory sequences on dendritic branches. *Trends Neurosci* 27:69-72.
- Meister M, Wong ROL, Baylor DA, Shatz CJ (1991) Synchronous bursts of action potentials in ganglion cells of the developing mammalian retina. *Science* 252:939-943.
- Mel BW, Schiller J (2004) On the fight between excitation and inhibition: location is everything. *Sci STKE* 2004:E44.
- Mohajerani MH, Cherubini E (2006) Role of giant depolarizing potentials in shaping synaptic currents in the developing hippocampus. *Crit Rev Neurobiol* 18:13-23.
- Murayama M, Perez-Garci E, Luscher HR, Larkum ME (2007) Fiberoptic system for recording dendritic calcium signals in layer 5 neocortical pyramidal cells in freely moving rats. *J Neurophysiol* 98:1791-1805.
- Murphy TH, Baraban JM, Wier WG, Blatter LA (1994) Visualization of quantal synaptic transmission by dendritic calcium imaging. *Science* 263:529-532.
- Murthy VN, Sejnowski TJ, Stevens CF (2000) Dynamics of dendritic calcium transients evoked by quantal release at excitatory hippocampal synapses. *Proceedings of the National Academy of Sciences of the United States of America* 97:901-906.
- Nakajima K, Harada K, Ebina Y, Yoshimura T, Ito H, Ban T, Shingai R (1993) Relationship between resting cytosolic Ca²⁺ and responses induced by N-methyl-D-aspartate in hippocampal neurons. *Brain Res* 603:321-323.
- Nakamura T, Barbara JG, Nakamura K, Ross WN (1999) Synergistic release of Ca²⁺ from IP₃-sensitive stores evoked by synaptic activation of mGluRs paired with backpropagating action potentials. *Neuron* 24:727-737.
- Narayan S, Greif KF (2004) Transport of a synaptotagmin-YFP fusion protein in sympathetic neurons during early neurite outgrowth in vitro after transfection in vivo. *J Neurosci Methods* 133:91-98.
- Nevian T, Helmchen F (2007) Calcium indicator loading of neurons using single-cell electroporation. *Pflugers Arch* 454:675-688.

Bibliography

- Nevian T, Larkum ME, Polsky A, Schiller J (2007) Properties of basal dendrites of layer 5 pyramidal neurons: a direct patch-clamp recording study. *Nat Neurosci* 10:206-214.
- O'Donovan MJ (1999) The origin of spontaneous activity in developing networks of the vertebrate nervous system. *Curr Opin Neurobiol* 9:94-104.
- Oertner TG (2002) Functional imaging of single synapses in brain slices. *Exp Physiol* 87:733-736.
- Palmer LM, Stuart GJ (2009) Membrane Potential Changes in Dendritic Spines during Action Potentials and Synaptic Input. *J Neurosci* 29:6897-6903.
- Pare D, Lang EJ, Destexhe A (1998) Inhibitory control of somatodendritic interactions underlying action potentials in neocortical pyramidal neurons in vivo: an intracellular and computational study. *Neuroscience* 84:377-402.
- Pavlidis P, Madison DV (1999) Synaptic transmission in pair recordings from CA3 pyramidal cells in organotypic culture. *J Neurophysiol* 81:2787-2797.
- Petrozzino JJ, Pozzo Miller LD, Connor JA (1995) Micromolar Ca²⁺ transients in dendritic spines of hippocampal pyramidal neurons in brain slice. *Neuron* 14:1223-1231.
- Poirazi P, Mel BW (2001) Impact of active dendrites and structural plasticity on the memory capacity of neural tissue. *Neuron* 29:779-796.
- Polsky A, Mel BW, Schiller J (2004) Computational subunits in thin dendrites of pyramidal cells. *Nat Neurosci* 7:621-627.
- Rall W, Burke RE, Smith TG, Nelson PG, Frank K (1967) Dendritic location of synapses and possible mechanisms for the monosynaptic EPSP in motoneurons. *J Neurophysiol* 30:1169-1193.
- Ramón y Cajal S (1911) *Histologie du Système Nerveux de l'Homme et des Vertébrés*. Paris: A. Maloine.
- Ramón y Cajal S (1888) Estructura de los centros nerviosos de las aves. *Revista trimestral de histología normal y patológica* 1:1-10.
- Regehr WG, Tank DW (1992) Calcium concentration dynamics produced by synaptic activation of CA1 hippocampal pyramidal cells. *J Neurosci* 12:4202-4223.
- Robain O, Barbin G, Billette d, V, Jardin L, Jahchan T, Ben Ari Y (1994) Development of mossy fiber synapses in hippocampal slice culture. *Brain Res Dev Brain Res* 80:244-250.
- Sanes JR, Lichtman JW (2001) Induction, assembly, maturation and maintenance of a postsynaptic apparatus. *Nat Rev Neurosci* 2:791-805.
- Scheiffele P (2003) Cell-cell signaling during synapse formation in the CNS. *Annu Rev Neurosci* 26:485-508.

Bibliography

- Scheiffele P, Fan J, Choih J, Fetter R, Serafini T (2000) Neuroligin expressed in nonneuronal cells triggers presynaptic development in contacting axons. *Cell* 101:657-669.
- Schiller J, Schiller Y, Stuart G, Sakmann B (1997) Calcium action potentials restricted to distal apical dendrites of rat neocortical pyramidal neurons. *J Physiol* 505 (Pt 3):605-616.
- Seifert M, Schmidt E, Baumeister R (2006) The genetics of synapse formation and function in *Caenorhabditis elegans*. *Cell Tissue Res* 326:273-285.
- Sholl DA (1953) Dendritic organization in the neurons of the visual and motor cortices of the cat. *J Anat* 87:387-406.
- Siksou L, Triller A, Marty S (2009) An emerging view of presynaptic structure from electron microscopic studies. *J Neurochem* 108:1336-1342.
- Sipila ST, Schuchmann S, Voipio J, Yamada J, Kaila K (2006) The Na-K-Cl cotransporter (NKCC1) Promotes Sharp Waves in the Neonatal Rat Hippocampus. *J Physiol* ..
- Sorra KE, Harris KM (1993) Occurrence and three-dimensional structure of multiple synapses between individual radiatum axons and their target pyramidal cells in hippocampal area CA1. *J Neurosci* 13:3736-3748.
- Stein V, Nicoll RA (2003) GABA generates excitement. *Neuron* 37:375-378.
- Stevens CF, Wang Y (1995) Facilitation and depression at single central synapses. *Neuron* 14:795-802.
- Stirling RV, Bliss TV (1978) Hippocampal mossy fiber development at the ultrastructural level. *Prog Brain Res* 48:191-198.
- Stoppini L, Buchs P-A, Muller D (1991) A simple method for organotypic cultures of nervous tissue. *J Neurosci Meth* 37:173-182.
- Stosiek C, Garaschuk O, Holthoff K, Konnerth A (2003) In vivo two-photon calcium imaging of neuronal networks. *Proceedings of the National Academy of Sciences* 100:7319.
- Stricker C, Field AC, Redman SJ (1996) Statistical analysis of amplitude fluctuations in EPSCs evoked in rat CA1 pyramidal neurones in vitro. *J Physiol* 490 (Pt 2):419-441.
- Stuart G, Spruston N, Sakmann B, Hausser M (1997) Action potential initiation and backpropagation in neurons of the mammalian CNS. *Trends Neurosci* 20:125-131.
- Stuart GJ, Dodt HU, Sakmann B (1993) Patch-clamp recordings from the soma and dendrites of neurons in brain slices using infrared video microscopy. *Pflugers Arch-Eur J Physiol* 423:511-518.
- Stuart GJ, Palmer LM (2006) Imaging membrane potential in dendrites and axons of single neurons. *Pflugers Arch* ..

Svoboda K, Yasuda R (2006) Principles of two-photon excitation microscopy and its applications to neuroscience. *Neuron* 50:823-839.

Tang FJ, Dent EW, Kalil K (2003) Spontaneous calcium transients in developing cortical neurons regulate axon outgrowth. *J Neurosci* 23:927-936.

Tessier-Lavigne M, Goodman CS (1996) The molecular biology of axon guidance. *Science* 274:1123-1133.

Thivierge JP (2009) How does non-random spontaneous activity contribute to brain development? *Neural Netw.*

Thomas D, Tovey SC, Collins TJ, Bootman MD, Berridge MJ, Lipp P (2000) A comparison of fluorescent Ca²⁺ indicator properties and their use in measuring elementary and global Ca²⁺ signals. *Cell Calcium* 28:213-223.

Todman D (2008) Henry Dale and the discovery of chemical synaptic transmission. *Eur Neurol* 60:162-164.

Togashi H, Abe K, Mizoguchi A, Takaoka K, Chisaka O, Takeichi M (2002) Cadherin regulates dendritic spine morphogenesis. *Neuron* 35:77-89.

Tsubokawa H, Ross WN (1996) IPSPs modulate spike backpropagation and associated [Ca²⁺]_i changes in the dendrites of hippocampal CA1 pyramidal neurons. *J Neurophysiol* 76:2896-2906.

Vaughn JE (1989) Fine structure of synaptogenesis in the vertebrate central nervous system. *Synapse* 3:255-285.

Williams SR, Stuart GJ (2003) Role of dendritic synapse location in the control of action potential output. *Trends Neurosci* 26:147-154.

Wong ROL (1999) Retinal waves and visual system development. *Annu Rev Neurosci* 22:29-47.

Yaksi E, Friedrich RW (2006) Reconstruction of firing rate changes across neuronal populations by temporally deconvolved Ca²⁺ imaging. *Nat Methods* 3:377-383.

Yang SN, Tang YG, Zucker RS (1999a) Selective induction of LTP and LTD by postsynaptic [Ca²⁺]_i elevation. *J Neurophysiol* 81:781-787.

Yang SN, Tang YG, Zucker RS (1999b) Selective induction of LTP and LTD by postsynaptic [Ca²⁺]_i elevation. *J Neurophysiol* 81:781-787.

Yates PA, Holub AD, Mclaughlin T, Sejnowski TJ, O'Leary DD (2004) Computational modeling of retinotopic map development to define contributions of EphA-ephrinA gradients, axon-axon interactions, and patterned activity. *J Neurobiol* 59:95-113.

Yuste R, Majewska A, Cash SS, Denk W (1999) Mechanisms of calcium influx into hippocampal spines: heterogeneity among spines, coincidence detection by NMDA receptors, and optical quantal analysis. *J Neurosci* 19:1976-1987.

Bibliography

Zito K, Scheuss V, Knott G, Hill T, Svoboda K (2009) Rapid functional maturation of nascent dendritic spines. *Neuron* 61:247-258.

Zucker RS (1999a) Calcium- and activity-dependent synaptic plasticity. *Curr Opin Neurobiol* 9:305-313.

Zucker RS (1999b) Calcium- and activity-dependent synaptic plasticity. *Curr Opin Neurobiol* 9:305-313.

8 ACKNOWLEDGEMENTS

First of all I want to thank Christian Lohmann for the supervision of my thesis and for training me in preparing and presenting talks, seminars and posters. Thank you for never running out of ideas.

I am very grateful to Tobias Bonhoeffer for being my *Doktorvater* and giving me the opportunity to do my PhD-Thesis in his department. Especially, I want to thank for the fast and reliable way to give advice and support.

Thanks to Axel Borst and Valentin Stein for their scientific support and their fruitful discussions and suggestions as members of my thesis committee.

Thanks to the Lohmann group for tolerating Bavarian habits, even in the Netherlands, and for listening to concerns and complaints and sometimes even to Bavarian music. Also thanks to the entire Bonhoeffer and Stein group, and to the former “Blocksberghehen”. You made working much easier and nicer.

Vielen Dank an alle Freunde, die mich im „niederländischen Exil“ besucht haben und die mich jederzeit mit offenen Armen empfangen haben und immer Zeit für mich hatten oder sie sich genommen haben. Besonderen Dank an Xaver Sewald für aufschlußreiche Gespräche auch über wissenschaftliche Probleme und Sorgen, und ihm sowie Christof Ettinger und Mario Schröppel, für Ihre Freundschaft und die unerschöpflichen Ideen, die mir oft über weniger erfolgreiche Perioden geholfen haben.

Un agradecimiento muy personal a Susana Gomis-Rüth. Te doy gracias no solo por la paciencia infinita en tus correcciones, mejoras y sugerencias, sino también muy especialmente por siempre estar a mi lado cuando te necesito!

Am dankbarsten bin ich meiner Familie, meiner Tante für Ihre Unterstützung und die viele Schweizer Schokolade und vor allem meinen zwei jugendlichen „Alten“, die mir alles ermöglichten und mich immer unterstützten und mich zusammen mit „Schneegal“ stets aufbauten und motivierten.

9 CURRICULUM VITAE

Personal Data

Name: Thomas Alexander Kleindienst
Address: Spielhahnstr. 4a
83059 Kolbermoor
Germany
E-mail: tomkl@gmx.de
Date of birth: August 24th, 1978
Place of birth: Landshut, Germany
Citizenship: German

Education

Since 01/2006 PhD under supervision of Dr. Christian Lohmann and Prof. Dr. Tobias Bonhoeffer at the *Netherlands Institute for Neuroscience, Department Synapse and Network Development, Amsterdam and Max-Planck-Institute of Neurobiology, Department of Cellular- and Systems Neurobiology, Munich*

08/2004 - 12/2005 Diploma thesis at the *Max-Planck-Institute of Neurobiology, Department of Cellular- and Systems Neurobiology, Munich*

05/2000 - 12/2005 Diploma in biology at the *Ludwig-Maximilians-Universität, Munich*, major subject: neurobiology, minor subjects: biochemistry, microbiology, ecology
Diploma final grade: 1.2

05/1999 - 05/2000 Civilian service at Bayrisches Rotes Kreuz, Munich

09/1998 - 05/1999 Undergraduate study: chemistry

09/1988 - 06/1998 Gymnasium Bad Aibling, Bad Aibling
Abitur final grade: 2.1